

UNIVERSITY OF MICHIGAN



**REPAIR AND STRENGTHENING OF REINFORCED CONCRETE  
BEAMS USING CFRP LAMINATES**

**Volume 6: Behavior of Beams Subjected to Freeze-Thaw Cycles**

by

Antoine Naaman  
Maria del Mar Lopez

Project Coordinator: Roger D. Till, MDOT  
Project Advisor: Thomas D. Gillespie, GLCTTR

Report No. UMCEE 98 - 32  
April, 1999

The University of Michigan  
Department of Civil and Environmental Engineering  
Ann Arbor, MI 48109-2125, USA

Technical Report Documentation Page

1. Report No. RC - 1372		2. Government Accession No.		3. Recipient's Catalog No.	
4. Title and Subtitle Repair and Strengthening of Reinforced Concrete Beams using CFRP Laminates. <b>Volume 6: Behavior of Beams Subjected to Freeze-Thaw Cycles</b>				5. Report Date April, 1999	
7. Author (s) Antoine E. Naaman Maria del Mar Lopez				6. Performing Organization Code UMCEE 98 - 32	
9. Performing Organization Name and Address The University of Michigan, Dept. of Civil and Env. Engineering 2340 G.G. Brown Bldg. Ann Arbor, MI 48109-2125				8. Performing Org Report No. RC - 1372	
12. Sponsoring Agency Name and Address Michigan Department of Transportation Construction and Technology Division P.O. Box 30049 Lansing, MI 48909				10. Work Unit No. (TRAIS)	
				11. Contract/Grant No.	
15. Supplementary Notes				13. Type of Report & Period Covered Research Report 1997-1998	
				14. Sponsoring Agency Code	
16. Abstract					
<p>Repair and strengthening techniques using glued-on carbon fiber reinforced plastic (CFRP) plates (also called sheets, tow sheets, and thin laminates) form the basis of a new technology being increasingly used for bridges and highway superstructures.</p> <p>The study described in this report (Volumes 1 to 7) focused on the use of carbon fiber reinforced plastic (CFRP) laminates for repair and strengthening of reinforced concrete beams. Its primary objectives are: 1) to ascertain the applicability of CFRP adhesive bonded laminates for repair and strengthening of reinforced concrete beams; 2) to synthesize existing knowledge and develop procedures for implementation in the field; 3) to identify key parameters for successful design and implementation; and 4) to adapt this technique to the specific conditions encountered in the state of Michigan.</p> <p>This report consists of 7 volumes:          Volume 1 – Summary Report          Volume 2 – Literature Review          Volume 3 – Behavior of Beams Strengthened for Bending          Volume 4 – Behavior of Beams Strengthened for Shear          Volume 5 – Behavior of Beams Under Cyclic Loading at Low Temperature          Volume 6 – Behavior of Beams Subjected to Freeze-Thaw Cycles          Volume 7 – Technical Specifications</p> <p>The part of the investigation dealing with the flexural testing of reinforced concrete beams with glued-on CFRP plates subjected to different numbers of freeze-thaw cycles is the subject of this volume (volume 6). Results are also analyzed, compared, and discussed. The experimental program comprised forty-eight reinforced concrete beams. The specimens were subjected to up to 300 freeze-thaw cycles according to ASTM C666. For every parameter, three beams were tested in bending at 0, 100, 200 and 300 cycles. Parameters investigated were two different adhesive systems, the Tonen CFRP sheet system (MBrace), and the Sika CFRP system (Carbodur); and a cracking stage where a precracked condition simulates cracking conditions in the field prior to strengthening. Control specimens (RC beams with no CFRP laminate externally glued-on) were also subjected to 0, 100, 200 and 300 cycles freeze-thaw cycles. Conclusions are drawn and some recommendations for design are suggested.</p>					
17. Keywords bond, carbon fiber, composites materials, laminates, rehabilitation, reinforced concrete, repair, strengthening systems			18. Distribution Statement No restrictions. This document is available to the public through the Michigan Department of Transportation		
19. Security Classification (report) Unclassified		20. Security Classification (Page) Unclassified		21. No. of pages	22. price

## Michigan Department of Transportation - Technical Advisory Group

Roger D. Till, *Project Coordinator*  
*Materials and Technology Laboratories*

David Juntunen  
*Materials and Technology Laboratories*

Jon Reincke  
*Materials and Technology Laboratories*

Glenn Bukoski  
*Construction*

Steve Beck  
*Design*

Raja Jildeh  
*Design*

Michel Tarazi  
*Design*

Steve O'Connor  
*Engineering Services*

Sonny Jadun  
*Maintenance*

John Nekritz  
*Federal Highway Administration*

## Great Lakes Center for Trucks and Transit Research

Thomas D. Gillespie, *Project Advisor*  
University of Michigan Transportation Research Institute

## University of Michigan - CEE Research Team

Antoine Naaman, *Project Director*

Sang Yeol Park, *Research Fellow*

Maria del Mar Lopez, *Graduate Research Assistant*

Luke R. Pinkerton, *Graduate Research Assistant*

UMCEE 98 - 32  
MDOT Contract No: 96-1067BAB

Project Director: Antoine E. Naaman, UM  
Project Coordinator: Roger D. Till, MDOT  
Project Advisor: Thomas D. Gillespie, GLCTTR

April, 1999

**key words:**

adhesives  
bending  
bond  
carbon fiber  
composite materials  
concrete  
durability  
epoxy  
fatigue  
freeze thaw  
FRP sheets  
low temperature  
repair  
rehabilitation  
shear  
strengthening systems

Department of Civil and Environmental Engineering  
University of Michigan, 2340 G.G. Brown building  
Ann Arbor, MI 48109-2125  
Tel: 1-734-764-8495; Fax: 1-734-764 4292

The publication of this report does not necessarily indicate approval or endorsement of the findings, opinions, conclusions, or recommendations either inferred or specifically expressed herein, by the Regents of the University of Michigan, the Michigan Department of Transportation, or the Great Lakes Center for Trucks and Transit Research.

## ACKNOWLEDGMENTS

The research described in this report was supported jointly by a grant from the Michigan Department of Transportation and the Great Lakes Center of Truck and Transit Research which is affiliated with the University of Michigan Transportation Research Institute. Matching funds for student tuition and for equipment were also provided by the University of Michigan.

The research team received valuable support, counsel, and guidance from the Technical Advisory Group. The support and encouragement provided by Roger Till, project coordinator representing the Michigan Department of Transportation, is deeply appreciated.

The authors are thankful to the Sika Corporation (Bob Pisha) for the donation of the carbodur laminate as well as Sikadur epoxy material. The partial contribution of Tonen Corporation with the MBrace composite strengthening system, and the help of Howard Kliger are also appreciated.

The opinions expressed in this report are those of the authors and do not necessarily reflect the views of the sponsors.

## TABLE OF CONTENTS

ACKNOWLEDGMENTS .....	iii
LIST OF FIGURES.....	vi
LIST OF TABLES .....	vi
PREFACE .....	vii
ABSTRACT .....	viii
EXECUTIVE SUMMARY .....	ix
<b>1. INTRODUCTION.....</b>	<b>1</b>
1.1. Organization of this Report .....	1
<b>2. LITERATURE REVIEW .....</b>	<b>2</b>
2.1.1. DE - University of Delaware, Delaware Department of Transportation.....	2
2.1.2. CAN - Canadian Institutes and Universities .....	2
2.1.3. EMPA - Swiss Federal Laboratories for Materials Testing and Research.....	6
2.1.4. Other Research On Freeze-Thaw.....	6
<b>3. EXPERIMENTAL PROGRAM .....</b>	<b>7</b>
3.1. Parameters of study .....	7
3.2. Material Properties .....	8
3.2.1. Concrete .....	8
3.2.2. Steel mesh.....	9
3.2.3. Strengthening Systems .....	9
3.3. Design and Fabrication of Specimens.....	12
3.4. Test Set-Up and Instrumentation .....	13
3.4.1. Freeze-Thaw Cycles.....	13
3.4.2. Bending Test.....	16
<b>4. TEST RESULTS .....</b>	<b>16</b>
<b>5. ANALYSIS AND INTERPRETATION.....</b>	<b>23</b>
5.1. Failure Modes .....	23

5.2. Shear Strength.....	26
5.3. Flexural Strength .....	31
5.4. Delamination Length .....	34
<b>6. CONCLUSIONS .....</b>	<b>37</b>
<b>7. RECOMMENDATIONS .....</b>	<b>38</b>
<b>8. REFERENCES WITH SOURCE CLASSIFICATION.....</b>	<b>39</b>
<b>9. APPENDIX A .....</b>	<b>41</b>
<b>10. APPENDIX B.....</b>	<b>48</b>
<b>11. APPENDIX C .....</b>	<b>55</b>
<b>12. APPENDIX D .....</b>	<b>58</b>

## LIST OF FIGURES

Figure 3.1 Stress-Displacement Curve of the Steel Mesh .....	10
Figure 3.2 Reinforcement Detail of the Cross Section .....	12
Figure 3.3 Flexural Test Load Set-up .....	14
Figure 3.4 Schematic Representation of the Freeze-Thaw Test (ASTM C666-procedure B).....	15
Figure 3.5 Freeze-Thaw Profile Applied .....	16
Figure 4.1 Load-Deflection Curves for 0 F.T. Cycles .....	19
Figure 4.2 Load-Deflection Curves for 100 F.T. Cycles .....	19
Figure 4.3 Load-Deflection Curves for 200 F.T. Cycles .....	20
Figure 4.4 Load-Deflection Curves for 300 F.T. Cycles .....	20
Figure 4.5 Load-Deflection Curves for Tonen Precracked Beams.....	21
Figure 4.6 Load-Deflection Curves for Tonen Not Precracked Beams .....	21
Figure 4.7 Load-Deflection Curves for Sika Precracked Beams.....	22
Figure 5.1 Failure Modes for Specimens with CFRP Plates .....	25
Figure 5.2 Tonen Precracked: Normalized Max. Shear Stress vs Number of F.T. Cycles.....	29
Figure 5.3 Tonen not Precracked: Normalized Max. Shear Stress vs Number of F.T. Cycles .....	29
Figure 5.4 Sika Precracked: Normalized Max. Shear Stress vs Number of F.T. Cycles.....	30
Figure 5.5 Average Normalized Max. Shear Stress at Failure vs Number of F.T. Cycles .....	30
Figure 5.6 Moment-Deflection Curves for 0 F.T. Cycles .....	32
Figure 5.7 Moment-Deflection Curves for 100 F.T. Cycles.....	32
Figure 5.8 Moment-Deflection Curves for 200 F.T. Cycles.....	33
Figure 5.9 Moment-Deflection Curves for 300 F.T. Cycles.....	33
Figure 5.10 Tonen Precracked: Delamination Length vs. Number of F.T. Cycles.....	34
Figure 5.11 Tonen not precracked: Delamination Length vs. Number of F.T. Cycles.....	34
Figure 5.12 Sika Precracked: Delamination Length vs. Number of F.T. Cycles.....	35

## LIST OF TABLES

Table 2.1 Test Parameters Found in Literature Review of Freeze-Thaw (F.T.) Tests.....	3
Table 3.1 Parameters of the Freeze-Thaw Beam Tests.....	8
Table 3.2 Compression Test Results .....	9
Table 4.1 Summary of the Test Results.....	17
Table 4.2 Maximum Shear Force and Moment.....	18
Table 5.1 Values of Normalized Maximum Shear Stress.....	24

## PREFACE

This project titled: "*Repair and Strengthening of Reinforced Concrete Beams using CFRP Laminates*" is aimed at providing experimental verification and recommendations for implementation of a new technology, in which thin fiber reinforced plastic laminates are glued-on the surface of concrete beams in order to strengthen them.

The primary objectives of the project were:

- To ascertain the applicability of Carbon Fiber Reinforced Plastic (CFRP) glued-on plates for repair and strengthening of concrete beams;
- To synthesize existing knowledge and develop procedures for implementation in the field;
- To adapt this technique to the specific conditions encountered in the state of Michigan.

The project consisted of 8 tasks as follows:

- A report containing a literature review and a comprehensive synthesis of the latest state of knowledge on the glued-on FRP technique (Task 1);
- Laboratory testing and verification of the selected CFRP glued-on technique according to the proposed experimental program: bending (Task 2), shear (Task 3), freeze-thaw (Task 4), temperature and high cyclic amplitude load (Task 5);
- An interim and final report summarizing the experimental results (Task 6). The interim report will cover the bending and freeze-thaw tests;
- A summary of field specifications and "how to" details for implementation in field applications;
- Guidelines for design based on the experience developed from the experimental work (Task 7);
- Field monitoring of application of the technique to one bridge selected by MDOT (Task 8a);
- Bridge testing before and after application of the glued-on plate (Task 8b to be conducted by professor A. Nowak, U of M)

This report summarizes the experimental program on freeze-thaw tests as per Task 4.

## ABSTRACT

Repair and strengthening techniques using glued-on carbon fiber reinforced plastic (CFRP) plates (also called sheets, tow sheets, and thin laminates) form the basis of a new technology being increasingly used for bridges and highway superstructures.

The study described in this report is part of a larger investigation on the use of carbon fiber reinforced plastic (CFRP) sheets for repair and strengthening of reinforced and prestressed concrete beams. Its primary objectives are: 1) to ascertain the applicability of CFRP glued-on plates for repair and strengthening of concrete beams, 2) to synthesize existing knowledge, 3) to identify optimum parameters for successful implementation, 4) to develop procedures for implementation in the field, and 5) to adapt the technique to the specific conditions encountered in the state of Michigan.

The experimental program includes four main parts: 1) tests of RC beams strengthened in bending; 2) tests of RC beams strengthened in shear; 3) freeze-thaw tests of strengthened beams followed by their test in bending; and 4) tests in bending and shear of strengthened beams under low temperature ( $-29^{\circ}\text{C}$ ) and high amplitude cyclic loading.

The part of the investigation dealing with the flexural testing of reinforced concrete beams with glued-on CFRP plates subjected to different numbers of freeze-thaw cycles is the subject of this report. Results are also analyzed, compared, and discussed. The experimental program comprised forty-eight reinforced concrete beams. The specimens were subjected to up to 300 freeze-thaw cycles according to ASTM C666. For every parameter, three beams were tested in bending at 0, 100, 200 and 300 cycles. Parameters investigated were two different adhesive systems, the Tonen CFRP sheet system (MBrace), and the Sika CFRP system (Carbodur); and a cracking stage where a precracked condition simulates cracking conditions in the field prior to strengthening. Control specimens (RC beams with no CFRP laminate externally glued-on) were also subjected to 0, 100, 200 and 300 cycles freeze-thaw cycles. Conclusions are drawn and some recommendations for design are suggested.

The experience gained during this project should contribute to a better understanding of the behavior of these new strengthening systems under different environmental conditions.

## EXECUTIVE SUMMARY

This report presents the summary of experimental work, laboratory testing, and analysis of results for task 4 of the current research project which deals with flexural testing of reinforced concrete beams with glued-on CFRP plates subjected to an increasing number of freeze-thaw cycles. Results are also analyzed, compared, and discussed.

Based on the results from the experimental work, the following conclusions were drawn:

1. For the control reinforced concrete specimens no decrease in the moment capacity or shear strength due to the freeze-thaw cycles was observed. However, a decrease in the maximum deflection was observed.
2. For specimens strengthened with CFRP sheets an overall decrease in the moment capacity as well as the maximum deflection was observed with an increase in number of freeze-thaw (F.T.) cycles. Precracked beams using the Tonen system presented the higher rate of decrease of moment capacity (38% average for 300 F.T. cycles). Non-precracked beams also strengthened with the Tonen system led to an average decrease of 20% for 300 F.T. cycles.
3. The maximum moment capacity of beams strengthened with the Sika system decreased 13% on average for 200 F.T. cycles and 4% average for 300 F.T. cycles. This variation was attributed to the influence of different type of failure modes.
4. The average deflection at maximum load was very sensitive to the effect of the freeze-thaw cycles and the cracking condition. For the Tonen precracked beams a reduction of 43% in deflection was found after 300 F.T. cycles whereas for the Tonen non-precracked beams the decrease was of 19%. Beams using the Sika system showed a smaller rate of decrease in deflection at maximum load (15% average for 200 F.T. cycles and 7% for 300 F.T. cycles)
5. With the Tonen system, the values of normalized shear stress ( $v_n$ ) for the same number of freeze-thaw cycles were higher for the flexure-delamination failure than for the shear-delamination failure. It was concluded that shear cracks accelerate the interfacial crack propagation.
6. With the Tonen system, precracking the beam influences the decrease in the average normalized shear stress with the freeze-thaw cycles. For 300 freeze-thaw cycles, precracked beams had a decrease of 39% (compared with the strength at zero F.T. cycles) whereas the decrease for the non precracked beams was 22%. However the normalized shear stress after 300 F.T. cycles remained almost the same:  $v = 0.20\sqrt{f'_c}$  for

precracked beams, and  $v=0.19\sqrt{f_c}$  for non-precracked beams. It can be shown that at zero F.T. cycles the cracking condition influences the capacity of the beam, whereas after 300 F.T. cycles, the freezing and thawing effect dominates.

7. For the Sika system, ignoring vertical shear failure, the decrease in the normalized average shear stress at failure load due to the effect of the freeze-thaw cycles seemed to be less significant than for the Tonen system. A decrease of 10% was observed for 300 freeze-thaw cycles, leading to a value of  $0.36\sqrt{f_c}$ .
8. For both strengthening systems (Tonen and Sika), the delamination length found in specimens that failed either by shear-delamination or flexure-delamination was located between the end of the CFRP laminate and the maximum bending moment region.
9. The delamination length was quite uniform for both strengthening systems. For the Tonen system, values of delamination length varied between 140 to 180 mm. For the Sika system, the range was even more narrow, 220-250 mm. No influence of either the number of freeze-thaw cycles or the type of failure mode was observed on delamination length.

Some recommendations for design and retrofit use based on this study are summarized as follows:

1. Freeze-Thaw (F.T.) cycles influence the behavior of reinforced concrete beams with glued-on Carbon Fiber Reinforced Plastic (CFRP) laminates. According to this study, with the Tonen system a maximum decrease of 29% of flexural capacity could be expected after 200 FT and 38% after 300 F.T. cycles. With the Sika system, the maximum decrease observed was of 13% after 200 F.T. cycles. It should be pointed out that the influence of the Freeze-Thaw cycles may also affects the concrete strength, but its effect cannot be easily observed from testing a reinforced concrete beam in bending; it is possible that this dual effect explains the decrease in strength. Unless some additional tests are carried out, as a first design approximation, it is recommended that a reduction of 40% in horizontal shear strength be taken to account for freeze-thaw exposure.
2. The value of the horizontal interfacial shear strength can be taken conservatively as  $0.17\sqrt{f_c}$  for both strengthening systems. Preliminary analyses indicate that this value may be close to 1.70 MPa for Tonen system and 2.64 MPa for the Sika system, considering the effect of the different strengthening level provided by the two systems. Further study of the interface bond behavior is needed in order to refine this value.
3. The minimum value of the development length (or anchorage) of the CFRP laminate should be based on the value of  $0.17\sqrt{f_c}$ . This value could be modified by results from further investigations. It is recommended that the bonded length of the CFRP should

be as long as possible in order to avoid an interfacial bond failure and to have a more efficient use of the CFRP sheet strength.

4. Since delamination seems to be controlled by the interface bond between the CFRP laminate and the concrete, which is also controlled by the concrete strength, it is strongly recommended to insure very good surface preparation before application of the strengthening system.

# 1. INTRODUCTION

This study is part of a research project at the University of Michigan supported by the Michigan Department of Transportation and the Great Lakes Center for Truck and Transit Research. The project title is "Repair and Strengthening of Reinforced and Prestressed Concrete Beams Using Carbon Fiber Reinforced Plastic (CFRP) Glued-on Plates". The study is aimed at providing experimental verification and recommendations for implementation of a new technology, in which thin fiber reinforced plastic laminates are glued-on the surface of concrete beams in order to strengthen them.

The primary objectives of this project are to ascertain the applicability of CFRP glued-on plates for repair and strengthening of concrete beams, to synthesize existing knowledge and develop procedures for implementation in the field, and to adapt this technique to the specific conditions encountered in the State of Michigan. The project consists of 8 tasks. Task 4 deals with the flexural testing of reinforced concrete beams with glued-on CFRP plates subjected to different numbers of freeze-thaw cycles. It is the subject of this report.

## 1.1 Organization of this Report

This report presents the summary of experimental work, laboratory testing, and analysis of the results for task 4 of the current research project: Flexural test of reinforced concrete beams with glued-on CFRP plates subjected to an increasing number of freeze-thaw cycles.

Chapter 2 summarizes known prior research on CFRP laminates subjected to freeze-thaw cycles. It describes how the proposed experimental project studies some of the unknowns about the performance of this strengthening technique.

Chapter 3 presents the experimental program. The main experimental parameters, the material properties, fabrication of specimens, and test set-up and instrumentation are specified.

Chapter 4 presents the test results from the bending tests of specimens subjected to the different freeze-thaw cycles.

Chapter 5 presents the interpretation and analysis of the experimental results.

Chapter 6 presents the conclusions based on this experimental study.

Chapter 7 summarizes the recommendations for design and retrofit use based on this study.

Chapter 8 provides an extensive list of references.

Chapters 9, 10, 11 and 12 present appendixes A, B, C and D.

## 2. LITERATURE REVIEW

The rehabilitation technique of external reinforcement of concrete elements by the use of CFRP sheets can not be effectively utilized in cold regions without investigating the durability of this new material in low temperature environments.

In the following sections the results of a literature review, aimed at investigating freeze-thaw durability of concrete elements strengthened by CFRP sheets are summarized. Table 2.1. highlights the most important parameters found in this literature review.

### 2.1.1. DE - University of Delaware, Delaware Department of Transportation

Reference: [DE-2]

At the University of Delaware, tests were performed to investigate the environmental durability of composite fiber materials: Aramid, E-glass and graphite (carbon) fibers. The environmental durability studies involved subjecting the 60 small scale size beam specimens to aggressive environments (the beams were exposed to repeated wet/dry and freeze/thaw cycles while submerged in a solution of calcium chloride.) Exposure times were varied and the flexural capacity of the exposed beam was compared with that of control beams. Once the beams completed the environmental cycling they were loaded to failure in four point bending. The results of the test indicate that the beams reinforced with the graphite fabric have greater environmental durability than those with Aramid or E-glass. After being subjected to environmental conditions, only graphite reinforced beams maintained nearly all of their strength advantage over the unwrapped beams. While both the Aramid and E-glass reinforced beams showed a 36 % decrease in strength after 100 wet/dry cycles, the graphite reinforced beams dropped in strength by only 19 % (as compared to a 12 % drop in strength of the unstrengthened beams). For the freeze-thaw test, a decrease of 21% on the strength of the graphite reinforced beams was reported after 100 freeze-thaw (F.T.) cycles (compare with 17% of unwrapped.) Of the two conditions showed above, the wet/dry cycling led to greater degradation. The tests also revealed that the environmental exposure could lead to a changed mode of failure compared to non-exposed specimens. Partial debonding was experienced prior to failure.

### 2.1.2. CAN - Canadian Institutes and Universities

Reference: [CAN-2]

Hoang et al. conducted an experimental program where beams of dimensions 51 x 76 x 279 mm were externally reinforced with a carbon/epoxy composite sheet and tested under flexure after being submitted to different environments.

Table 2.1 Test Parameters Found in Literature Review of Freeze-Thaw (F.T.) Tests

Reference	No. specimens	No. cycles	Tests Procedures	Type of FRP	Variable	Comments
DE-2	60 beams 38.1x 28.6x330mm Reinf $\varnothing$ = 2.38mm Adhes. = Sikadur 32 Aggregate size = 3.175 mm	50, 100	Epoxy-concrete compatibility ASTM C884-87 Freeze-thaw (F.T.) ASTM C672-84 Flexural test (4 pts) after environmental cycling	Aramid, E-glass, Graphite (Carbon)	type of FRP: Aramid, E-glass, Graphite (Carbon)	<ul style="list-style-type: none"> <li>Graphite has higher env. durability than Aramid and E-glass.</li> <li>For CFRP 21% decrease in strength compared with 17% for control beams.</li> <li>Wet/dry cycles more critical than Freeze-thaw test.</li> <li>Change in failure mode due to environmental exposure.</li> <li>Partial debonding prior to failure.</li> </ul>
DE-3	Field application Foulk Road bridge	(1 year)	6 beams	CFRP	<ul style="list-style-type: none"> <li>Performance during its first year.</li> <li>Evaluation of bond characteristics.</li> <li>Durability of joints</li> </ul>	<ul style="list-style-type: none"> <li>All of the single layer applications of CFRP were well bonded (5 beams).</li> <li>1 beam with 2 layers of the highest strength sheet was not well bonded. Assumed due to insufficient resin saturation during the bonding process.</li> </ul>
XX-9	2 coupons 25.4 x 9.53 x 304.8 mm	300	Cut edges coated with epoxy 2% water solution Temp = 0-40 F F.T. (ASTM C666) Flexure (ASTM D790)	Fiber glass composite	Edge coated-uncoated Salt water	<ul style="list-style-type: none"> <li>Lost 20-30% flexural strength, rigidity and toughness.</li> <li>Loss due to only salt water exposure = 5-10%.</li> </ul>
XX-25	FRP rods embedded in a concrete cube of 100 mm length	300	bond test CP110 ASTM and RILEM	GFRP, CFRP and Vynylon FRP bar	Bond strength	<ul style="list-style-type: none"> <li>No great influence of the bond strength due to F. T. Cycles.</li> </ul>

Reference	No. specimens	No. cycles	Tests Procedures	Type of FRP	Variable	Comments
XX-26	Information Not Available (N.A.)	N.A.	N.A.	CGFRP grid (74% glass, 26% Carbon)	Range T	<ul style="list-style-type: none"> <li>Increase ultimate tensile strength by 11% and 2.5% mod. Elasticity for a fall in Temp. of -30C.</li> <li>Decrease of 9.5% and 2.5% respect. for increase from room T to 50C.</li> </ul>
XX-22	N.A.	N.A.	N.A.	N.A.	Combine env. Expos. Crack propagation	<ul style="list-style-type: none"> <li>The freezer condition had little effect on crack propagation.</li> </ul>
CAN-1	42 columns, 15 were subjected to FT test 152 x 305 mm	200	Cycling = -18C to +20C	CFRP wrap	% of Reinf. # of CFRP layers Env. Conditions: F.T. test Low Temperature water	<ul style="list-style-type: none"> <li>CFRP wrapped concrete columns exposed to F. T. cycling showed a significant increase in strength (3 times) compared to unwrapped columns exposed to the same cond.</li> <li>A second layer of CFRP provided an increase of 15% in strength.</li> <li>The wrapped columns subjected to F.T. cycling failed in a more catastrophic manner than those at room Temperature.</li> </ul>
CAN-2	18 beams	N.A.	40C one week, -23C one week for 2 months Flexural test (3pt. Bending)	N.A.	Accelerated env. Exposure	<ul style="list-style-type: none"> <li>7% Reduction in strength for beams subjected to hot-cold cycles.</li> <li>Results from hot-cold cycles are quite close to those for long term exposure.</li> <li>The effect of Temperature is more important than humidity in reducing the bonding strength.</li> </ul>
CAN-4	12 beams 102 x 152 x 1220 mm	50	F.T. cycle -18C to +20C (cold room overnight to water bath)	CFRP	- # of CFRP sheet (0,1) - Orientation of sheet (long vs. Transv.) - Freeze-thaw vs. Room Temperature	<ul style="list-style-type: none"> <li>No decrease in ultimate strength due to F.T. cycles</li> <li>Strengthening with CFRP improves strength and ductility.</li> <li>No difference in failure mode when compared with control beams.</li> <li>F.T. cycling affects cracking behavior but does not affect ultimate behavior.</li> </ul>
CAN-5	13 cycliders 150 x 300 mm	50	F.T. cycle same as CAN-4	CFRP	-1 and 2 CFRP wraps -F.T. vs room Temp.	<ul style="list-style-type: none"> <li>CFRP wraps are effective in strengthening concrete columns after exposure to F.T. cycling</li> </ul>

Unidirectional graphite/epoxy composite sheets were made by autoclave-vacuum molding using Newport NCT-301 composite prepeg. Thickness varied from 0.33 mm for 3 layers to 6 mm for 45 layers. Ciba-Geigy's structure epoxy adhesives AW106 and Rp1700-1 were used for the bonding procedure.

Results showed that accelerated environmental exposure by water immersion for 60 days had a slight positive effect on the load bearing capacity. Exposure to hot-cold cycles for 60 days and long term outdoor exposure up to 28 months both reduced the load bearing capacity for about 7%. The authors found that the effect of temperature was more important than humidity. Thus hot-cold cycle was presented as an effective method for accelerated test.

Reference: [CAN-3]

Baumert et al. review in this paper the existing information on the low temperature response of reinforced concrete members strengthened with FRP sheets. It reviews the material behavior of concrete, steel, and FRP at low temperatures, and discusses the observed behavior of reinforced concrete beams, with and without FRP strengthening when subjected to low temperatures.

Experiments on tensile loading of unidirectional FRP at low temperature (Dutta, 1990) have shown that the longitudinal strength of these composites drops at low temperatures. It is generally believed that in unidirectional FRP with a high fiber volume fraction tensile loading is primarily governed by the fiber properties.

To investigate the effect of freeze-thaw cycles, 6 test beams were subjected to 100 freeze/thaw cycles of 20C to -25C before being tested to failure in four point bending at room temperature (Kaiser, 1989). Half of these beams were cracked prior to adhesion of the laminate. During temperature cycling, the frozen beams were thawed by flooding the freezers with water at a temperature of approximately 20C. It was expected that water would enter into cracks and expand with subsequent freezing, resulting in peeling of the laminate. All frozen beams were brought to room temperature before being tested. A comparison of the breaking loads of the frozen beams with the breaking loads of the control beams showed no negative influence on the ultimate load capacity.

Concrete beams strengthened with FRP sheets may increase in strength when subjected to short-term exposure to low temperatures. Long-term exposure of such members must be investigated to determine the effects of creep and aging of the materials.

Reference: [CAN-4]

Soudki and Green present the results of an investigation into the effects of freeze-thaw cycling on the flexural and shear behavior of beams post-strengthened with CFRP sheets. Of twelve rectangular beams with different steel and CFRP reinforcement configuration half were finally subjected to 50 freeze-thaw cycles and half were kept in room temperature. All the beams were finally subject to a 4 point flexural test. Researchers concluded that CFRP sheets are effective in strengthening flexural members exposed to freeze-thaw cycling. CFRP

sheets can be used as external shear and/or flexural reinforcement. Strengthening concrete beams with CFRP sheets improves strength and ductility. Failure modes observed were:

- bond peeling of CFRP sheet (BF).
- rupture of CFRP fibers (FD)

There was no difference in failure mode between beams subjected to freeze-thaw and those at room temperature. Freeze-thaw slightly affected cracking behavior of beams, but does not affect ultimate behavior. Finally, the theoretical predictions compared well with test results.

Reference: [CAN-5]

Soudki and Green present the results of an investigation into the effects of freeze-thaw cycling on the efficiency of using CFRP unidirectional fiber wraps for strengthening circular columns. Thirteen plain concrete circular cylinders (150 x 300 mm) were tested under axial compression loads, seven of them were wrapped with 1 or 2 CFRP sheets. Nine cylinders were subjected to 50 F.T. cycles while the remaining four cylinders were kept at room temperature. Regarding the freeze-thaw test, the cylinders were placed in a cold room at  $-18^{\circ}\text{C}$  for 16 hours (overnight), they were removed in the morning and thawed in a water bath at  $18^{\circ}\text{C}$  for 8 hours. Axial and circumferential strains were measured with strain gages placed on the cylinders after the completion of the 50 freeze-thaw cycles. Test results showed that the CFRP wraps enhance the axial compressive strength through confinement of the concrete in the radial direction. Considering the fact that the unwrapped specimens had a decrease on its axial strength of 46% after 50 F.T. cycles, the CFRP wrap (2 layers) was able to restore the level of strength of the unwrapped specimens at room temperature. The CFRP wraps appear to be efficient in strengthening concrete cylinders after exposure to freeze-thaw cycling in terms of strength, stiffness, and ductility. The wrapped cylinders subjected to freeze-thaw cycling failed in a more catastrophic fashion than those at room temperature.

### 2.1.3. EMPA - Swiss Federal Laboratories for Materials Testing and Research

Reference: [EMPA-1]

Meier reported that when a change of temperature takes place, the differences in the coefficients of thermal expansion of concrete and the carbon fiber composites resulted in thermal stresses at the joints between the two components. After 100 frost cycles ranging from  $+20^{\circ}\text{C}$  to  $-25^{\circ}\text{C}$ , no negative influence on the loading capacity of three post-strengthened beams tested was found.

### 2.1.4. Other Research On Freeze-Thaw

Reference: [XX-9]

Gomez et al. suggested that cycles of freezing and thawing temperatures may magnify the effects of water absorption: the expansion of the freezing water could cause further delamination and interfacial failure.

Two commercially available fiber glass composite coupons were placed in a 2% salt water solution and subjected to 300 cycles of freezing and thawing, with the temperature ranging between  $-17.8^{\circ}\text{C}$  and  $4.4^{\circ}\text{C}$ . Results indicates significant loss(20-30%) in flexural strength, rigidity, and toughness. For only salt water, the percentage reduction was 5-10%.

Reference: [XX-26]

Rahman et al. found that the ultimate tensile strength of Carbon-Glass Fiber Reinforced Plastic (CGFRP) grid (74% glass+26 % carbon) increased by 11 % and the modulus of elasticity by 2.5% when the temperature falls to  $-30^{\circ}\text{C}$ . On the other hand, tensile strength and modulus of elasticity decreased by 9.5% and 2.5%, respectively, when the temperature rose to  $50^{\circ}\text{C}$  from the room temperature.

Reference: [XX-27]

Shulley et. al investigated the durability of five different types of reinforcing fibers (3 carbon and 2 glass) bonded on steel using the wedge-crack extension test. Different types of fibers had different durabilities against different environments. The crack growth was affected by hot water( $65^{\circ}\text{C}$ ) , sea water, aqueous environment, and freeze-thaw (from  $-18^{\circ}\text{C}$  to  $20^{\circ}\text{C}$ ) in the order of importance of environmental effect. A sub-zero environment ( $-18^{\circ}\text{C}$ ) had little effect on crack growth (a slightly positive effects for some fibers).

### 3. EXPERIMENTAL PROGRAM

#### 3.1. Parameters of study

A number of freeze-thaw tests were undertaken on reinforced concrete beams with glued-on CFRP plates. The freeze-thaw equipment was available at the University of Michigan. ASTM C666 procedure B was followed (see Section 3.4: Test Set-up and Instrumentation). The specimens were subjected to up to 300 freeze-thaw cycles. For every parameter, three beams were tested in bending at 0, 100, 200 and 300 cycles.

Parameters investigated were:

- 1) Two different adhesive systems: the Tonen system, which was selected by the technical advisory group as the primary system to be studied, and the Sika system, which represents a feasible alternative.

- 2) Cracking stage. A precracked state simulates the cracking conditions in the field prior to strengthening. It was expected that water would enter into the cracks during the thawing cycle and expand with subsequent freezing, resulting in a more critical situation for the performance of the strengthening system. The influence of the presence of cracks was compared with that of specimens without initial cracks.
- 3) Control specimens (precracked reinforced concrete beams with no CFRP laminate externally glued-on) were also subjected to 0, 100, 200 and 300 cycles.

Table 3.1. presents the summary of the parameters tested.

**Table 3.1 Parameters of the Freeze-Thaw Beam Tests**

Parameters	Number of Freeze-thaw cycles				Total number of specimens (48)
	0	100	200	300	
Control beam (Precracked, no CFRP glued-on)	3	3	3	3	12
Sika System (Precracked beams)	3	3	3	3	12
Tonen System (Precracked beams)	3	3	3	3	12
Tonen System (not precracked beams)	3	3	3	3	12

A total of 48 beams were tested under four-point load.

### 3.2. Material Properties

#### 3.2.1. Concrete

The same type of concrete mix was utilized for the specimens and for the dummy beams that were used for calibration of the freeze-thaw chamber.

Nine mixtures were prepared. The cement used was ASTM Type III high early strength (meets MDOT Standard Specifications) and the fine aggregate had a gradation of 2NS. The coarse aggregate was provided by France Stone Company; its gradation was 26A and its Pit number was 58-9. This aggregate meets MDOT requirements regarding freeze-thaw dilation, with a dilation of 0.008% (MTM 115). The mix proportions (by weight) were:

Cement (ASTM type III) = 1.0 (418 Kg-f/m<sup>3</sup>)

Sand (saturated, surface-dry conditions) = 1.50 (626 Kg-f/m<sup>3</sup>)

Coarse Aggregate (saturated, surface dry conditions) = 2.54 (1062 Kg-f/m<sup>3</sup>)

Water = 0.38 (160 Kg-f/m<sup>3</sup>)

Two additives were used: an air entraining agent, in order to obtain a minimum air content of  $6\% \pm 1.5$  according to MDOT requirements, and a superplasticizer for better workability of the mix during pouring.

The volume of air contained in each mix was measured using a roll-a-meter. The average value obtained was 5% which falls within the admissible range. Compressive strength was obtained by testing cylinders after a curing time of at least 21 days. Average values are presented in Table 3.2.

**Table 3.2 Compression Test Results**

Mix number, Date	Number of cylinders	Date testing	Test data (KN)	$f_c$ (MPa) ave.	$\sqrt{f_c}$ ave.
1, October 30 1997	2	21 days	307.31-193.35	30.88	5.56
2, October 30 1997	2	21 days	250.60-183.66	26.79	5.18
3, Nov. 4 1997	3	46 days	344.28-295.57-330.04	39.88	6.32
4, Nov. 4 1997	4	46 days	166.8-215.28-290.68-288.05	29.65	5.45
5, Nov. 5 1997	3	45 days	236.63-310.25-296.90	34.70	5.89
6, Nov.5 1997	3	45 days	305.58-308.91-241.53	35.20	5.93
7, Nov. 10 1997	2	40 days	278.76-284.23	34.72	5.89
8, Nov. 10 1997	3	40 days	305.58-175.78-191.53	27.67	5.26
9, Nov. 24 1997	3	26 days	264.79-322.08-324.7	38.03	6.17

### 3.2.2. Steel mesh

Different possibilities were considered in order to define the appropriate amount of reinforcement (bending and shear) needed to allow precracking the beams and to guarantee shear capacity once the beams were strengthened with the CFRP laminates. A galvanized steel square welded wire mesh was chosen, with a wire spacing of 25.4 mm x 25.4 mm and a wire diameter of 1.6 mm. Tensile specimens of mesh coupons (304.8 mm long x 50.8 mm wide) were tested in order to obtain its tensile strength. Figure 3.1 presents a typical stress-displacement curve. Average tensile yield stress was found to be 400 MPa. Maximum elongation at failure, measured from machine displacement was 23 mm.

### 3.2.3. Strengthening Systems

#### *3.2.3.1. Tonen System*

The strengthening system was supplied by Master Builders. Its commercial name is: MBrace Composite Strengthening System. It has five components:

- MBrace Primer
- MBrace Putty filler (not used)
- MBrace Saturant Resin
- MBrace Fiber Reinforcement (MBrace CF130 Carbon fiber system)

- MBrace Topcoat (not used)

MBrace Putty filler was not used since it is intended to be used to patch cracks in old concrete and the concrete used did not require this surface preparation. MBrace Topcoat is an optional finishing layer for painting appearance and UV protection. Since the testing of the beams was to be performed indoors, this finishing was not used in this experimental program.

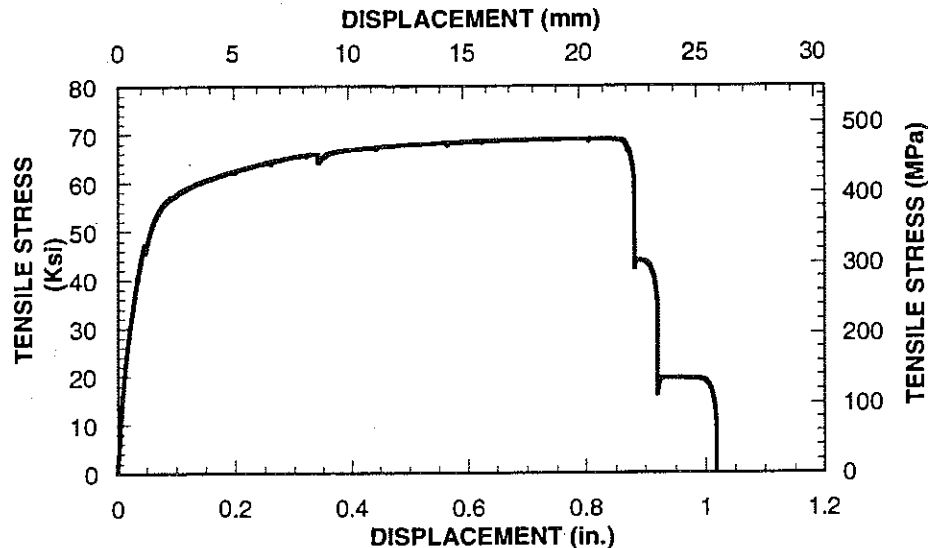


Figure 3.1 Stress-Displacement Curve of the Steel Mesh

Typical Properties of MBrace CF 130 (provided by the supplier):

Fiber Reinforcement: Carbon Fiber, High Tensile

Fiber Density: 1.82 g/cm<sup>3</sup>

Fiber Modulus: 2.35 x 10<sup>6</sup> kg-force/cm<sup>2</sup>

Fiber Areal Weight Density: 300g/m<sup>2</sup>

Sheet Width: 50 cm

Tensile Strength: 590 kg-f/cm-sheet width

35,500 kg-f/cm<sup>2</sup>

Tensile Modulus: 38,800 kg-f/cm-sheet width

2.35 x 10<sup>5</sup> kg-f/cm<sup>2</sup>

Design Thickness: 0.165 mm/ply

Tensile Elongation at ultimate: 1.5%

Typical Properties of MBrace Saturant (i.e., epoxy resin as called by the supplier):

Volatile Organic Compounds: 20 g/liter

Flash Point: 72°C

Mixed Viscosity @ 20°C: 1,600 cps

Color: Blue

Weight/Gallon: 1.04±0.024 kg/L

Shelf Life @ 20°C : 18 months

Flexural Strength: 43 MPa  
 Tensile Strength: 78 MPa  
 Compressive Strength: 88 MPa  
 Work Time @ 20°C : 30 minutes

Typical Properties of MBrace Primer (i.e., primer resin as called by the supplier):

Generic type: Amine-cured liquid epoxy  
 Solids content: 100%  
 Color: clear Amber  
 Weight/Gallon: Part A 1139g/L  
                   Part B 996 g/L  
 Tensile Strength: 13 to 15.8 MPa  
 Tensile Modulus (Tangent): 689 to 826.8 MPa  
 Tensile elongation: 20-30%  
 Tensile bond strength (steel): 17 MPa  
 Work Time @ 20°C : 45 hours

*3.2.3.2. Sika System*

The Sika Company provided the Carbodur strengthening system. Components of this system are:

- Sika Carbodur CFRP (Carbon fiber laminate strips).
- Sikadur 30 (epoxy adhesive).

Typical Properties of Sika CFRP Strips (provided by the supplier):

Tensile Strength: 2,400 MPa  
 Modulus of Elasticity: 150 x10<sup>3</sup> MPa  
 Density: 1.6 g/cm<sup>3</sup>  
 Thickness: 1.2 mm  
 Sheet width: 50 or 80 mm  
 Elongation at ultimate: 1.4%

Typical Properties of Sikadur 30(provided by the supplier):

Application Temperature: 18-30°C  
 Pot Life @23°C : 70 min  
 Compressive Strength (14 day) >58.6 MPa  
 Shear Strength: 24.8 MPa  
 Tensile Strength @7 day: 24.8 MPa  
 Elongation at break: 1%

### 3.3. Design and Fabrication of Specimens

Typical freeze-thaw test of concrete beams according to ASTM C-666 requires beams of dimensions 76 mm x 76 mm x 406 mm (ASTM C666). For this particular freeze-thaw test and considering that the beams were to be tested under flexural loads, the dimensions of the reinforced concrete beams for the freeze-thaw tests was 76 mm x 76 mm x 1016 mm, see Figure 3.2.

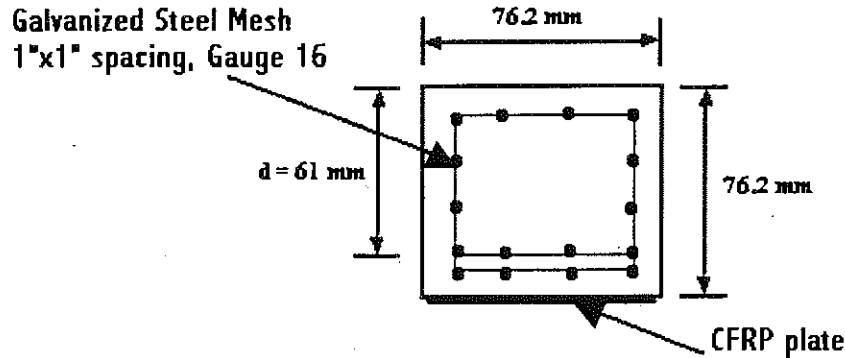


Figure 3.2 Reinforcement Detail of the Cross Section

Prior investigators ([X-27], [EMPA-1], [CAN-3], [CAN-4]) have indicated that the freeze-thaw cycles had little effect on the CFRP laminate itself. However, the bond strength at the interface between the concrete and the CFRP seems to be the controlling parameter.

The reinforced concrete beams were designed with enough longitudinal reinforcement to support the precracking load without failure. The width and length of the CFRP sheet for both systems was calculated assuming that once the interface between the concrete and the CFRP reaches the value of the shear bond strength of the concrete ( $0.17\sqrt{f_c}$ ), peeling off of the CFRP laminate will occur, see Appendix A. A width of 76.2 mm for the CFRP was used for the Tonen system and 80 mm was used for the Sika system.

For the Tonen system, a minimum value of development length of 371 mm was found to be necessary in order to prevent interfacial failure between the CFRP sheet and the concrete surface, leading to a peeling-off of the CFRP. However because the objective of this project was to evaluate the influence of the freeze-thaw cycles on bond, a shorter length was selected namely 254 mm as the development length for the CFRP sheet. The total length of the CFRP was 660 mm (see Figure 3.3).

For the Sika system, the minimum value of development length calculated was 872 mm. Following the same line of thought presented above, a smaller value (356 mm) was adopted. The total length of the CFRP was 864 mm.

The moment capacity for each system was different since the Sika laminate provides almost 5 times the tensile load of the Tonen laminate per unit width. From Appendix A it can be seen that the moment capacity of the reinforced concrete beam strengthened with the Sika plate system is 1.7 times the moment capacity for the reinforced concrete beam strengthened with the Tonen sheet system. This difference will be considered in the analysis of the test results.

For the fabrication of the specimens, plexiglass molds were utilized in order to obtain a smooth surface finish. The steel mesh was placed inside the molds leaving a 13 mm cover around the perimeter of the cross section (see Figure 3.2). Thermocouples were installed in three dummy beams and three specimens. Once the specimens were installed in the freeze-thaw chamber, the thermocouples provided information to the computerized controller to adjust the conditions inside the freeze-thaw chamber in order to meet the target profile.

The concrete was mixed in a laboratory concrete mixer. All specimens were removed from their molds 24 hours after pouring, and were placed in a water tank for 21 days. Specimens that were placed in the freeze-thaw chamber had at least 3 weeks of age.

### 3.4. Test Set-Up and Instrumentation

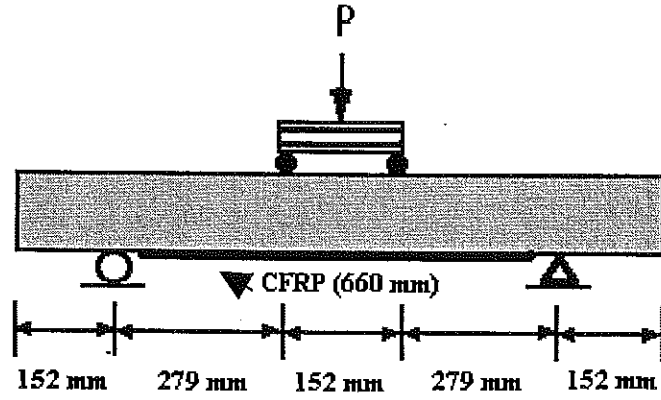
#### 3.4.1. Freeze-Thaw Cycles

As mentioned in the introduction, the freeze-thaw equipment available at the University of Michigan allowed exposure as per ASTM C666, Procedure B requirements. The freeze-thaw machine was programmed to run freeze-thaw cycles according to the Michigan Test Method for Testing Concrete for Durability by Rapid Freezing in Air and Thawing in Water (MTM 115-97). This method conforms to the general requirements of ASTM C666, Procedure B.

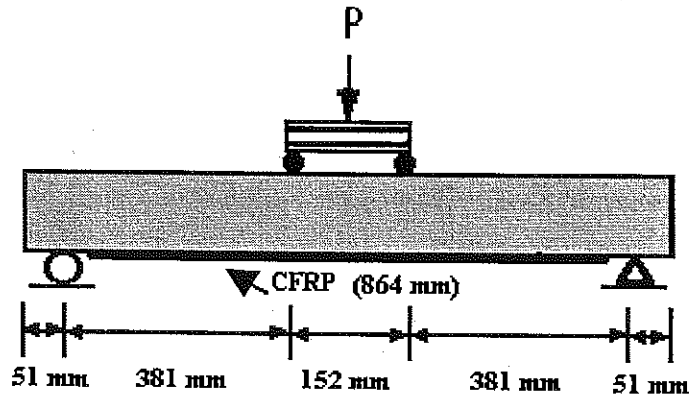
The nominal freezing and thawing cycle for this method consisted of alternately lowering the temperature of the specimens from 4.4°C to -17.8°C and raising it from -17.8°C to 4.4°C within the temperature limitations of ASTM C666. The nominal cycle length was 3 hours. Figure 3.4 shows a schematic representation of the freeze-thaw test.

The freeze-thaw machine was programmed with a profile defined to follow, as close as possible, the nominal freezing and thawing cycle adopted by MDOT. The profile was tried using 24 dummy beam specimens. Once the profile was tested with the dummy beams and showed compliance with MDOT requirements, the "real" specimens were tested. Figure 3.5 presents the readings from the freeze-thaw machine after its calibration.

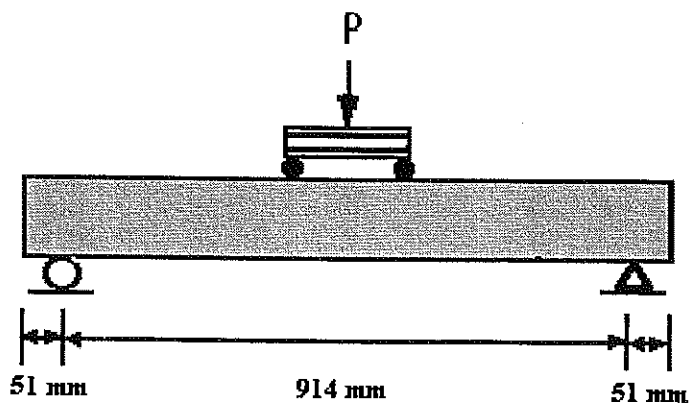
After 100, 200 and 300 number of freeze-thaw cycles, 12 specimens were removed each time from the chamber and placed into a water tank at room temperature until the time of flexural testing.



Tonen System: Load Set-Up



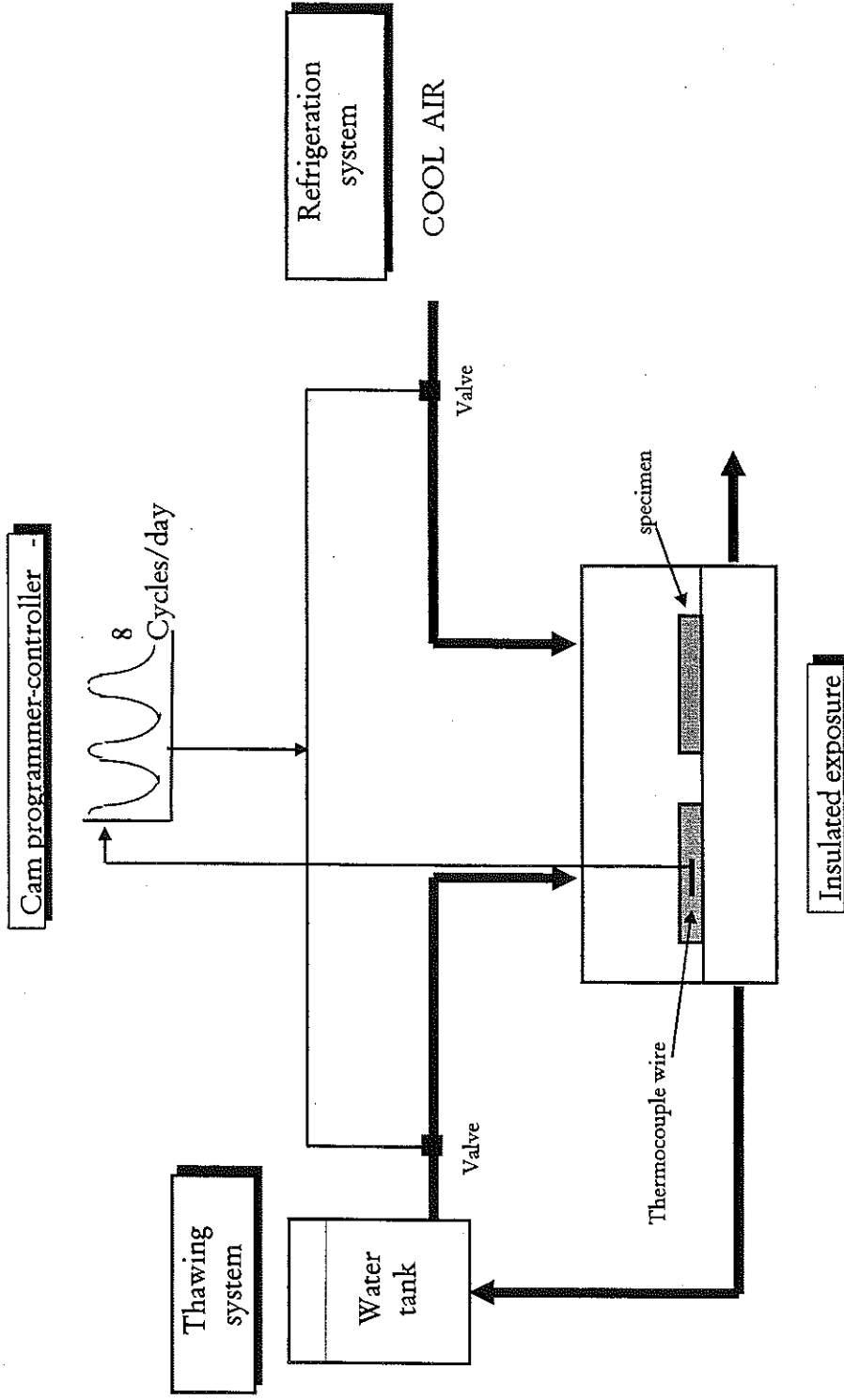
Sika System: Load Set-Up



Control Beams: Load Set-Up

Figure 3.3 Flexural Test Load Set-up

Figure 3.4 Schematic Representation of the Freeze-Thaw Test (ASTM C666-procedure B)



The use of the water tank was suggested by the TAG to guarantee 100% wet conditions at the time of testing. The age of the specimens at the time of the flexural test was at least 4 weeks.

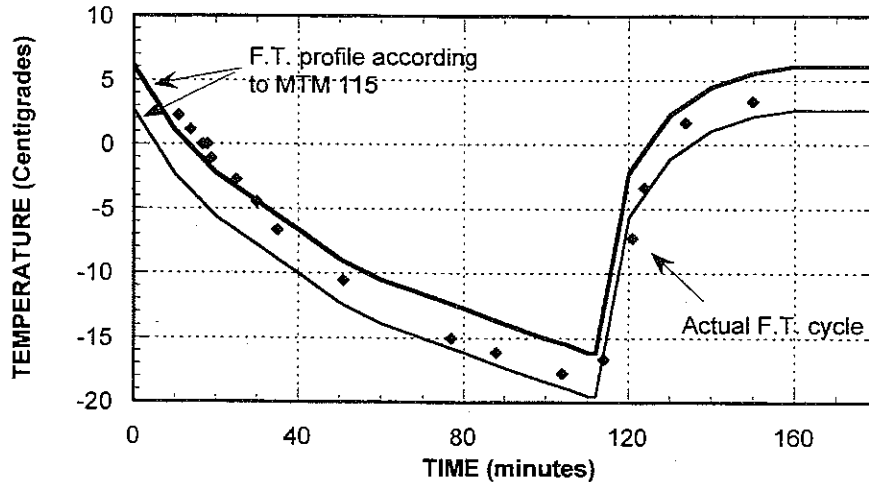


Figure 3.5 Freeze-Thaw Profile Applied

#### 3.4.2. Bending Test

All the specimens were tested at room temperature under four-point load in an INSTRON testing Machine, Model 4206, with a load cell of 133,000 N capacity. The specimens were tested under displacement control. The rate of loading was 0.25 mm/min. Applied loads and displacements were recorded from the load cell and the crosshead of the machine. The bending tests were also video taped. Pictures were taken during and at the end of each test. Some photos of failure modes are shown in appendix D.

## 4. TEST RESULTS

A total of 48 beams were tested under 4 point bending. The applied loads versus displacements were recorded and the type of failure observed.

Table 4.1 presents a summary of these results: Peak load, deflection at failure, and type of failure are reported for each beam tested. Table 4.2 presents the values of maximum shear force and maximum moment at failure.

Figures 4.1, 4.2, 4.3 and 4.4 present typical load-displacement curves for the Sika and Tonen systems at 0, 100, 200 and 300 freeze-thaw cycles, respectively. Figure 4.5 to 4.7 present load-displacement curves for the Tonen precracked, Tonen not precracked and Sika precracked beams.

Table 4.1 Summary of the Test Results

Number of Cycles	Parameter	Peak Load (KN)	Deflection at Failure (mm)	Delamination Length (mm)	Type of Failure
0 cycles	No CFRP (precracked beam)	2.65	7.62	0.00	Yield and fracture of reinforcement
		2.52	7.11	0.00	Yield and fracture of reinforcement
		2.64	8.03	0.00	Yield and fracture of reinforcement
	Tonon sheet (precracked beam)	19.54	10.85	101.60	Shear-delamination (crack at 30° angle)
		20.49	12.37	279.40	Shear-delamination.
		19.90	11.15	69.85	Shear-delamination.
	Tonon sheet (non-precracked)	16.79	9.50	196.85	Flexure-delamination
		17.81	9.96	165.10	Flexure-delamination
		17.04	9.55	139.70	Flexure-delamination
	Sika sheet (precracked beam)	22.02	8.76	0.00	Shear (crack length = 178 mm)
		21.29	8.10	0.00	Shear
		23.99	9.58	254.00	Shear-delamination
100 cycles	No CFRP (precracked beam)	2.85	7.62	0.00	Yield and fracture of reinforcement
		2.81	7.11	0.00	Yield and fracture of reinforcement
		2.73	9.65	0.00	Yield and fracture of reinforcement
	Tonon sheet (precracked beam)	16.09	9.65	127.00	Shear-delamination (45° angle)
		15.81	9.91	152.40	Shear-delamination
		15.93	9.65	165.10	Shear-delamination-flexure (50° angle)
	Tonon sheet (non-precracked)	16.46	10.16	152.40	Shear-delamination
		16.46	9.40	177.80	Shear-delamination
		10.98	8.64	139.70	Shear-delamination
	Sika sheet (precracked beam)	19.55	7.11	0.00	Shear (crack length = 229 mm)
		20.39	7.87	0.00	Shear (crack length = 229 mm)
		20.18	7.62	0.00	Shear
200 cycles	No CFRP (precracked beam)	2.94	6.86	0.00	Yield and fracture of reinforcement
		2.96	6.86	0.00	Yield and fracture of reinforcement
		2.53	7.62	0.00	Yield and fracture of reinforcement
	Tonon sheet (precracked beam)	15.40	6.10	139.70	Shear-delamination (40° angle)
		13.34	6.86	0.00	Shear-delamination
		13.78	7.62	215.90	Shear-delamination (60° angle)
	Tonon sheet (non-precracked)	14.06	7.37	139.70	Flexure-delamination
		13.34	7.37	177.80	Shear-delamination (45° angle)
		14.44	7.62	203.20	Flexure-delamination (75° angle)
	Sika sheet (precracked beam)	19.57	7.62	203.20	Delamination-flexure (25° angle)
		19.64	7.37	241.30	Delamination-shear (45° angle)
		19.49	7.62	0.00	Shear (crack length = 203 mm)
300 cycles	No CFRP (precracked beam)	2.94	6.35	0.00	Yield and fracture of reinforcement
		2.49	6.35	0.00	Yield and fracture of reinforcement
		2.75	6.10	0.00	Yield and fracture of reinforcement
	Tonon sheet (precracked beam)	12.66	6.86	177.80	Flexure-delamination
		12.45	6.35	165.10	Flexure-delamination
		12.13	6.35	190.50	Shear-delamination (40° angle)
	Tonon sheet (non-precracked)	13.22	7.87	152.40	Shear-delamination
		14.52	7.62	177.80	Shear-delamination (35° angle)
		13.74	8.13	0.00	Shear-delamination
	Sika sheet (precracked beam)	21.88	8.64	177.80	Shear-delamination (35° angle)
		21.33	8.38	241.30	Shear-delamination flexure (25° angle)
		21.14	7.62	254.00	Flexure-delamination (30° angle)

Table 4.2 Maximum Shear Force and Moment

Number of Cycles	Parameter	Shear Force (KN)	Max. Moment (KN-m)	Type of Failure
0 cycles	No CFRP (precracked beam)	1.33	0.51	Yield and fracture of reinforcement
		1.26	0.48	Yield and fracture of reinforcement
		1.32	0.50	Yield and fracture of reinforcement
	Tonen sheet (precracked beam)	9.77	2.73	Shear-delamination (crack at 30° angle)
		10.25	2.86	Shear-delamination.
		9.95	2.78	Shear-delamination.
	Tonen sheet (non-precracked)	8.40	2.35	Flexure-delamination
		8.90	2.49	Flexure-delamination
		8.52	2.38	Flexure-delamination
	Sika sheet (precracked beam)	11.01	4.20	Shear (crack length = 178 mm)
		10.65	4.06	Shear
		12.00	4.57	Shear-delamination
100 cycles	No CFRP (precracked beam)	1.42	0.54	Yield and fracture of reinforcement
		1.41	0.54	Yield and fracture of reinforcement
		1.37	0.52	Yield and fracture of reinforcement
	Tonen sheet (precracked beam)	8.05	2.25	Shear-delamination (45° angle)
		7.91	2.21	Shear-delamination
		7.97	2.23	Shear-delamination-flexure (50° angle)
	Tonen sheet (non-precracked)	8.23	2.30	Shear-delamination
		8.23	2.30	Shear-delamination
		5.49	1.55	Shear-delamination
	Sika sheet (precracked beam)	9.78	3.72	Shear (crack length = 229 mm)
		10.19	3.88	Shear (crack length = 229 mm)
		10.09	3.85	Shear
200 cycles	No CFRP (precracked beam)	1.47	0.56	Yield and fracture of reinforcement
		1.48	0.56	Yield and fracture of reinforcement
		1.27	0.48	Yield and fracture of reinforcement
	Tonen sheet (precracked beam)	7.70	2.15	Shear-delamination (40° angle)
		6.67	1.86	Shear-delamination
		6.89	1.93	Shear-delamination (60° angle)
	Tonen sheet (non-precracked)	7.03	1.96	Flexure-delamination
		6.67	1.86	Shear-delamination (45° angle)
		7.22	2.02	Flexure-delamination (75° angle)
	Sika sheet (precracked beam)	9.79	3.73	Delamination-flexure (25° angle)
		9.82	3.74	Delamination-shear (45° angle)
		9.75	3.71	Shear (crack length = 203 mm)
300 cycles	No CFRP (precracked beam)	1.47	0.56	Yield and fracture of reinforcement
		1.25	0.47	Yield and fracture of reinforcement
		1.37	0.52	Yield and fracture of reinforcement
	Tonen sheet (precracked beam)	6.33	1.77	Flexure-delamination
		6.22	1.74	Flexure-delamination
		6.07	1.69	Shear-delamination (40° angle)
	Tonen sheet (non-precracked)	6.61	1.85	Shear-delamination
		7.26	2.03	Shear-delamination (35° angle)
		6.87	1.92	Shear-delamination
	Sika sheet (precracked beam)	10.94	4.17	Shear-delamination (35° angle)
		10.68	4.07	Shear-delamination flexure (25° angle)
		10.57	4.02	Flexure-delamination (30° angle)

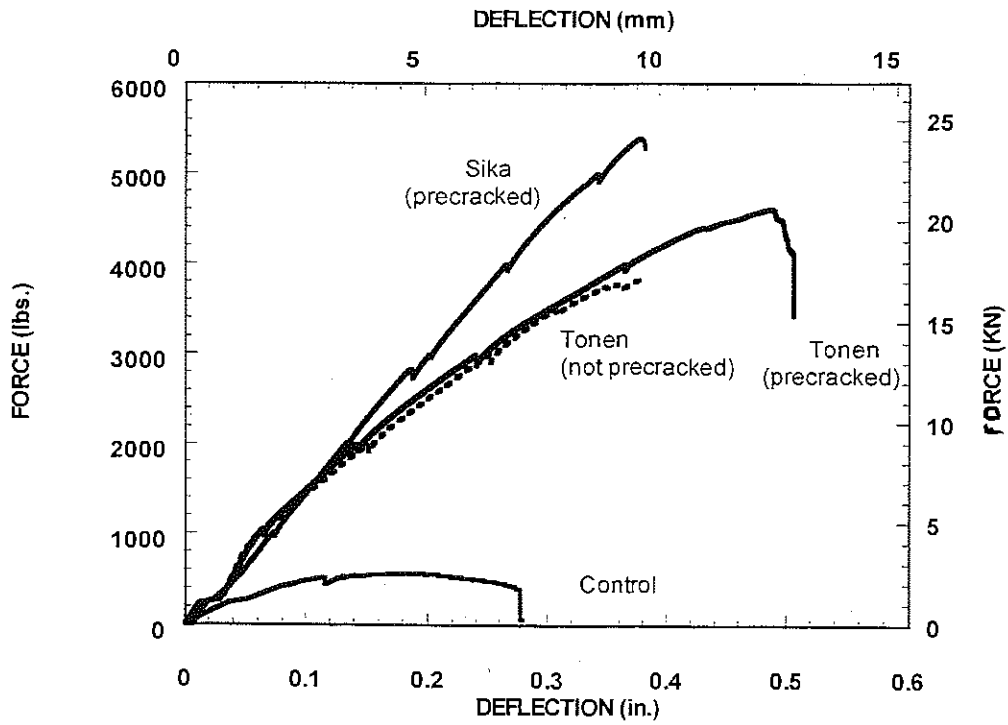


Figure 4.1 Load-Deflection Curves for 0 F.T. Cycles

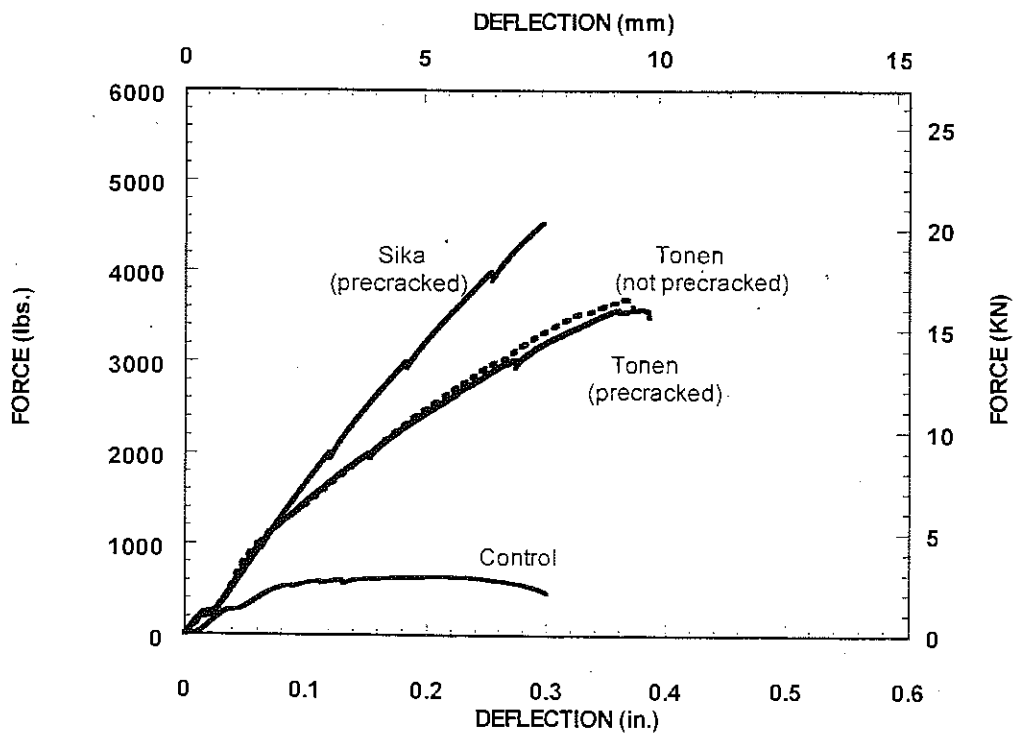


Figure 4.2 Load-Deflection Curves for 100 F.T. Cycles

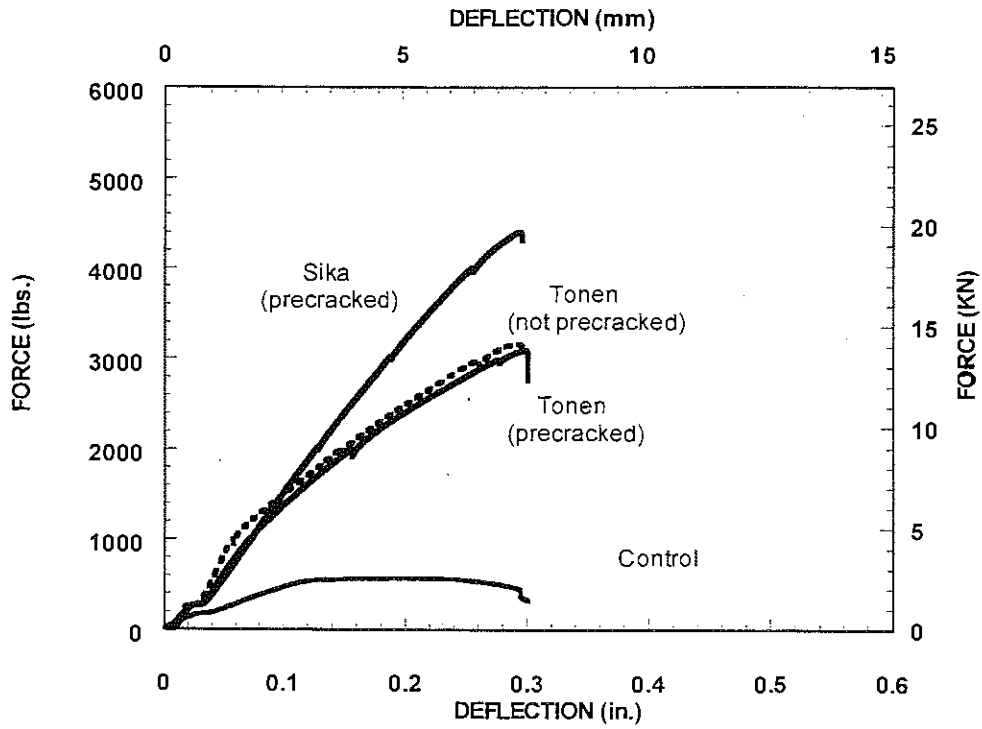


Figure 4.3 Load-Deflection Curves for 200 F.T. Cycles

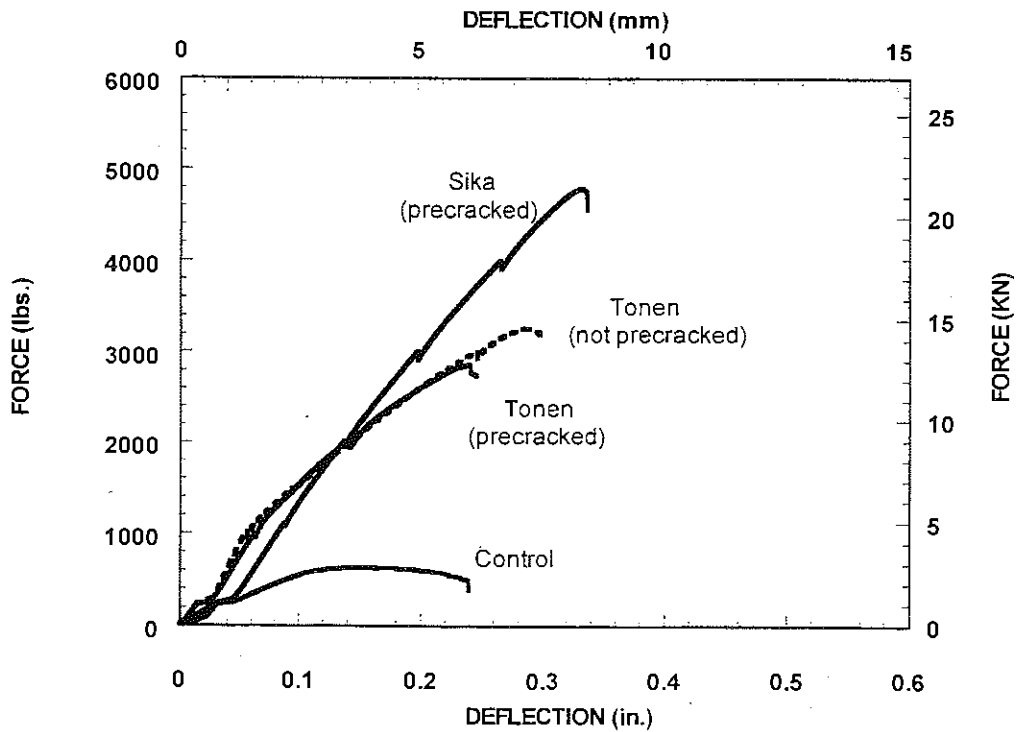


Figure 4.4 Load-Deflection Curves for 300 F.T. Cycles

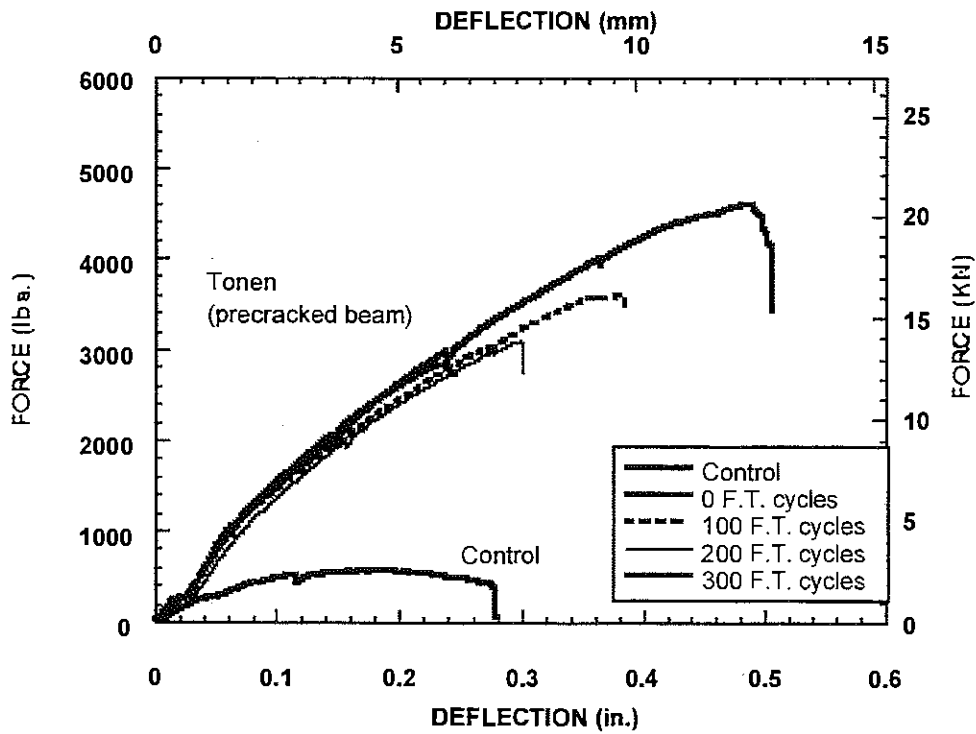


Figure 4.5 Load-Deflection Curves for Tonen Precracked Beams

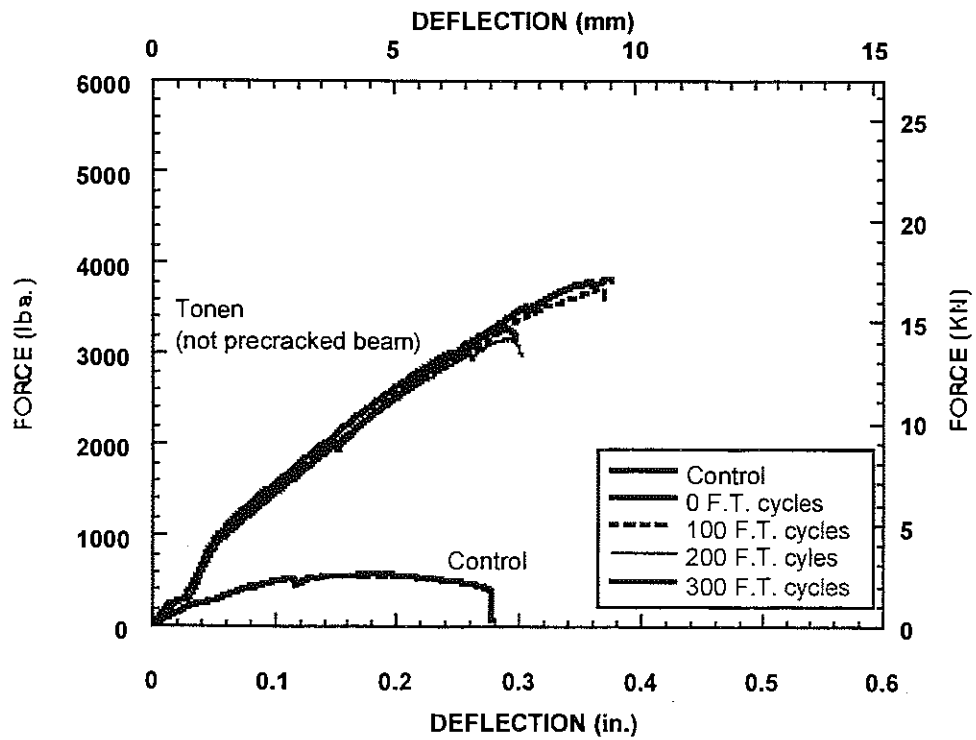


Figure 4.6 Load-Deflection Curves for Tonen Not Precracked Beams

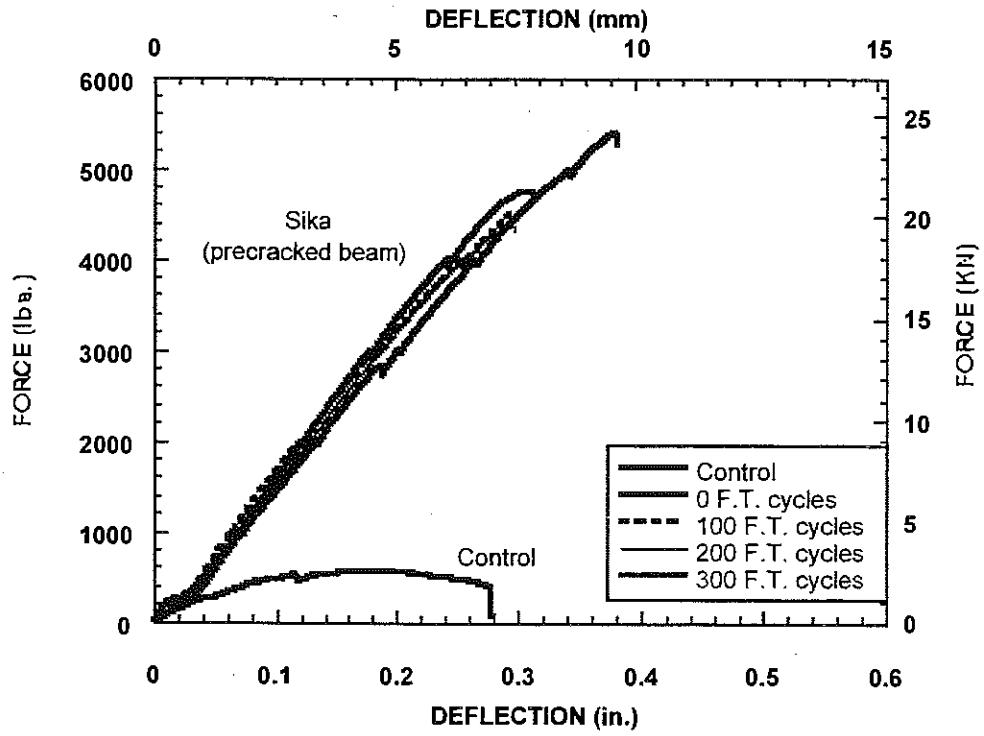


Figure 4.7 Load-Deflection Curves for Sika Precracked Beams

## 5. ANALYSIS AND INTERPRETATION

As was indicated in section 3.3 the specimens were designed in a way to make failure by debonding of the CFRP likely. Therefore, beams reinforced by the Tonen and the Sika system had a different reinforcement ratios and were expected to have different levels of moment capacity but failure was expected to occur by the CFRP peeling-off. Both delamination length and the corresponding type of failure observed in each test are analyzed.

It is expected that this analysis will indicate how the bond strength and development length of the CFRP laminates are affected by the number of freeze-thaw cycles.

### 5.1. Failure Modes

Four different types of failure mode were found during the testing of the 48 beams:

1. Yielding and immediate fracture of the steel mesh reinforcement at the tension level of the beam. This type of failure is characteristic of under-reinforced beams (control beams with no CFRP).
2. The CFRP delaminates at the interface with the concrete surface. This interfacial failure started at a flexural crack (flexure-delamination).
3. CFRP delaminates at the interface with the concrete surface. This interfacial failure started at a shear crack (shear-delamination).
4. Vertical shear failure of the reinforced beam at the end of the CFRP laminate (shear).

Figure 5.1 shows the different types of failure mode. Table 5.1 also presents the type of failure observed for each specimen tested.

For the Tonen precracked beams, a very uniform pattern was observed. All the specimens at 0, 100 and 200 F.T. cycles failed by shear-delamination. For 300 F.T. cycles, two beams failed by flexure-delamination and one failed by shear delamination.

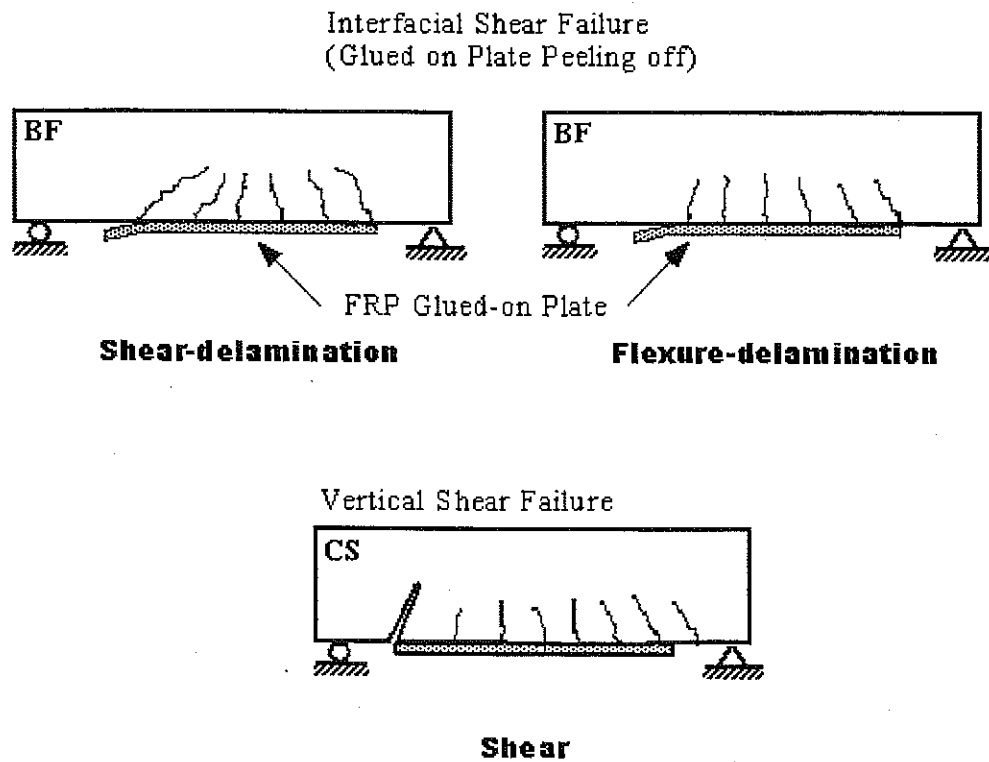
For the Tonen non-precracked beams, the type of failure was also consistent, all the specimens failed by delamination. For all the specimens at 0 F.T. cycles, flexure-delamination occurred. For the specimens at 100 and 300 F.T. cycles, shear-delamination occurred. At 200 F.T. cycles, two beams failed by flexure-delamination and one failed by shear-delamination.

For the Sika precracked beams, the pattern was not as uniform. For the specimens at 0 F.T. cycles, two beams failed by shear and one beam failed by shear-delamination. At 100 F.T. cycles, all the beams failed by shear. For the specimens at 200 F.T. cycles, each beam failed in a different failure mode (shear, shear-delamination, flexure-delamination). Finally, for the specimens at 300 F.T. cycles, two beams failed by shear-delamination and one by flexure-delamination.

It was important to find a possible correlation between each type of failure and the strength of the beams strengthened with the Sika or the Tonen system. It was also important to discover the influence of the number of freeze-thaw cycles on the bond strength.

Table 5.1 Values of Normalized Maximum Shear Stress

Number of cycles	Parameter	Shear Force (KN)	$\sqrt{f_c}$ ( $\sqrt{\text{MPa}}$ )	Normalized Shear Stress $V_n$	Type of Failure
0 cycles	No CFRP (precracked beam)	1.33	5.89	0.04	Yield and fracture of reinforcement
		1.26	5.18	0.04	Yield and fracture of reinforcement
		1.32	5.89	0.04	Yield and fracture of reinforcement
	Tonen sheet (precracked beam)	9.77	5.18	0.32	Shear-delamination (crack at 30° angle)
		10.25	5.93	0.30	Shear-delamination.
		9.95	5.18	0.33	Shear-delamination.
	Tonen sheet (non-precracked)	8.40	6.17	0.23	Flexure-delamination
		8.90	6.17	0.25	Flexure-delamination
		8.52	6.17	0.24	Flexure-delamination
	Sika sheet (precracked beam)	11.01	5.89	0.32	Shear (crack length = 178 mm)
		10.65	5.18	0.35	Shear
		12.00	5.18	0.40	Shear-delamination
100 cycles	No CFRP (precracked beam)	1.42	5.93	0.04	Yield and fracture of reinforcement
		1.41	5.93	0.04	Yield and fracture of reinforcement
		1.37	5.89	0.04	Yield and fracture of reinforcement
	Tonen sheet (precracked beam)	8.05	5.89	0.24	Shear-delamination (45° angle)
		7.91	5.89	0.23	Shear-delamination
		7.97	5.89	0.23	Shear-delamination-flexure (50° angle)
	Tonen sheet (non-precracked)	8.23	5.89	0.24	Shear-delamination
		8.23	5.89	0.24	Shear-delamination
		5.49	5.89	0.16	Shear-delamination
	Sika sheet (precracked beam)	9.78	5.89	0.29	Shear (crack length = 229 mm)
		10.19	5.93	0.30	Shear (crack length = 229 mm)
		10.09	5.93	0.29	Shear
200 cycles	No CFRP (precracked beam)	1.47	5.44	0.05	Yield and fracture of reinforcement
		1.48	5.44	0.05	Yield and fracture of reinforcement
		1.27	5.44	0.04	Yield and fracture of reinforcement
	Tonen sheet (precracked beam)	7.70	5.56	0.24	Shear-delamination (40° angle)
		6.67	6.17	0.19	Shear-delamination
		6.89	5.56	0.21	Shear-delamination (60° angle)
	Tonen sheet (non-precracked)	7.03	5.44	0.22	Flexure-delamination
		6.67	5.44	0.21	Shear-delamination (45° angle)
		7.22	5.44	0.23	Flexure-delamination (75° angle)
	Sika sheet (precracked beam)	9.79	5.44	0.31	Delamination-flexure (25° angle)
		9.82	5.18	0.33	Delamination-shear (45° angle)
		9.75	5.44	0.31	Shear (crack length = 203 mm)
300 cycles	No CFRP (precracked beam)	1.47	6.31	0.04	Yield and fracture of reinforcement
		1.25	6.31	0.03	Yield and fracture of reinforcement
		1.37	5.44	0.04	Yield and fracture of reinforcement
	Tonen sheet (precracked beam)	6.33	5.56	0.20	Flexure-delamination
		6.22	5.56	0.19	Flexure-delamination
		6.07	5.56	0.19	Shear-delamination (40° angle)
	Tonen sheet (non-precracked)	6.61	5.89	0.19	Shear-delamination
		7.26	6.31	0.20	Shear-delamination (35° angle)
		6.87	5.89	0.20	Shear-delamination
	Sika sheet (precracked beam)	10.94	5.18	0.36	Shear-delamination (35° angle)
		10.68	5.18	0.36	Shear-delamination flexure (25° angle)
		10.57	5.18	0.35	Flexure-delamination (30° angle)



Notes:

Flexure-delamination: CFRP peeling-off started at a flexural crack

Shear-delamination: CFRP peeling-off caused by shear cracks

Shear: Shear failure of the reinforced beam at the end of the CFRP laminate

**Figure 5.1 Failure Modes for Specimens with CFRP Plates**

## 5.2. Shear Strength

The design calculations for the specimens showed proximity of the shear failure load to the CFRP peeling-off (delamination) load, particularly with the Sika system. It was expected that if the specimen did not fail by delamination, shear failure would immediately follow.

As stated before, for the control specimens the failure was by fracture of the steel mesh following yielding of the reinforcement. This type of failure was in accordance with the under reinforced nature of the beam. The values obtained for shear force for the control specimens were very close (average = 1.37 KN), showing them to be indifferent to the influence of the number of freeze-thaw cycles. However, a decrease of 17% in the deflection at failure was observed after 300 freeze-thaw cycles.

For the strengthened specimens, the first step in the analysis process was to compare the values of maximum shear force and displacement versus number of freeze-thaw cycles. For the Tonen system (precracked and non-precracked beams) it was clear that there was a decrease in the value of the shear force as well as the maximum deflection with an increase in the number of freeze-thaw cycles. However, this behavior did not seem to be so obvious for the Sika specimens. Contribution of the different types of failure modes and the strength of the concrete of each mix should be evaluated more accurately such as is presented next.

By the traditional theory for *homogeneous, elastic, uncracked* beams, shear stresses,  $v$ , can be calculated using the equation:

$$v = \frac{V \times Q}{I \times b} \quad (1)$$

where  $V$  is the vertical shear force on the cross section;  $Q$  is the moment of inertia of the cross section,  $Q$  is the first moment about the neutral axis of the part of the cross-sectional area above the point where the shear stresses are being calculated and  $b$  is the width of the member. However, because the reinforced concrete beam at the failure load is beyond the elastic range and it is a cracked section, equation 1 is not accurate to calculate shear stresses.

ACI design equation (11-3) computes the shear strength provided by the concrete as:

$$V_c = 0.17\sqrt{f_c} bd \quad (\text{SI units}) \quad (2)$$

where  $V$  is the vertical shear force,  $b$  the thickness of the web and  $d$  is the distance of the area of tensile steel to the maximum compression strain. ACI considers the shear strength to be based on an average shear stress on the full effective cross section  $b*d$  (see commentary R11.1). The average shear stress of the concrete is therefore equal to  $0.17 \sqrt{f_c}$ . Based on this idea, average shear stress can be taken as:

$$v = \frac{V}{b \times d} \quad (3)$$

However, since the CFRP has a significant contribution to the force equilibrium of the section, the real position of "d" is located near the centroid of the laminate. Therefore, the use of "h" instead of "d" in the calculation of the  $v$  will give a more accurate evaluation of the shear stress:

$$v = \frac{V}{b \times h} \quad (4)$$

In order to eliminate the contribution of the strength of the concrete mix, normalized shear stresses ( $v_n$ ) were calculated from the original data. The shear force obtained from the experimental data was divided by the square root of the compressive strength ( $\sqrt{f_c}$ ) times the width ( $b = 76.2$  mm) times the height of the beam ( $h = 76.2$  mm):

$$v_n = \frac{V}{b \times h \times \sqrt{f_c}} \quad (5)$$

In the calculation of  $v_n$ ,  $v$  was normalized with respect to  $f_c$  in order to be able to compare its value with the assumed design shear strength of concrete ( $0.17\sqrt{f_c}$ , MPa). Table 5.1 presents the values of normalized shear stresses for each specimen. Figures 5.2, 5.3, and 5.4 show the normalized shear stress at failure versus number of freeze-thaw cycles for each strengthening system. Figure 5.5 compares the average values of normalized shear stresses at failure.

For the Tonen System, the normalized maximum shear stress ( $v_n$ ) decreased with an increase number of freeze-thaw cycles. For the beams with precracking, the decrease in stress was more significant (26% for 100 F.T. cycles, 32% for 200 F.T. cycles, and 39% for 300 F.T. cycles on the average) than for the non cracking beams (11% for 100 F.T. cycles, 9% for 200 F.T. cycles, and 22% for 300 F.T. cycles).

For the Sika system a more irregular pattern was presented. Comparing the average value of normalized maximum shear stress at 0 freeze-thaw cycles, a decrease of 18% was obtained for 100 F.T. cycles, 12% for 200 F.T. cycles, and 0% for 300 F.T. cycles. It is expected that a more consistent pattern will be obtained if discrimination is made with respect to the type of failure.

For all the tests observed, values were higher than 0.17 for the normalized shear stress.

As is shown in appendix B, this normalized shear stress is only an indirect measure of the value of horizontal interfacial shear stress at the level of the CFRP laminate. However, in order to find the exact value of the interfacial shear stress ( $\tau$ ) that leads to delamination failure, another set of experiment should be carried out. The effect of freeze-thaw cycles and the shear capacity of the specimens are variables that influence interfacial shear strength and should be weighted. For this report, the normalized shear stress ( $v_n$ ) will be used to measure indirectly the influence of the freeze-thaw cycles on the bond strength of the specimens tested.

Normalized shear stresses decreased with an increasing number of freeze-thaw cycles for the Tonen precracked beams. Maximum and minimum values of normalized shear stress for the specimens were 0.32 and 0.19. For the Tonen system without precracking, the maximum and minimum values of normalized shear stress were closer: 0.25 and 0.19.

For the Sika system with precracked beams, maximum and minimum values of normalized shear stress were 0.40 and 0.29.

For the control specimens, the average value of normalized shear stress was 25% of the design value and was indifferent to the number of freeze-thaw cycles. This low value was related to

the type of failure (yielding of reinforcement) showing that the control beams did not develop their maximum capacity in shear.

It can be concluded that the values of normalized shear stress were higher than 0.19 for the Tonen system and 0.29 for the Sika system. In no case was the value of 0.40 surpassed.

Yoshizawa et al. [FTS-5] have found that the bond strength of the CFRP sheets increases with an increase in the number of CFRP layers. From appendix A, preliminary design of the beam capacity with Tonen and Sika system indicated that the moment capacity of the beam with Sika system was 1.7 higher than the moment capacity of the beam with the Tonen system. From the experimental data analyzed above, it was found that for each number of F.T. cycles, the values of normalized shear stress for the Sika system were always higher than the ones for the Tonen system, corroborating Yoshizawa et al.' statement [FTS-5].

Considering the different failure modes, it was observed that for the Tonen system with precracking the values of normalized shear stress were higher for the flexure-delamination failure than for the shear-delamination for the same number of freeze-thaw cycles, see Figure 5.2. This result can be explained if it is assumed that in the flexure-delamination failure, the CFRP laminate can still carry tensile load between the flexural cracks whereas for the shear-delamination failure, the effect of a diagonal crack accelerate the interfacial crack propagation. Researchers at Ibaraki University [XX-46] described a similar phenomenon. However, the overall pattern of decrease of strength was followed no matter what type of failure was considered. It can be concluded that for the Tonen system with precracking, an increasing number of freeze-thaw cycles led to a decrease in the shear capacity of 39% for 300 F.T. cycles ( $\bar{v}_n=0.19$ ).

In the Tonen system without precracking, the values of normalized shear stress were also higher for the flexure-delamination failure than for the shear-delamination for the same number of freeze-thaw cycles, see Figure 5.3. There was also a consistent decrease in strength with an increase in the number of freeze-thaw cycles. It can be concluded that for this set of specimens an increase in number of freeze-thaw cycles led to a 22% decrease in the shear capacity for 300 F.T. cycles ( $v_n=0.20$ ).

For the Sika system with precracking, the occurrence of vertical shear failure was considered a premature failure that did not allow measuring the effect of the freeze-thaw cycles on the bond strength of the CFRP glued-on system. Considering only the values for shear-delamination and flexure-delamination, it was observed that the decrease in strength was 10% for 300 F.T. cycles whereas a decrease of 20% was observed after 200 freeze-thaw cycles (see Figure 5.4).

For the Tonen system a precracking stage influences the decrease in strength due to the effect of the freeze-thaw cycles. A decrease of the average shear stress of 22% for 300 freeze-thaw cycles was obtained for the non-precracked beams whereas for the precracked beams this value was 39%. However the average value for the normalized shear stress at 300 freeze-thaw cycles for both conditions was very close:  $v_n=0.20$  for precracked beams, and  $v_n=0.19$  without precracking. It can be shown that at 0 F.T. cycles the cracking condition influences the capacity of the beam, whereas after 300 F.T. cycles, the freezing and thawing effect dominates, see Figure 5.5.

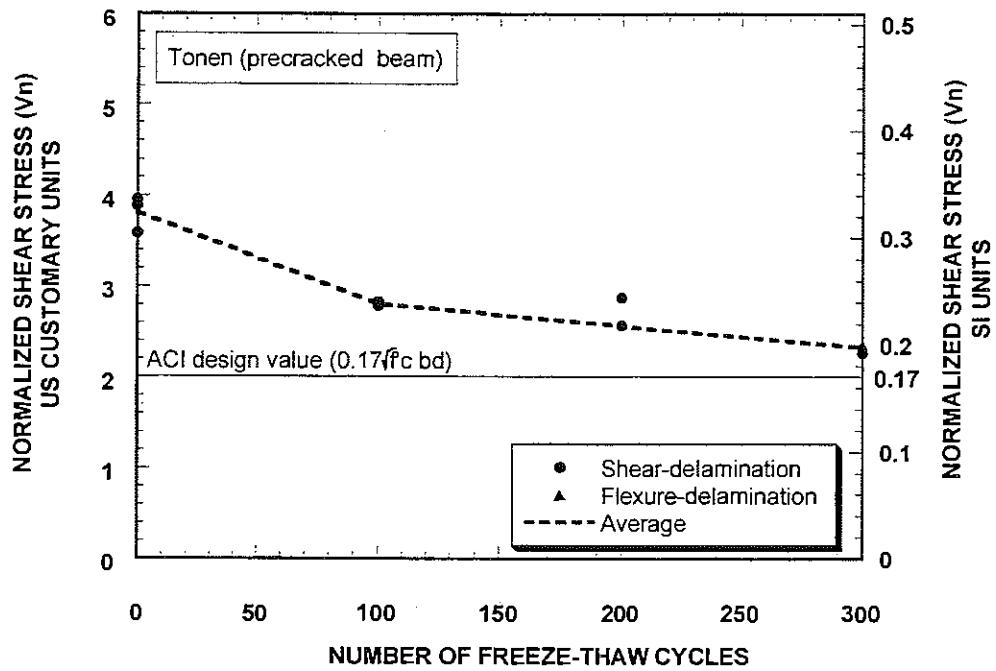


Figure 5.2 Tonen Precracked: Normalized Max. Shear Stress vs Number of F.T. Cycles

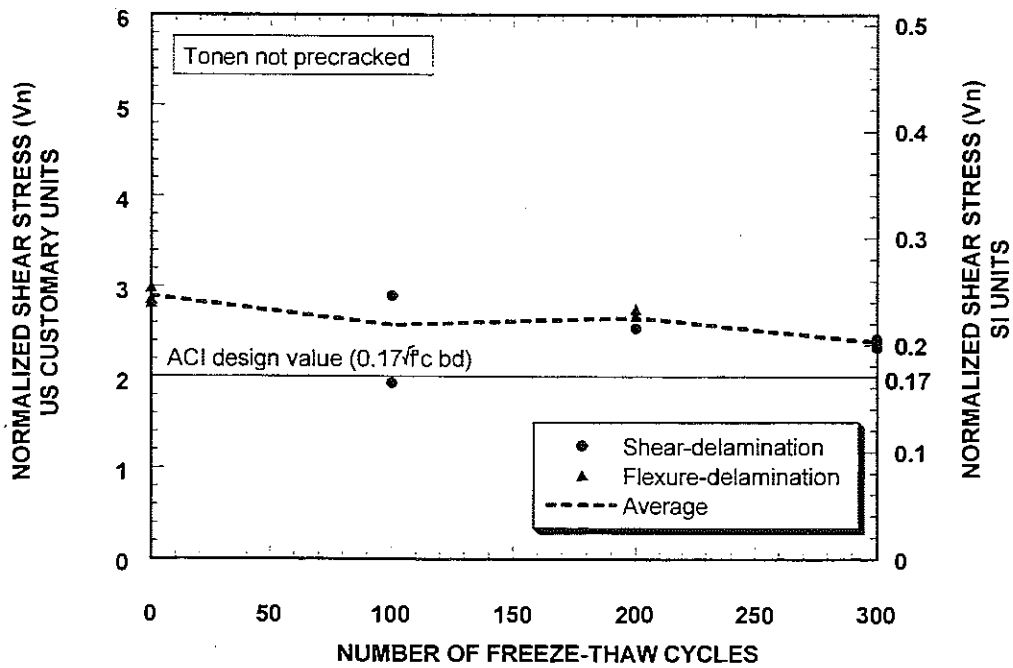


Figure 5.3 Tonen not Precracked: Normalized Max. Shear Stress vs Number of F.T. Cycles

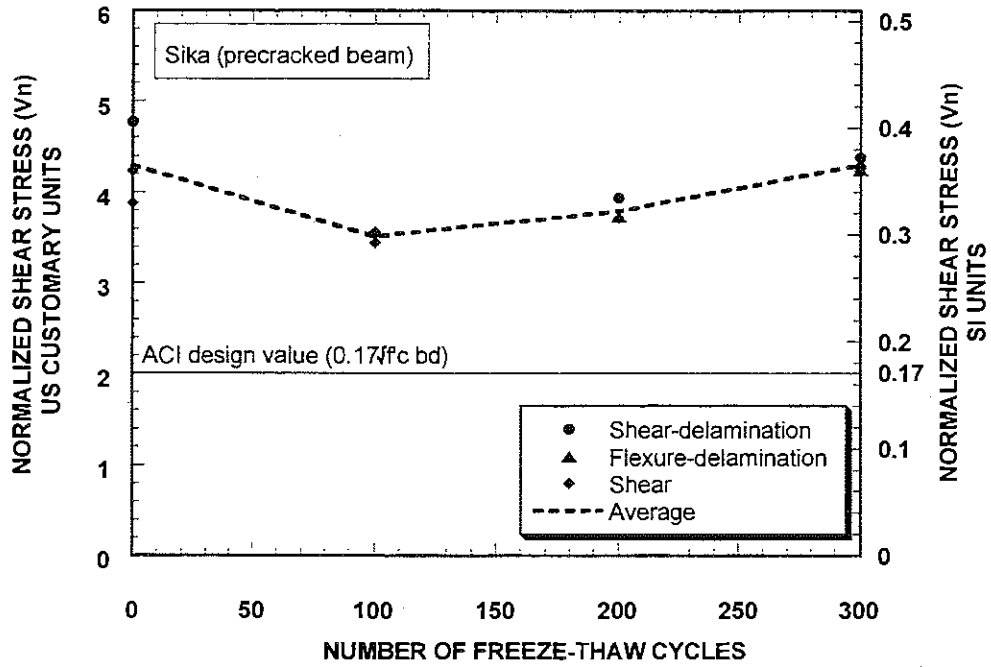


Figure 5.4 Sika Precracked: Normalized Max. Shear Stress vs Number of F.T. Cycles

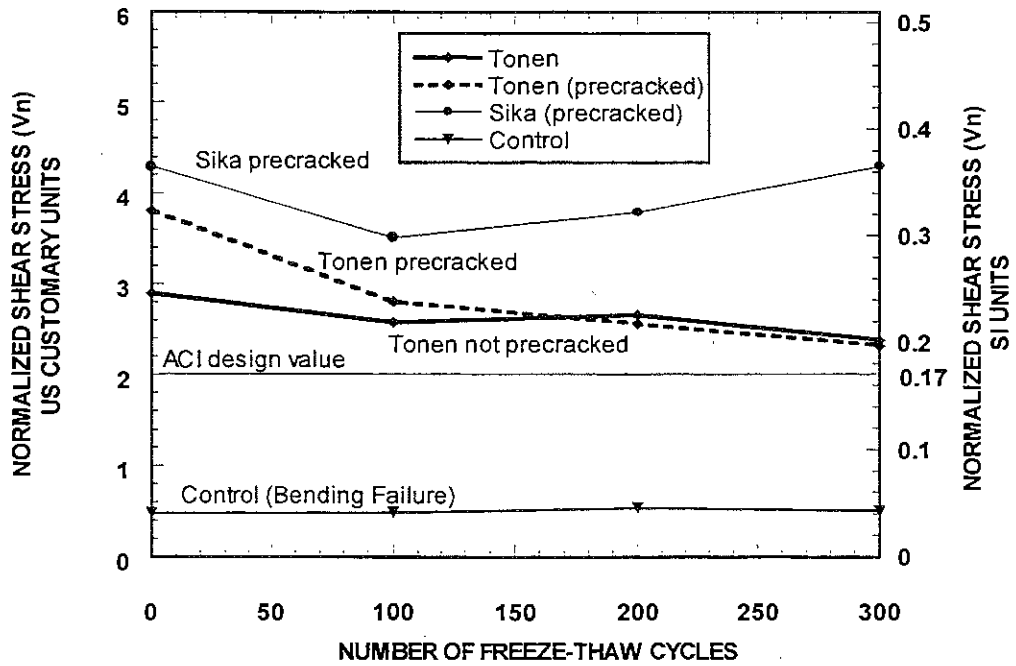


Figure 5.5 Average Normalized Max. Shear Stress at Failure vs Number of F.T. Cycles

For the Sika system, ignoring shear failure, the decrease in strength was less significant but also less consistent. Only a decrease of 10% ( $v_n=0.36$ ) was observed after 300 freeze-thaw cycles.

### 5.3. Flexural Strength

Moment-deflection curves were plotted for 0, 100, 200 and 300 freeze-thaw cycles. Figures 5.6 to 5.9 show typical moment-deflection curves for the Tonen and Sika systems as well as the control beams for these numbers of cycles. See appendix C for additional moment-deflection curves for each strengthening system.

A decrease in the moment capacity of the strengthened specimens as well as maximum deflection was observed for an increasing number of freeze-thaw cycles. These findings were analogous to those for shear strength.

The same stiffness was observed for all the specimens (including control specimens) at the pre-yielding stage. At the post yielding stage, the Sika system had a higher stiffness than the Tonen system (for both precracked and non-precracked beams).

For the control specimens no decrease in the moment capacity due to the freeze-thaw cycles was observed. However, as mentioned before, a decrease in the maximum deflection was also observed.

For the Tonen system a decrease in the moment capacity was found for both precracked and non-precracked beams. For the precracked beams, a decrease of the average moment capacity of 27% was found for 100 F.T. cycles, 29% for 200 F.T. cycles and 38% for 300 F.T. For the non-precracked beams the decrease was less drastic (15% was found for 100 F.T. cycles, 19% for 200 F.T. cycles and 20% for 300 F.T.).

The maximum deflection was very sensitive to the effect of the freeze-thaw cycles. For precracked beams, a reduction of 15% for the average deflection value was found for 100 F.T. cycles, 40% for 200 F.T. cycles and 43% for 300 F.T. For the non-precracked beams, a value of 3% was found for the average deflection at 100 F.T. cycles, 23% for 200 F.T. cycles and 19% for 300 F.T.

For the Sika system a variation in the moment capacity was also found. A decrease of 11% for the average value of the moment capacity was found for 100 F.T. cycles, 13% for 200 F.T. cycles and 4% for 300 F.T. For average deflection values, a decrease of 15% was found for 100 F.T. cycles, 15% for 200 F.T. cycles and 7% for 300 F.T.

As noted above, for the Tonen and Sika systems an overall decrease in the moment capacity as well as the maximum deflection was observed for an increase in the number of freeze-thaw cycles. The Tonen system presented the higher rate of decrease of moment capacity for the precracked beams (38% for 300 F.T. cycles). As expected the lower rate was found in the Sika system considering that, as indicated before, the predominant failure mode was shear.

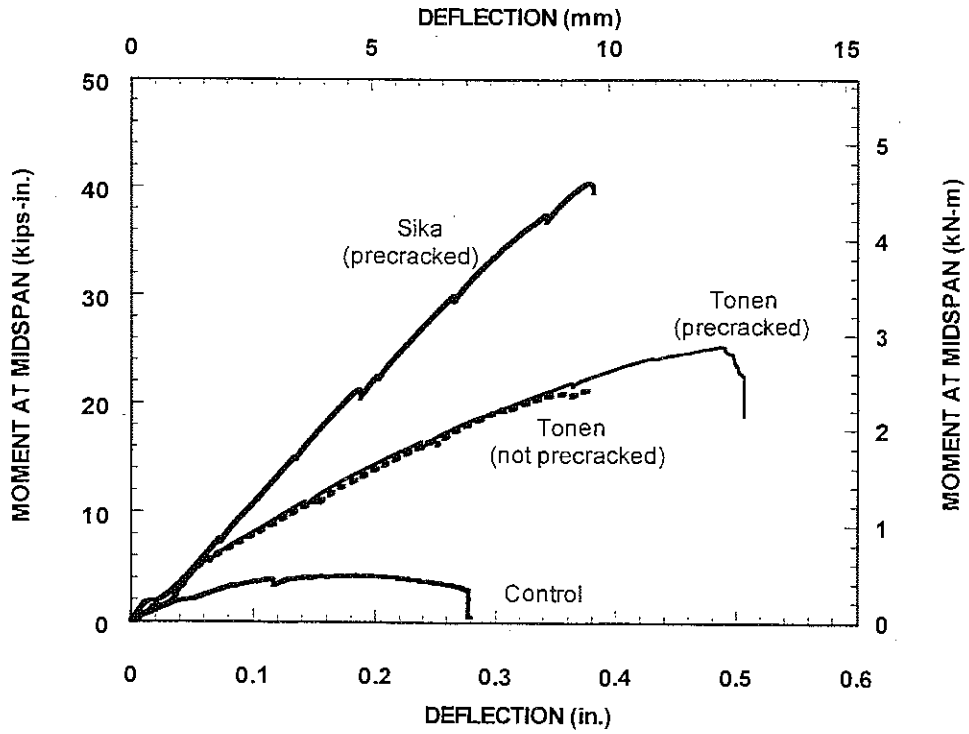


Figure 5.6 Moment-Deflection Curves for 0 F.T. Cycles

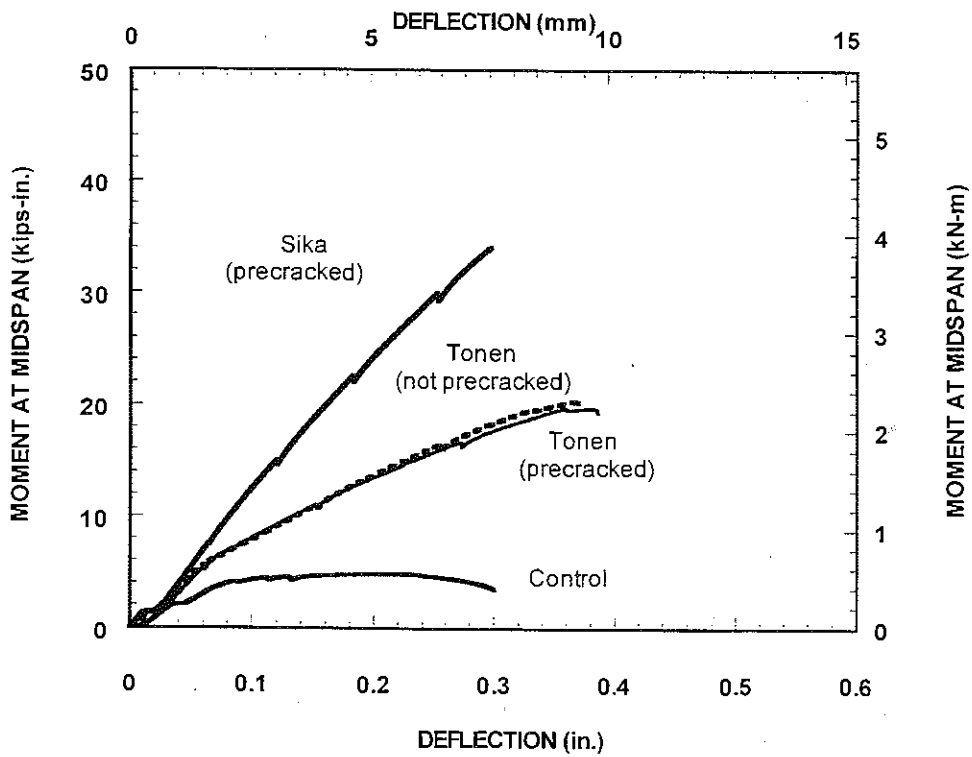


Figure 5.7 Moment-Deflection Curves for 100 F.T. Cycles

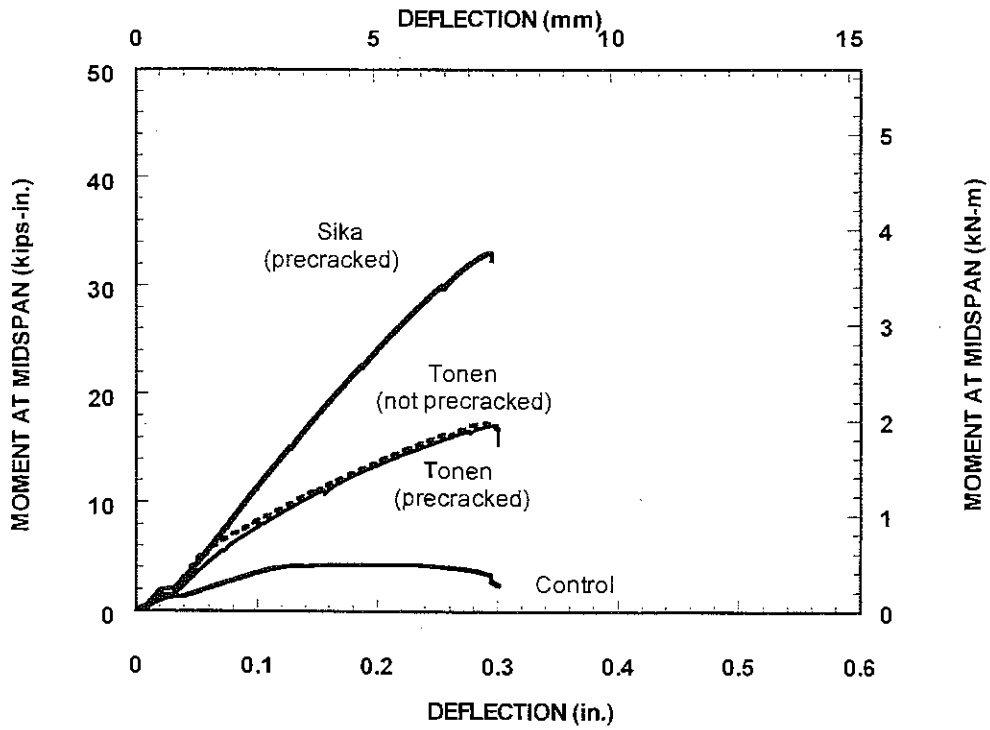


Figure 5.8 Moment-Deflection Curves for 200 F.T. Cycles

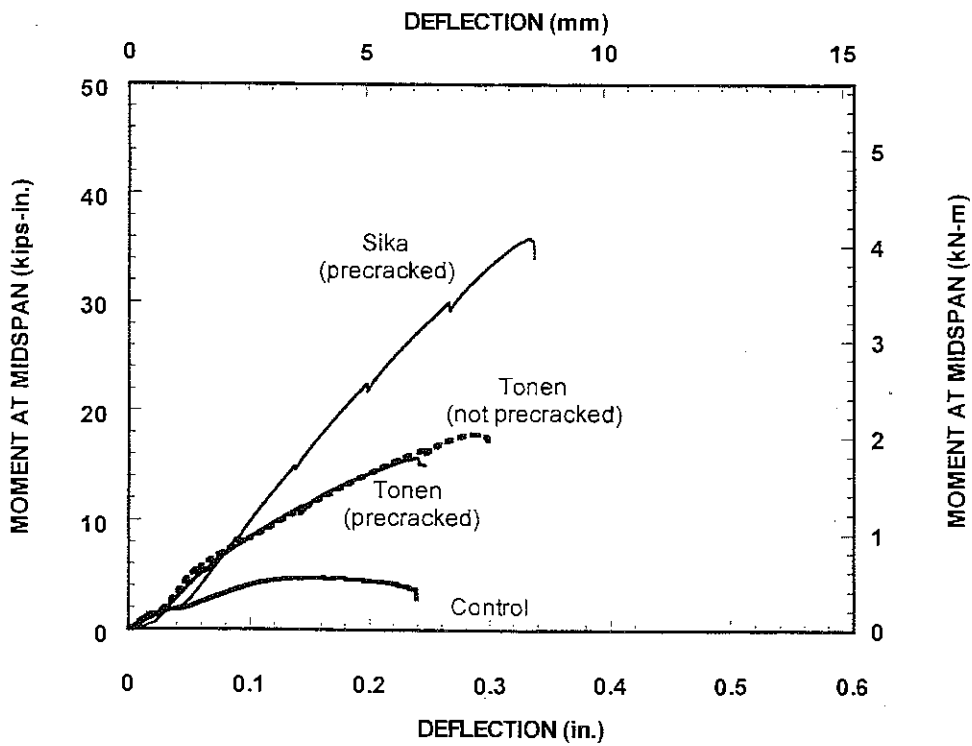


Figure 5.9 Moment-Deflection Curves for 300 F.T. Cycles

Researchers at the University of Bologna [XX-47] found that for their specimens strengthened with rigid CFRP plates (like the Sika system), high shear stress concentration at the end of the plate was responsible for the failure mechanism of the beam.

#### 5.4. Delamination Length

Delamination length was calculated with respect to the total length of the corresponding CFRP laminate. Figures 5.10, 5.11 and 5.12 present the delamination length versus number of freeze-thaw cycles for each one of the strengthening systems.

For all the systems, the delamination length found in specimens that failed either by shear-delamination failure or flexure-delamination was located between the end of the CFRP laminate and the maximum bending area. Confirming the possibility that the experimental observation that the delamination process starts at the tip of a shear or flexural crack

For the Tonen system, a relatively uniform pattern was found for both cases. For the precracked beams, the average delamination length was 23% of the total length for 0 F.T. cycles, 22% for 100 F.T. cycles, 27% for 200 F.T. cycles and 27% for 300 F.T. cycles. For the non-precracked beams, there was no significant variation in the average value of delamination length for each number of freeze-thaw cycles: the average delamination value was 25% for 0 F.T. cycles, 24% for 100 F.T. cycles, 26% for 200 F.T. cycles and 25% for 300 F.T. cycles. For both cases no major differences were found in delamination length for different types of failure modes.

For the Sika system, the variation in average values of delamination length was more significant for all the failure modes. Disregarding the specimens that failed by vertical shear (where the delamination length is considered as 0%), a more uniform pattern could be seen: 29% for 0 F.T., 26% for 200 F.T. cycles and 26% for 300 F.T. cycles. For the Sika system no major differences were found in delamination length for either shear-delamination or flexure-delamination failure.

It can be concluded that the delamination length showed a uniform pattern for both strengthening systems. For the Tonen system, values of delamination length fall within the 22-27% range of the total length. For the Sika system, the range was even more narrow, 26-29%. No influence of either the number of freeze-thaw cycles or the type of failure mode was observed.

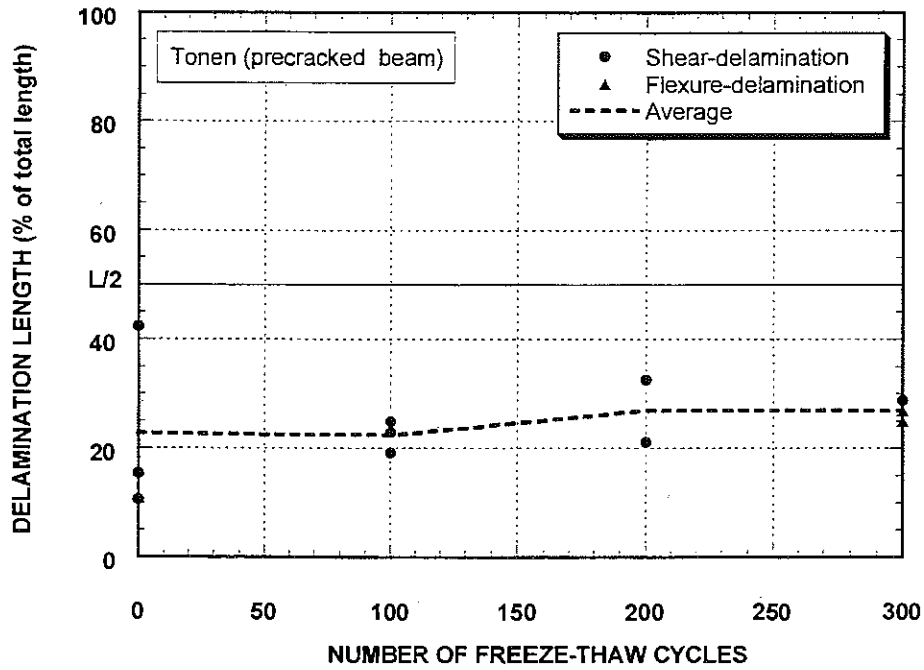


Figure 5.10 Tonen Precracked: Delamination Length vs. Number of F.T. Cycles

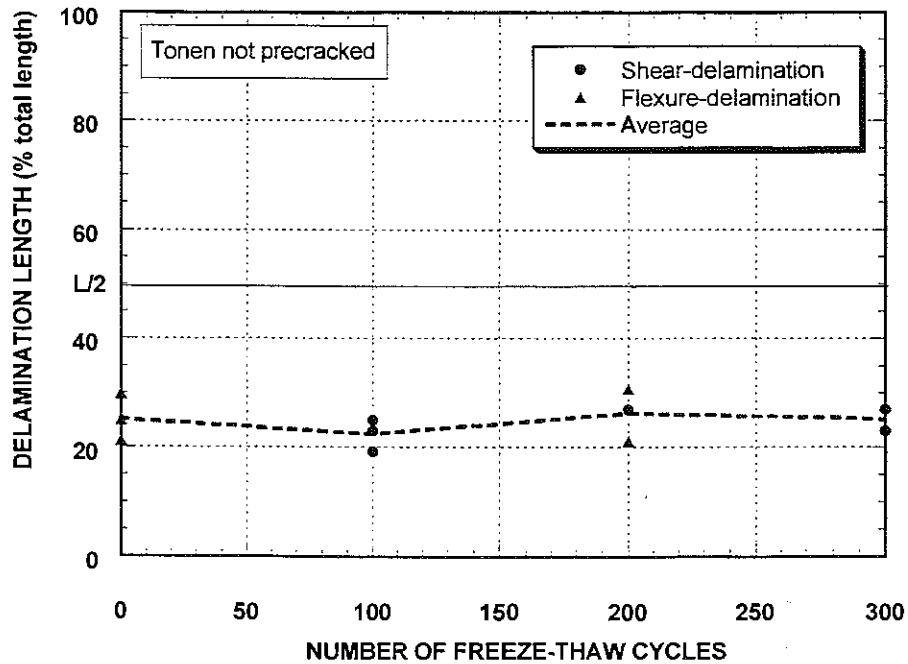


Figure 5.11 Tonen not precracked: Delamination Length vs. Number of F.T. Cycles

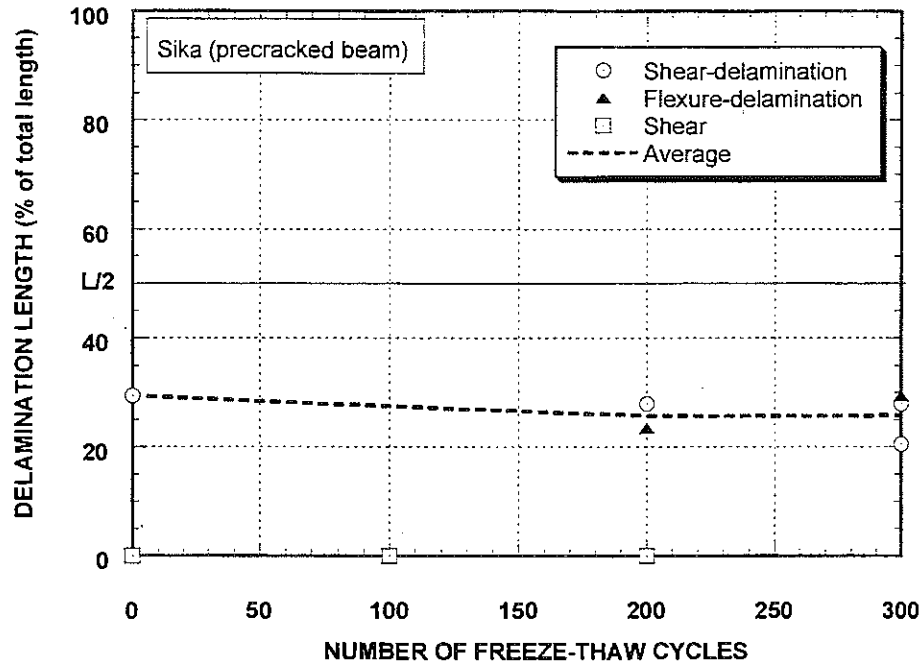


Figure 5.12 Sika Precracked: Delamination Length vs. Number of F.T. Cycles

## 6. CONCLUSIONS

1. For the control specimens no decrease in the moment capacity or shear strength due to the freeze-thaw (F.T.) cycles was observed. However, a decrease in the maximum deflection was observed.
2. For specimens strengthened with CFRP sheets an overall decrease in the moment capacity as well as the maximum deflection was observed with an increase in number of freeze-thaw cycles. Precracked beams using the Tonen system presented the higher rate of decrease of moment capacity (38% average for 300 F.T. cycles). Non-precracked beams also strengthened with the Tonen system led to an average decrease of 20% for 300 F.T. cycles.
3. The maximum moment capacity of beams strengthened with the Sika system decreased 13% on average for 200 F.T. cycles and 4% average for 300 F.T. cycles. This variation was attributed to the influence of different type of failure modes.
4. The average deflection at maximum load was very sensitive to the effect of the freeze-thaw cycles and the cracking condition. For the Tonen precracked beams a reduction of 43% in deflection was found after 300 F.T. cycles whereas for the Tonen non-precracked beams the decrease was of 19%. Beams using the Sika system showed a smaller rate of decrease in deflection at maximum load (15% average for 200 F.T. cycles and 7% for 300 F.T. cycles)
5. With the Tonen system, the values of normalized shear stress ( $v_n$ ) for the same number of freeze-thaw cycles were higher for the flexure-delamination failure than for the shear-delamination failure. It was concluded that shear cracks accelerate the interfacial crack propagation.
6. With the Tonen system, precracking the beam influences the decrease in the average normalized shear stress with the freeze-thaw cycles. For 300 freeze-thaw cycles, precracked beams had a decrease of 39% (compared with the strength at zero F.T. cycles) whereas the decrease for the non precracked beams was 22%. However the normalized shear stress after 300 F.T. cycles remained almost the same:  $v=0.20\sqrt{f'_c}$  for precracked beams, and  $v=0.19\sqrt{f'_c}$  for non-precracked beams. It can be shown that at zero F.T. cycles the cracking condition influences the capacity of the beam, whereas after 300 F.T. cycles, the freezing and thawing effect dominates.
7. For the Sika system, ignoring vertical shear failure, the decrease in the normalized average shear stress at failure load due to the effect of the freeze-thaw cycles seemed to be less significant than for the Tonen system. A decrease of 10% was observed for 300 freeze-thaw cycles, leading to a value of  $0.36\sqrt{f'_c}$ .
8. For both strengthening systems (Tonen and Sika), the delamination length found in specimens that failed either by shear-delamination or flexure-delamination was located between the end of the CFRP laminate and the maximum bending moment region.

9. The delamination length was quite uniform for both strengthening systems. For the Tonen system, values of delamination length varied between 140 to 180 mm. For the Sika system, the range was even more narrow, 220-250 mm. No influence of either the number of freeze-thaw cycles or the type of failure mode was observed on delamination length.

## 7. RECOMMENDATIONS

1. Freeze-Thaw (F.T.) cycles influence the behavior of reinforced concrete beams with glued-on Carbon Fiber Reinforced Plastic (CFRP) laminates. According to this study, with the Tonen system a maximum decrease of 29% of flexural capacity could be expected after 200 FT and 38% after 300 F.T. cycles. With the Sika system, the maximum decrease observed was of 13% after 200 F.T. cycles. It should be pointed out that the influence of the Freeze-Thaw cycles may also affects the concrete strength, but its effect cannot be easily observed from testing a reinforced concrete beam in bending; it is possible that this dual effect explains the decrease in strength. Unless some additional tests are carried out, as a first design approximation, it is recommended that a reduction of 40% in horizontal shear strength be taken to account for freeze-thaw exposure.
2. The value of the horizontal interfacial shear strength can be taken conservatively as  $0.17 \sqrt{f_c}$  for both strengthening systems. Preliminary analyses indicate that this value may be close to 1.70 MPa for Tonen system and 2.64 MPa for the Sika system, considering the effect of the different strengthening level provided by the two systems. Further study of the interface bond behavior is needed in order to refine this value.
3. The minimum value of the development length (or anchorage) of the CFRP laminate should be based on the value of  $0.17 \sqrt{f_c}$ . This value could be modified by results from further investigations. It is recommended that the bonded length of the CFRP should be as long as possible in order to avoid an interfacial bond failure and to have a more efficient use of the CFRP sheet strength.
4. Since delamination seems to be controlled by the interface bond between the CFRP laminate and the concrete, which is also controlled by the concrete strength, it is strongly recommended to insure very good surface preparation before application of the strengthening system.

## 8. REFERENCES WITH SOURCE CLASSIFICATION

### SOA - State of the Art Reports & Review Documents

- SOA-1. "State-of-the-art Report on Fiber Reinforced Plastic (FRP) Reinforcement for Concrete Structures". ACI Committee 440, 1996.
- SOA-2. "US Research Projects", International Research on Advanced Composites for construction (IRACC-96), Bologna, June 9-11, 1996.

### CAN - Canadian Institutes and Universities

- CAN-1. Soudki Khaled and Green Mark F. "Performance of CFRP Retrofitted Concrete Columns at low Temperatures". From Proceeding of the Advanced Composite Materials in Bridges and Structures. Canadian Society for Civil Engineering, Montreal, Quebec, 1996.
- CAN-2. Hoa S.V., Xie M. and Xiao X.R. "Repair of Steel Reinforced Concrete with Carbon/Epoxy Composites" From Proceeding of the Advanced Composite Materials in Bridges and Structures. Canadian Society for Civil Engineering, Montreal, Quebec, 1996.
- CAN-3. Baumert M.E., Green M.F. and Erki M.A. "A Review of low Temperature Response of Reinforced Concrete Beams strengthened with FRP sheets". From Proceeding of the Advanced Composite Materials in Bridges and Structures. Canadian Society for Civil Engineering, Montreal, Quebec, 1996.
- CAN-4. Soudki Khaled and Green Mark F "Freeze-Thaw Durability of Concrete Beams Strengthened by Carbon Fiber Sheets". ACI Fall Convention, 3-8 Nov. 1996, New Orleans.
- CAN-5. Soudki Khaled and Green Mark F "Freeze-Thaw Response of CFRP Wrapped Concrete" Concrete International. Vol. 19, No. 8, pp. 64-67, 1997.

### EMPA - Swiss Federal Laboratories for Materials Testing and Research

- EMPA-1. Meier U., "Strengthening of Structures Using Carbon Fibre/Epoxy Composites", Construction and Building materials, Vol.9, No.6, pp.341-351, 1995.

### DE - University of Delaware, Delaware Department of Transportation

- DE-1. Chajes M.J., Thomson T.A., Januszka T.F., Finch W.W., "Flexural Strengthening Of Concrete Beams Using Externally Bonded Composite Materials". 1994.
- DE-2. Chajes, M.J., Mertz, D.R., Thomson, T.A., and Farschman, C.A., "Durability of Composite Material Reinforcement," Proceedings of the Third Materials Engineering Conference on Infrastructure: New Materials and Methods of Repair, Kim, D.B., Editor, ASCE, 1994, pp. 598-605.

### XX - Other Research Institutions

- XX-9 Gomez J., Casto B., "Freeze-Thaw Durability of Composite Materials", 1<sup>st</sup> International Conference Composites in Infrastructure, ICCI, Tucson, Arizona, January 1996, pp.947-955.
- XX-26 Rahman R.H., Taylor, D.A., and Kingsley C.Y., "Evaluation of FRP as Reinforcement for Concrete Bridges," Proceedings of International Symposium on FRP Reinforcement for Concrete Structures, Nanni, A., and Dolan, C., Editors, ACI, SP-138, Detroit, 1993, pp. 71-80.
- XX-27 Shulley, S.B., Huang, X., Karbhari, V.M., and Gillespie, J.W., "Fundamental Consideration of Design and Durability on Composite Rehabilitation Schemes for Steel Girders with Web Distress," Proceedings of the Third Materials Engineering Conference on Infrastructure: New Materials and Methods of Repair, Kim, D.B., Editor, ASCE, 1994, pp. 1187-1194.
- XX-46 Blaschko M., Niedermeier R., and Zilch K., "Bond Failure Modes of Flexural Members Strengthened with FRP", Proceeding of the Second International Conference on Composites in Infrastructure, H. Saadatmanesh and M.R. Ehsani, Editors, Tucson, AZ 1998, pp. 315-327.
- XX-47 Arduini M., Di Tommaso A., Nanni A., "Brittle Failure in FRP Plate and Sheet Bonded Beams", ACI Structural Journal, V. 94, No. 4, July-August 1997, pp.363-370.

ASTM - American Standard Specifications

- ASTM-1. ASTM C666-92. Standard Test method for Resistance of Concrete to Rapid Freezing and Thawing.

## 9. APPENDIX A

### Design of Reinforced Concrete Beams with CFRP

Design of the reinforced concrete beams strengthened with the CFRP sheets was defined prior to the experimental tests. Expected maximum load was necessary to define the load cell to be used for the experimental load set-up. Based on the stresses found from this previous analysis, a value of development length (or anchorage) of the CFRP sheets was also found. In order to assure that failure will be by delamination it was agreed to use a CFRP length that will have an anchorage value smaller than the one predicted previously. Calculations of the stresses and strains for the concrete-CFRP section at ultimate as well as development lengths for the two strengthening systems are presented as follows:

For this particular analysis the cross section was considered as a laminate with different layers of material. The upper layer is composed by concrete (not cracked) and steel subjected to compressive stresses. The thickness of this layer corresponds to the depth of the neutral axis of the section. A second layer is made of steel and concrete cracked where only the steel carries tensile stresses. The third layer is composed by the CFRP laminate placed in a longitudinal orientation ( $\theta = 0^\circ$ ) and subjected to tensile stresses due to the bending external moment. Figure 1A shows the cross section to be analyzed by the strain compatibility method.

#### Stress-Strain Relationship for Steel and Concrete

For this analysis, concrete was considered a material that does not carry any tensile load. The compressive stress-strain relation was based on the model proposed by Hognestad [3]. The ascending branch was modeled with a parabolic function. The descending branch was modeled with a linear function.

$e_{cm}$  = strain of the concrete at any particular point

$f_c$  = stress of the concrete corresponding to  $e_{cm}$

$f'_c$  = maximum compressive stress (3.45 MPa)

$e_o$  = strain corresponding  $f'_c$  (assumed 0.002 for this model)

note that  $e_o$  is the strain at peak load and that the strain at failure (generally taken by ACI as 0.003) is a result of the analysis.

$$\text{for } 0 \leq e_{cm} \leq e_o, \quad f_c = f'_c \left( 2 \left( \frac{e_{cm}}{e_o} \right) - \left( \frac{e_{cm}}{e_o} \right)^2 \right)$$

$$\text{for } e_o \leq e_{cm}, \quad f_c = f'_c (1 - 150 (e_{cm} - e_o))$$

Figure 2A shows the stress-strain relationship based on this model

The stress-strain relationship of the steel was chosen so it would fit to the experimental curves obtained from the tensile testing of the mesh coupons. A stress-displacement curve of the steel mesh is presented in Figure 3.1. of the main report.

$e_s$  = strain of the steel at a particular point

$f_s$  = stress of the steel at  $e_s$   
 $f_y$  = yielding stress of the steel = 400 MPa (from experimental data)  
 $f_{su}$  = 482 MPa (from experimental data)  
 $E_s$  = 200 GPa  
 $e_u$  = strain at failure = 0.10 (from experimental data)

for  $e_s \leq e_y$ ,  $f_s = E_s e_s$   
 for  $e_y \leq e_s \leq e_m$ ,  $f_s = f_y + (f_{su} - f_y) (2j - j_1)$   
 where  $j = (e_s - e_y) / (e_{sm} - e_y)$   $e_{sm} = 0.031$

Figure 3A show the strain-stress relationship based on this model.

#### Stress- Strain Relationship for CFRP Laminates

Since all the fibers of the CFRP sheets are unidirectional (in the longitudinal direction), it will be assumed that

$$\sigma_x = E_{CFRP} \epsilon_{CFRP}$$

where  $\sigma_x$  are the longitudinal stresses at the level of the CFRP and  $\epsilon_{CFRP}$  is the strain at that level of the CFRP.  $E_{CFRP}$  is the modulus of elasticity of the CFRP sheet.

- Tonen system mechanical properties:

Information provided by the supplier:  
 Modulus of Elasticity  $E_1 = 227.53$  GPa  
 Tensile strength  $\sigma_x = 3.48$  GPa  
 thickness  $t_f = 0.165$  mm  
 Strain at failure  $e_u = 1.5\%$

- Sika system mechanical properties:

Information provided by the supplier:  
 $E_1 = 150$  GPa  
 $t_f = 1.2$  mm  
 $e_u = 1.4\%$

#### Strain Compatibility Method

The strain compatibility method derives from one of the basic assumptions in flexure theory: it is assumed that stresses in the concrete and reinforcement can be computed from the strains using stress-strain curves for concrete and steel [5].

In order to find the moment capacity of the section, a compression strain of 0.003 for the concrete was assumed, based on ACI concrete block failure model.

The location of the neutral axis ( $kd$ ) was found through an iterative process where equilibrium of internal forces was checked for a defined value of  $e_m$ . Once equilibrium was reached, the

internal bending moment was calculated. Following this procedure, a moment-curvature curve can be calculated for a particular cross section, see Figure 1A.

#### Tonen System

$$kd = 18 \text{ mm}$$

$$e_{cm} = 0.003 \quad C_c = 35606 \text{ N}$$

$$e_{c1} = 0.00046 \quad C1 = 3256 \text{ N}$$

$$\sum C_i = 38862$$

$$e_{s2} = -0.00208 \quad T_{s2} = 1618 \text{ N}$$

$$e_{s3} = -0.00462 \quad T_{s3} = 1674 \text{ N}$$

$$e_{s4} = -0.00771 \quad T_{s4} = 6958 \text{ N}$$

$$e_{CFRP} = -0.00986 (< 1.5\%) \quad T_{CFRP} = 28426 \text{ N}$$

$$\sum T_i = 38676$$

$$M = 2435 \text{ N-m}$$

$$P = M \cdot 2/L = 17302 \text{ N}$$

#### Sika system

$$kd = 33 \text{ mm}$$

$$e_{cm} = 0.003 \quad C_c = 63300 \text{ N}$$

$$e_{c1} = 0.0016 \quad C1 = 2539 \text{ N}$$

$$\sum C_i = 65954$$

$$e_{c2} = 0.000229 \quad C2 = 115 \text{ N}$$

$$e_{s3} = -0.00115 \quad T_{s3} = 1039 \text{ N}$$

$$e_{s4} = -0.00277 \quad T_{s4} = 6530 \text{ N}$$

$$e_{CFRP} = -0.00481 (< 1.4\%) \quad T_{CFRP} = 66390 \text{ N}$$

$$\sum T_i = 67273$$

$$M = 4179 \text{ N-m}$$

$$P = M \cdot 2/L = 21937 \text{ N}$$

The strains in the CFRP laminated for all the cases are less than the maximum tensile strain (strain at failure).

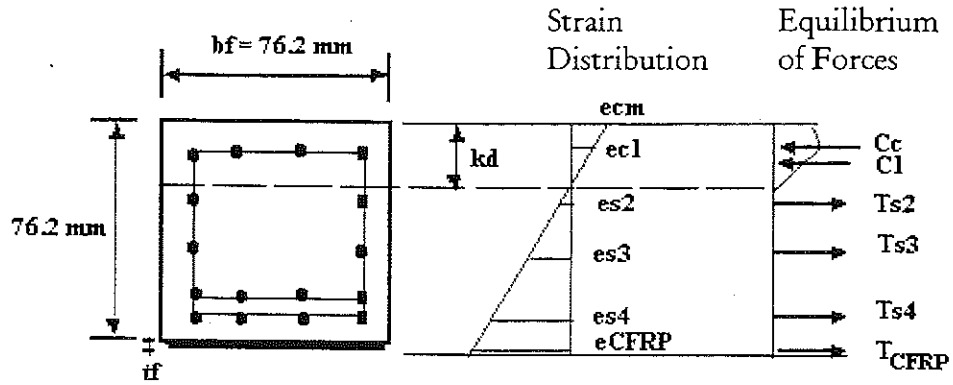


Figure 1A. Cross Section to be Analyzed Using Strain Compatibility Method

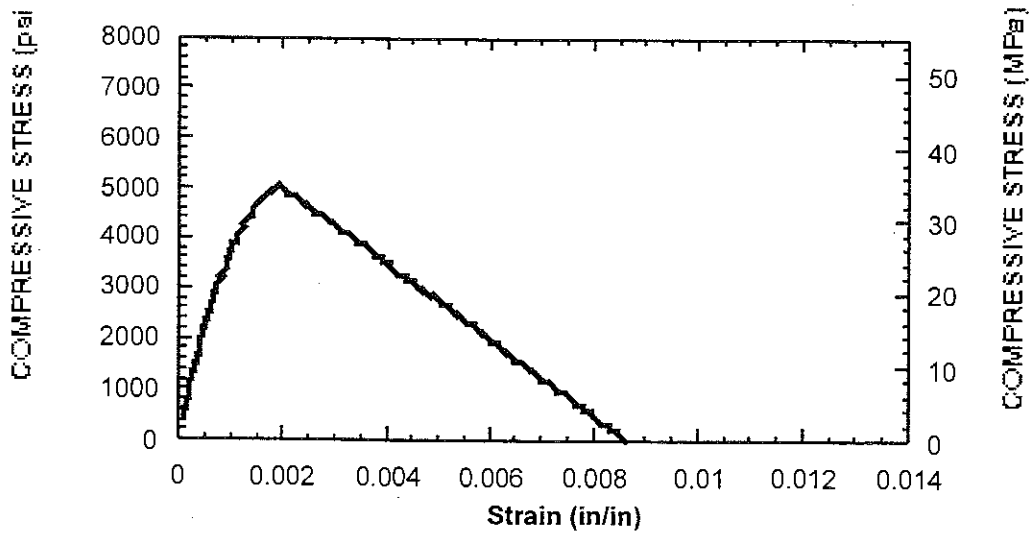


Figure 2A. Stress-Strain Relationship for Concrete in Compression

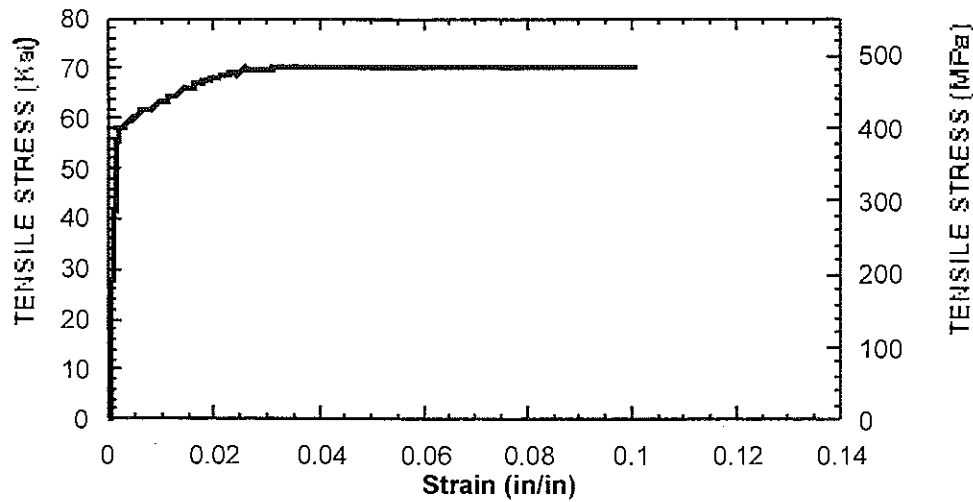


Figure 3A. Stress-Strain Relationship for Steel Mesh

### Prediction of the Delamination Length

- Uniform Shear Stress Model

According to the experimental data, it was found that most of the cases of failure of the bond interface between the CFRP sheet and the concrete laminate started at a flexural or shear crack next to one of the point loads and progressed toward the end of the CFRP sheet. Since the shear forces are uniform in the shear span of a four point bending test, an uniform interface shear stress ( $\tau_s$ ) model can be considered [5].

Therefore  $l_d = T_{CFRP} / (b * \tau_s) = (\sigma_{CFRP} * t_f) / \tau_s$ ,

And  $\sigma_{CFRP} = E_{CFRP} \epsilon_{CFRP}$

where  $l_d$  (development length) is the shear span for the CFRP laminate and  $T_{CFRP}$ ,  $\sigma_{CFRP}$  are the tensile force and stress of the CFRP sheet at the point under one of the concentrated loads, point A of the Figure 4A. The tensile force, stress and strains were found from the equilibrium of the section according to the strain-compatibility method presented in the previous section.  $t_f$  is the thickness of the CFRP plate and  $\tau_s$  is the shear strength of the interface, assume to be equal to the shear strength of the concrete  $\tau_c$ .

Shear Strength of the concrete  $\tau_c = 0.17\sqrt{f'_c} = 998 \text{ KPa}$   
(compressive strength of concrete,  $f'_c = 34.48 \text{ MPa}$ )

Values of  $l_d$  were calculated for every one of the strengthening systems.

### Tonen System

$$\sigma_{CFRP} = \epsilon_{CFRP} E_{CFRP} = 0.00986 * 227.53 = 2.24 \text{ GPa}$$

$$l_d = 2.26 * 0.165 / 0.998 = 371 \text{ mm}$$

The minimum value of development length required to avoid delamination is 371 mm. However because the objective of this project was to measure the influence of the freeze-thaw cycles on the bond strength of this system, it was of our research group interest to actually guaranty this type of failure. Therefore a smaller value than the one calculated previously was adopted (254 mm) as the development length for the CFRP sheet.

Total length of the Tonen CFRP ( $l_{cs}$ , see Figure 4A) = 660 mm.

### Sika System

$$\sigma_{CFRP} = \epsilon_{CFRP} E_{CFRP} = 0.00481 * 150.7479 = 0.725 \text{ GPa}$$

$$l_d = 0.725 * 1.2 / 0.998 = 872 \text{ mm}$$

The minimum value of development length required to avoid delamination is 872 mm.

Following the same line of thought presented above, we will use a smaller value for the development length. Since the maximum length of CFRP for the load set-up is 864 mm and this length gives a value of development length is 356 mm (smaller than 872 mm), it is agreed to use this value as the length for the Sika system.

These values of development length are included in the main report (see page 12) and are considered for analysis of the test results.

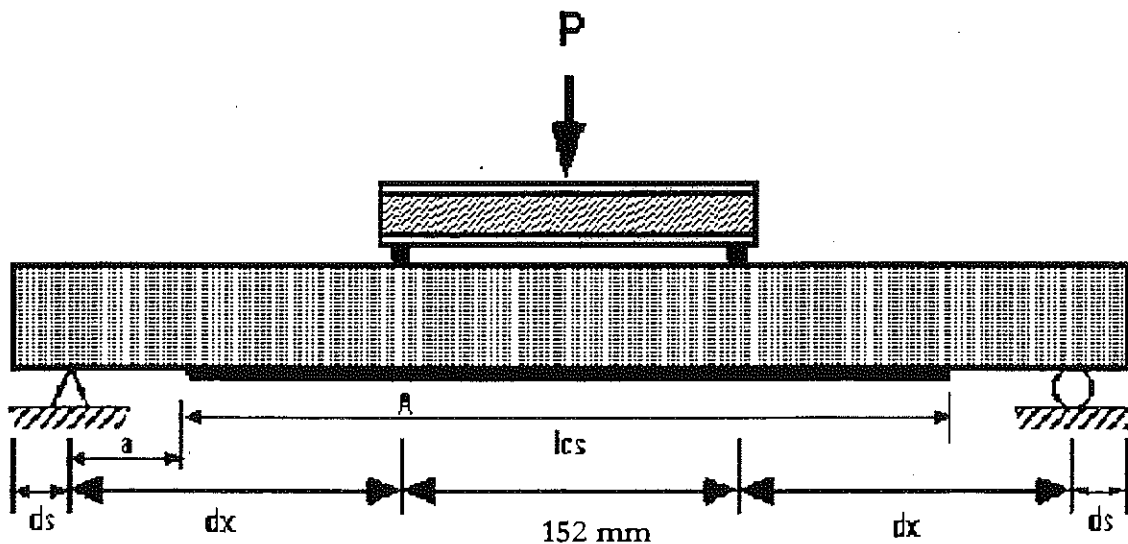


Figure 4A. Flexural Test Load Set-Up

## References

- [1] Blaschko M., Niedermeier R. and Zielch K. "Bond Failure Modes of Flexural Members Strengthened with FRP." Proceedings of the Second International conference on Composites in Infrastructure. Tucson, Arizona 1998.
- [2] Hyer, M. "Stress Analysis of Fiber-Reinforced Composite Materials. WCB/McGraw-Hill publishers. 1998.
- [3] Hognestad, E., Hanson, N.W. and McHenry, D., "Concrete Stress Distribution in Ultimate Strength Design," ACI Journal, Vol. 57, No. 2, February 1961
- [4] Malek A.M. and Saadatmanesh H. "Design Equations and Guidelines for Reinforced Concrete Beams Strengthened with FRP Plates." Proceedings of the Second International conference on Composites in Infrastructure. Tucson, Arizona 1998.
- [5] Wang, C.Y. and Ling F.S. "Prediction Model for the Debonding Failure of Cracked RC Beams with Externally Bonded FRP Sheets." Proceedings of the Second International conference on Composites in Infrastructure. Tucson, Arizona 1998.
- [6] Wu Z., Matsuzaki T. and Tanabe K., "Interface Crack propagation in FRP Strengthened Concrete Structures". Proceedings of the Third International Symposium of Non-Metallic (FRP) Reinforcement for Concrete Structures. Vol. 1, Oct. 1997.

## 10. APPENDIX B

### Interface Bond Modeling of Reinforced Concrete Beams Externally Reinforced with Glued-on Carbon Fiber Reinforced Plastic (CFRP) Sheets

The objective of this analysis is to predict the value of the interface shear strength between the CFRP laminate and the concrete when interface bond failure occurred. In order to avoid the influence of freeze-thaw cycles, which will be analyzed in the main report, only specimens at 0 F.T. cycles will be considered. Additionally, only specimens that failed by delamination will be considered.

Table 1B. Maximum External Moment and Shear Forces at 0 F.T. cycles

Strengthening System	Average Max. Shear Force (N)	Average Max. Moment (N-m)
Tonen (not precracked beam)	8669	2422
Tonen (precracked beam)	10062	2810
Sika (precracked beam)	11996	4603

From the failure loads, average values of moment capacity for the section A (see Figure 1B) under a point load were calculated and are presented in Table 1B.

Stresses and strains based on the strain compatibility method and equilibrium of forces were found for this section. The resulting moment was intended to match the values of external moment obtained from the experimental data (see Table 1B).

According to the experimental data, it was found that most of the cases of failure of the bond interface between the CFRP sheet and the concrete laminate started at a flexural or shear crack next to one of the point loads and progressed toward the end of the CFRP sheet. Stress-strain relationships for concrete, steel and the CFRP sheets were the same used in Appendix A.

Notation was also kept consistent with the one used on Appendix A. (See Figure 2B, Appendix B). Note that in the following results, the strain in the concrete top fiber can be larger than 0.003 and is a result of the analysis.

#### Tonen Not Precracked

$$kd = 19 \text{ mm}$$

$$e_{cm} = 0.0036 \quad C_c = 37984 \text{ N}$$

$$e_{c1} = 0.00288 \quad C_1 = 3272 \text{ N} \quad \sum C_i = 41300$$

$$e_{s2} = 0.00218 \quad T_{s2} = 1620 \text{ N}$$

$$e_{s3} = 0.00506 \quad T_{s3} = 1683 \text{ N}$$

$$e_{s4} = 0.00795 \quad T_{s4} = 6958 \text{ N} \quad \sum T_i = 42000$$

$$e_{CFRP} = 0.01103 (< 1.5\%) \quad T_{CFRP} = 31777 \text{ N}$$

$$M = 2503 \text{ N-m}$$

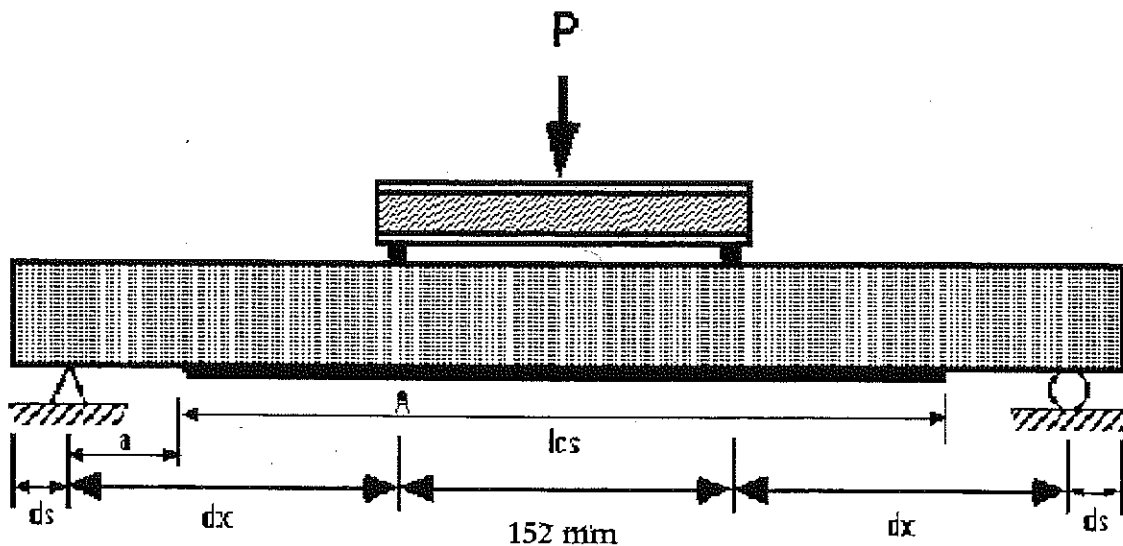


Figure 1B. Cross Section and Load Set-Up

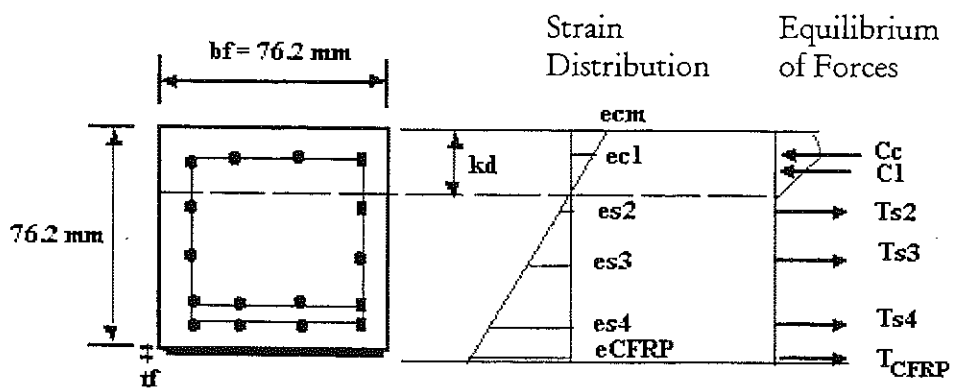


Figure 2B. Cross Section to be Analyzed Using Strain Compatibility Method

Tonen Precracked

$$kd = 22 \text{ mm}$$

$$e_{cm} = 0.005 \quad C_c = 42305 \text{ N}$$

$$e_{c1} = 0.00346 \quad C_1 = 3298 \text{ N} \quad \sum C_i = 45603$$

$$e_{s2} = 0.00193 \quad T_{s2} = 1560 \text{ N}$$

$$e_{s3} = 0.00539 \quad T_{s3} = 1690 \text{ N}$$

$$e_{s4} = 0.00885 \quad T_{s4} = 6781 \text{ N} \quad \sum T_i = 46000$$

$$e_{CFRP} = 0.0125 (< 1.5\%) \quad T_{CFRP} = 36012 \text{ N}$$

$$M = 2802 \text{ N-m}$$

Sika System

$$kd = 35.5 \text{ mm}$$

$$e_{cm} = 0.0040 \quad C_c = 70690 \text{ N}$$

$$e_{c1} = 0.00228 \quad C_1 = 3245 \text{ N} \quad \sum C_i = 74392$$

$$e_{c2} = 0.000566 \quad C_2 = 457 \text{ N}$$

$$e_{s3} = 0.00115 \quad T_{s3} = 929 \text{ N}$$

$$e_{s4} = 0.00287 \quad T_{s4} = 6544 \text{ N} \quad \sum T_i = 73863$$

$$e_{CFRP} = 0.00481 (< 1.4\%) \quad T_{CFRP} = 66390$$

$$M = 4459 \text{ N-m}$$

Since no tensile failure of the CFRP was observed, it was expected that the strains in the CFRP sheets for all cases were less than in the maximum tensile strain (strain at failure). The values obtained from this analysis corroborate this statement.

It should also be noted that the difference between the calculated and the experimental value of moment is due to the nature of the numerical iteration process. In all cases this difference was less than 3%.

**Prediction of the Bond Strength**

- **Uniform Shear Stress Model**

According to the experimental data, it was found that most of the cases of failure of the bond interface between the CFRP sheet and the concrete laminate started at a flexural or shear crack next to one of the point loads and progressed toward the end of the CFRP sheet. As shown in Appendix A, an uniform interface shear stress ( $\tau_s$ ) along the shear span was assumed as a first shear stress model.

Therefore 
$$\tau_s = (\sigma_{CFRP} * t_f) / (dx-a)$$

where  $(dx-a)$  is the shear span for the CFRP sheet (see Figure 1B),  $t_f$  is the thickness of the CFRP sheet and  $\sigma_{CFRP}$  is the tensile stress of the CFRP sheet at the point under one of the concentrated loads (point A in Figure 1B).

Values of  $\tau_s$  were calculated from every one of the final iterations presented above.

#### Tonen Not Precracked

$$\sigma_{CFRP} = \epsilon_{CFRP} E_{CFRP} = 0.011 * 227.53 = 2.50 \text{ GPa}$$

$$\tau_s = 2.50 * 0.165 / 254 = 1.63 \text{ MPa} (\approx 0.28 \sqrt{f_c})$$

From the experimental data it was observed that the interfacial debonding process occurred at the level of the concrete surface. ACI suggested a value of  $0.17\sqrt{f_c}$  (MPa) for the shear strength of the concrete ( $\tau_c$ ). It is considered that this value could be used as a control to avoid the interface bond failure.

#### Tonen Precracked

$$\sigma_{CFRP} = \epsilon_{CFRP} E_{CFRP} = 0.0125 * 227.53 = 2.84 \text{ GPa}$$

$$\tau_s = 2.84 * 0.165 / 254 = 1.85 \text{ MPa} (\approx 0.31 \sqrt{f_c})$$

As for the case of Tonen not precracked, the shear strength of the concrete controlled the interface bond failure. The values of  $\tau_s$  for both cases (precracked and not precracked) were larger than  $0.17\sqrt{f_c}$ .

#### Sika system (Precracked)

$$\sigma_{CFRP} = \epsilon_{CFRP} E_{CFRP} = 0.00481 * 150.7479 = 7.25 \text{ GPa}$$

$$\tau_s = 7.25 * 1.2 / 355.6 = 2.44 \text{ MPa} (\approx 0.43 \sqrt{f_c})$$

As for the Tonen system, it was found that the failure occurred at the level of the concrete surface.

#### • Non Uniform Shear Stress Model

For this model a strip of beam in the shear span of length  $dx$  was analyzed. From the equilibrium of axial forces a relation was found to estimate the interface CFRP-concrete shear stress value  $\tau_s$  (see Figure 3B). The value of  $\tau_s$  is assumed to be uniform along the length  $dx$ :

$$\frac{dT_{CFRP}}{dx} - \tau_s \cdot b_f = 0 \quad (1)$$

Values of  $\tau_s$  are obtained from solving (1). Since the variation of the compressive forces and tensile forces along the shear span are related to the nonlinearity of the stress-strain relationship of the concrete and steel, the evaluation of  $\tau_s$  will be done numerically.

$$\text{Therefore, for a strip of length } dx, \quad \tau = \frac{\frac{dT_{CFRP}}{dx}}{b_f} \quad (1)$$

### Tonen Not Precracked

Defining  $x = 0$  at point A (see Figure 1). Equilibrium of forces at this point was set using the strain compatibility method.

At  $x = 0$

$$\Sigma C = 41256, \Sigma T = 10261, \Sigma T_{CFRP} = 31777$$

For  $dx = 18$  mm,  $M = 2435$  N-m

$$\Sigma C = 38862, \Sigma T = 10190, \Sigma T_{CFRP} = 28426$$

from (1),  $\tau = (186167) / 0.0762 = 2.44$  MPa

### Tonen Precracked

At  $x = 0$

$$\Sigma C = 45603, \Sigma T = 10031, \Sigma T_{CFRP} = 36012$$

For  $dx = 20$  mm,  $M = 2601$  N-m

$$\Sigma C = 41256, \Sigma T = 10261, \Sigma T_{CFRP} = 31777$$

from (1),  $\tau = (211750) / 0.0762 = 2.78$  MPa

### Sika system

At  $x = 0$

$$\Sigma C = 70690, \Sigma T = 7473, \Sigma T_{CFRP} = 66390$$

For  $dx = 24$  mm,  $M = 4179$  N-m

$$\Sigma C = 65954, \Sigma T = 7569, \Sigma T_{CFRP} = 59704$$

from (1),  $\tau = (278583) / 0.0762 = 3.66$  MPa

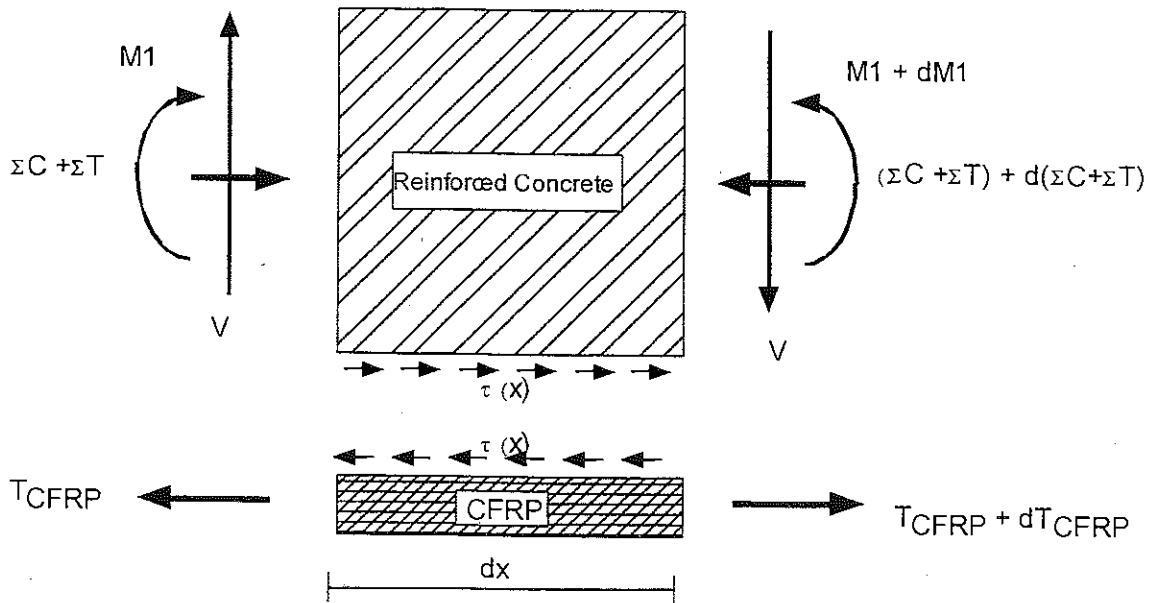


Figure 3B. Free Body Diagram

### • Comparison of Results

Table 2B presents a comparison of results of  $\tau_s$  values obtained from the uniform shear stress model and the non uniform shear stress model. The third column represents the calculation of the average vertical shear stress  $v_1 = V/(b_f*d)$ , where  $V$  = shear force( from Table 1B),  $b_f$  = width of concrete beam = 76.2 mm and  $d$  = distance from maximum compressive strain to centroid of steel at tension = 63.5 mm. The fourth column represents the calculation of the  $v_2=V/(b*h)$ , where  $h$  = height of the concrete beam = 76.2 mm.

As can be seen from Figure 4B, model 1 represents the lower bound and model 2 the upper bound of the values of the interface shear strength. Comparing these values with the calculation of  $v_1$  and  $v_2$ , we can conclude that the calculation of the average vertical shear stress is an indirect measure of the value of the interface shear for the Tonen system. Values of  $v_2$  represent the lowest bound (compared to model 1 and 2) and are therefore on the safe side (for a defined value of  $\tau_s$ ).

Values of  $\tau_s$  for the Sika system were higher than the ones for Tonen system. Recalling that for the Sika system at 0 freeze-thaw cycles, 2 out of 3 beams failed by vertical shear, it is possible that the values of  $\tau_s$  found are only approximate. Additionally,  $v_1$  and  $v_2$  values calculated were higher than the  $\tau_s$  values obtained from model 1 and 2. However,  $v_2$  was closer to the  $\tau_s$  values than  $v_1$ . Considering the shear strength of the concrete as  $0.17\sqrt{f_c} = 0.998$  MPa we can conclude that this value can be taken conservatively as the interfacial bond strength.

**Table 2B.  $\tau_s$  values obtained from analysis.**

System	Model1 (uniform $\tau_s$ ) MPa	Model2 (discontinuous $\tau_s$ ) MPa	$v_1=V/bd$ (MPa)	$v_2= V/bh$ (MPa)
Tonen not precracked	1.63	2.44	1.79	1.48
Tonen precracked	1.85	2.78	2.08	1.73
Sika precracked	2.44	3.66	4.99	4.14

It can be concluded that for an accurate prediction of the bond strength at the interface either model 1 or 2 should be analyzed for all the experimental data obtained. However the values of  $V/bh$  obtained follow the same trend as those of either Model 1 or 2, and are recommended as a first approximation in design.

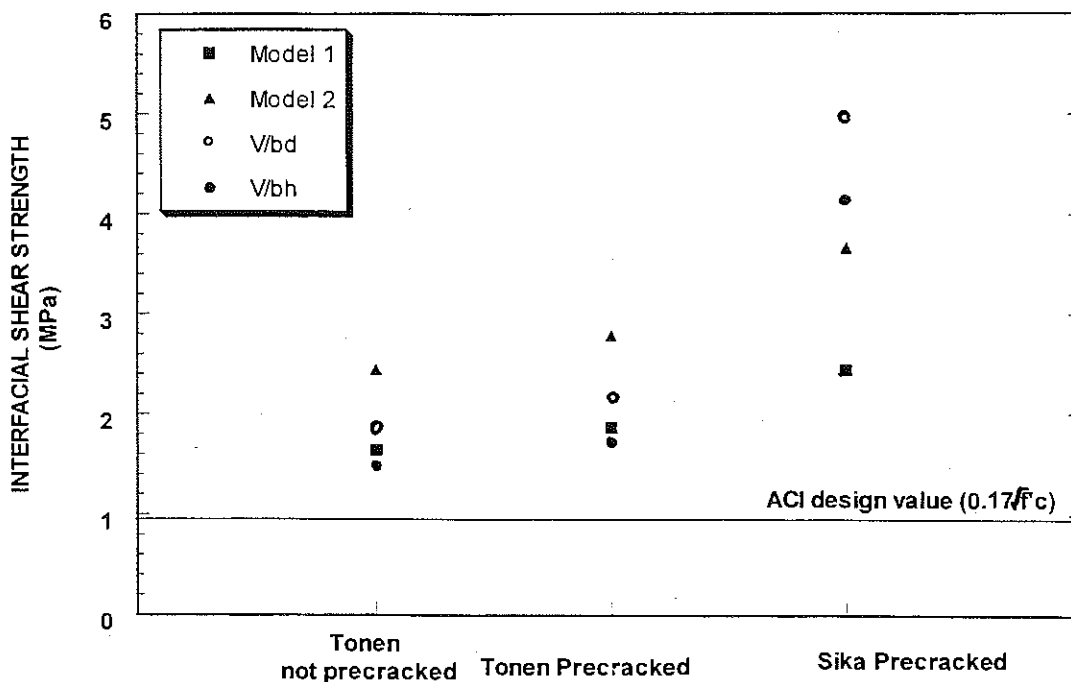


Figure 4B. Interfacial Shear Strength Values

## References

- [1] Blaschko M., Niedermeier R. and Zielch K. "Bond Failure Modes of Flexural Members Strengthened with FRP." Proceedings of the Second International conference on Composites in Infrastructure. Tucson, Arizona 1998.
- [2] Hyer, M. "Stress Analysis of Fiber-Reinforced Composite Materials. WCB/McGraw-Hill publishers. 1998.
- [3] Hognestad, E., Hanson, N.W. and McHenry, D., "Concrete Stress Distribution in Ultimate Strength Design," ACI Journal, Vol. 57, No. 2, February 1961
- [4] Malek A.M. and Saadatmanesh H. "Design Equations and Guidelines for Reinforced Concrete Beams Strengthened with FRP Plates." Proceedings of the Second International conference on Composites in Infrastructure. Tucson, Arizona 1998.
- [5] Wang, C.Y. and Ling F.S. "Prediction Model for the Debonding Failure of Cracked RC Beams with Externally Bonded FRP Sheets." Proceedings of the Second International conference on Composites in Infrastructure. Tucson, Arizona 1998.
- [6] Wu Z., Matsuzaki T. and Tanabe K., "Interface Crack propagation in FRP Strengthened Concrete Structures". Proceedings of the Third International Symposium of Non-Metallic (FRP) Reinforcement for concrete Structures. Vol 1, Oct., 1997.

APPENDIX C

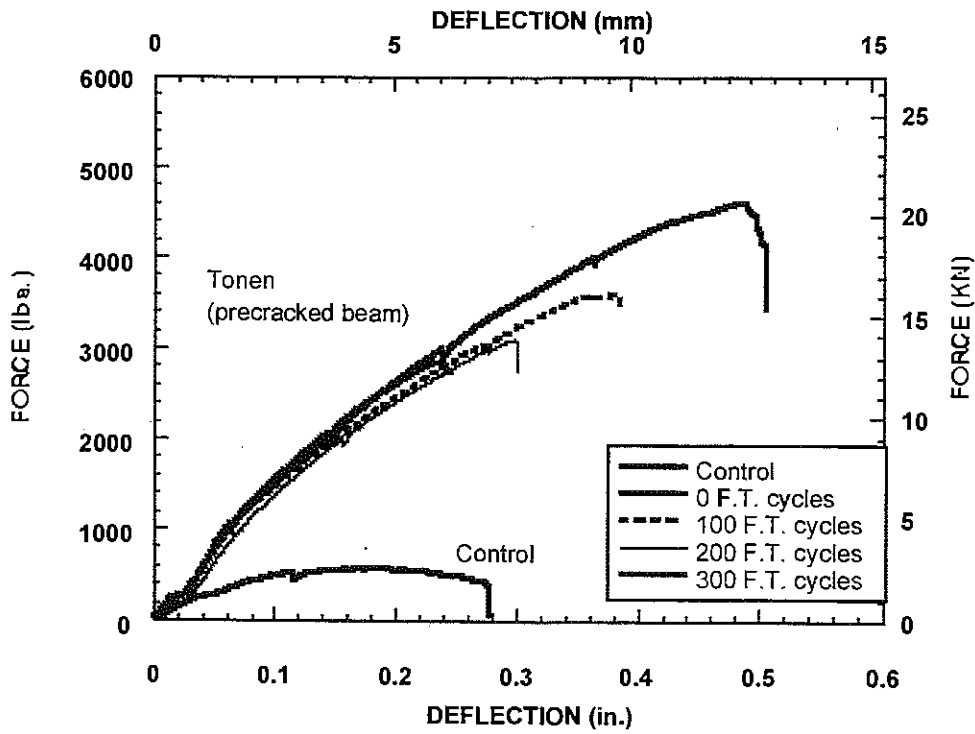


Figure 1C Load-Deflection Curves for Tonen Precracked Beams

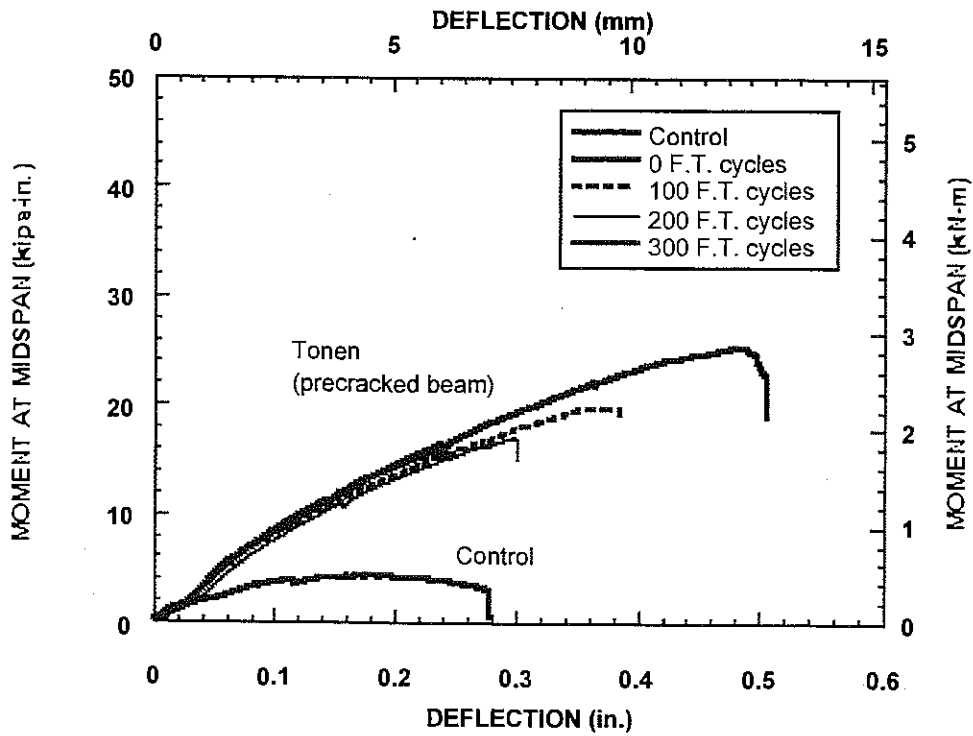


Figure 2C Moment-Deflection Curves for Tonen Precracked Beams

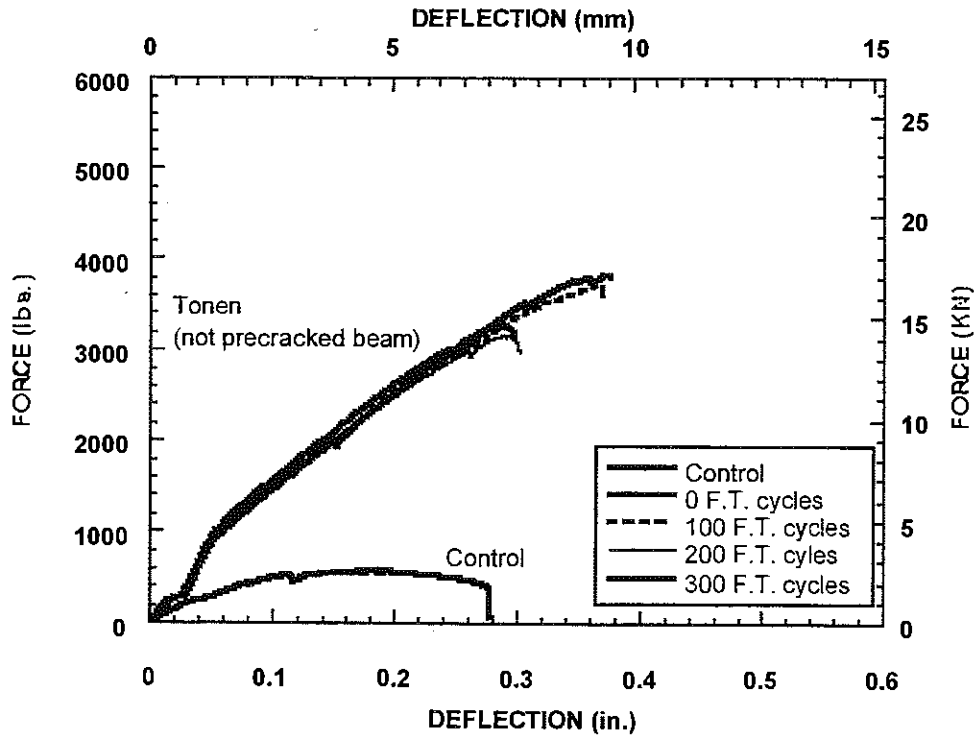


Figure 3C Load-Deflection Curves for Tonen Not Precracked Beams

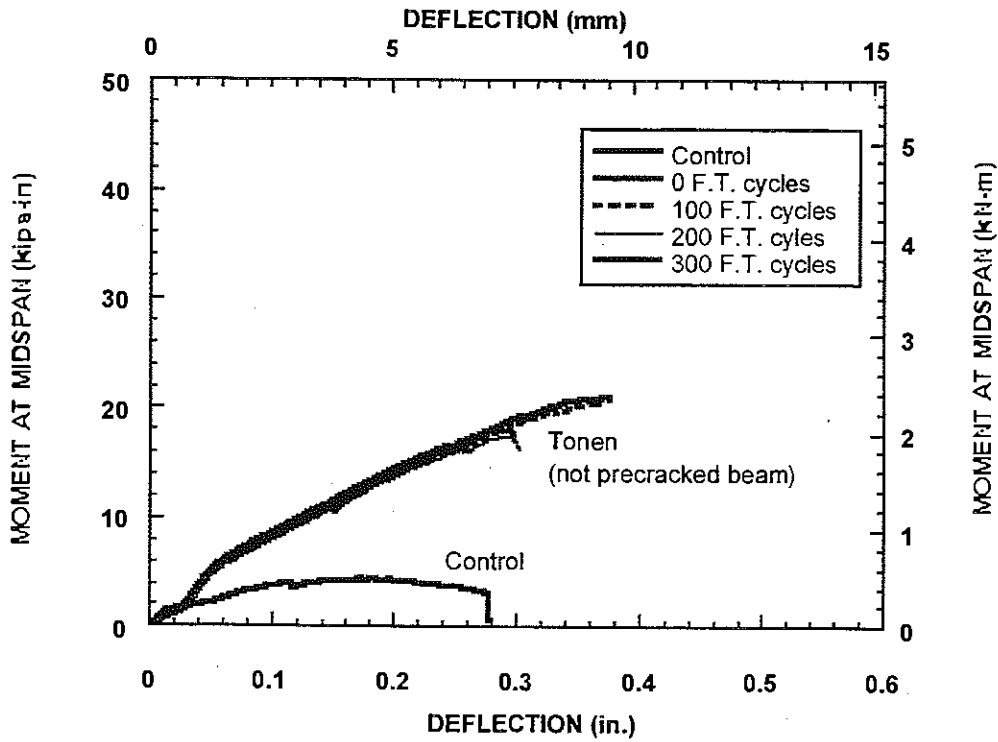


Figure 4C Moment-Deflection Curves for Tonen Not Precracked Beams

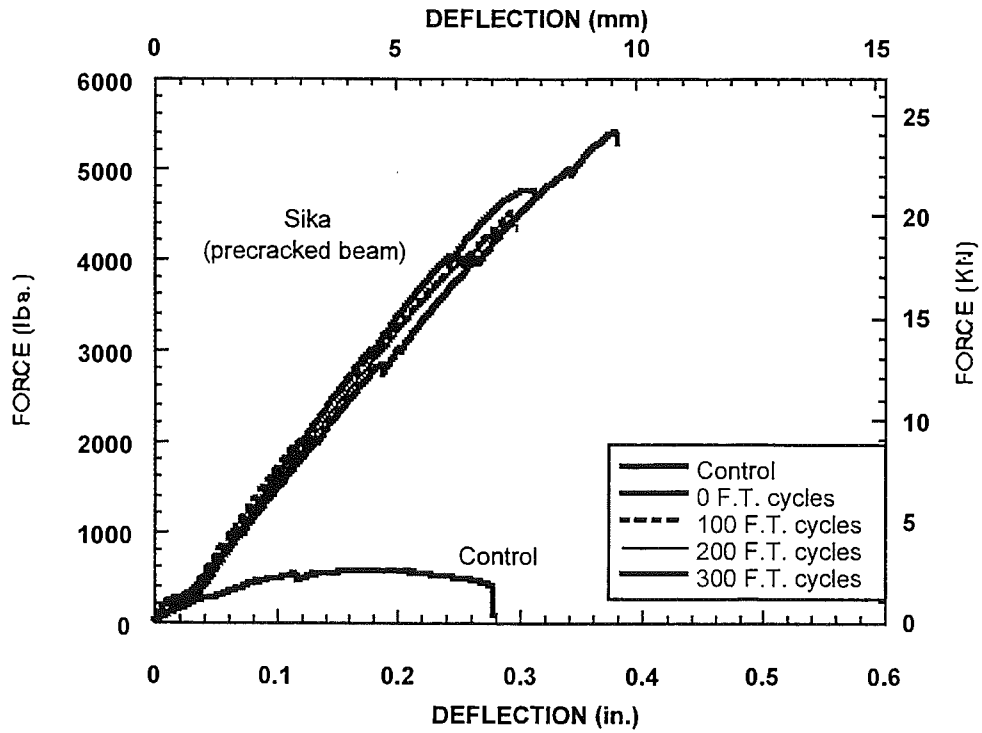


Figure 5C Load-Deflection Curves for Sika Precracked Beams

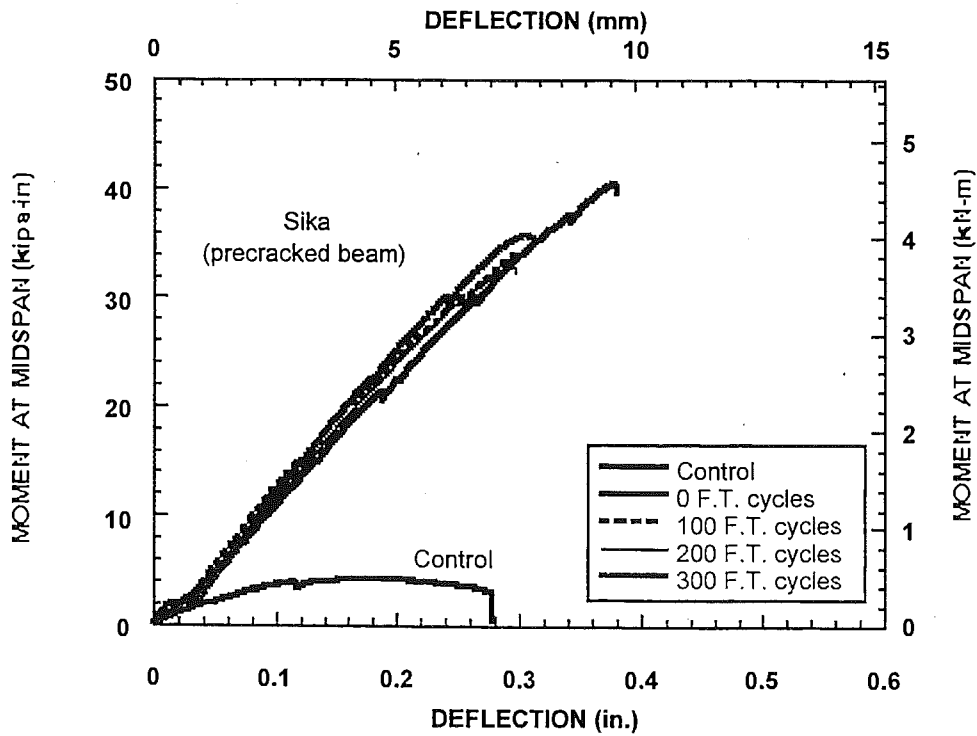
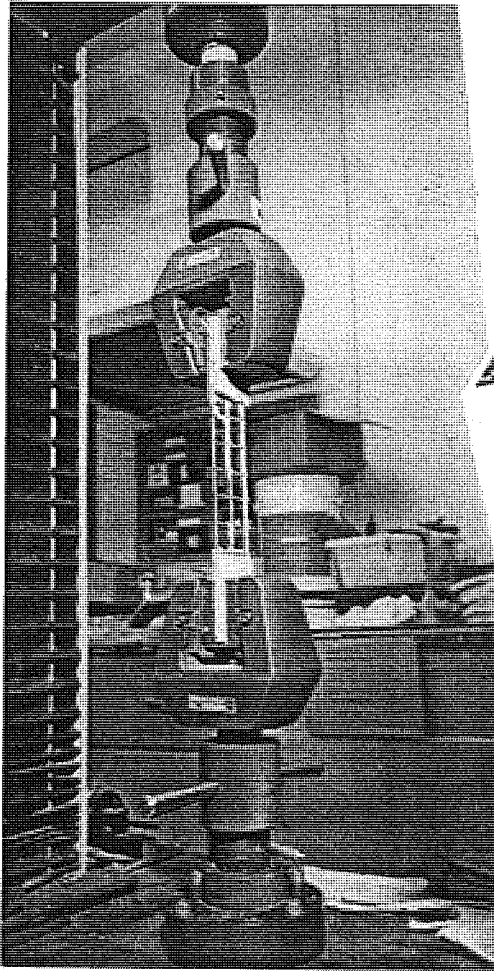


Figure 2C Moment-Deflection Curves for Sika Precracked Beams

**APPENDIX D**

**1. MATERIALS**

**1.1 STEEL**



**Figure 1. Tensile Test of Steel Mesh Coupons**

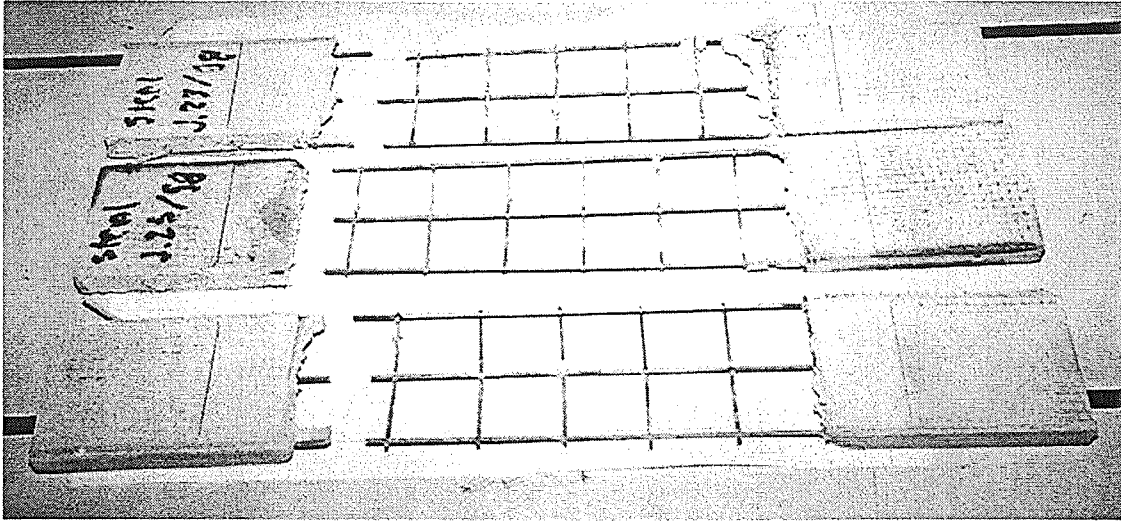


Figure 2. Steel Mesh Coupons

## 2. TEST SET-UP

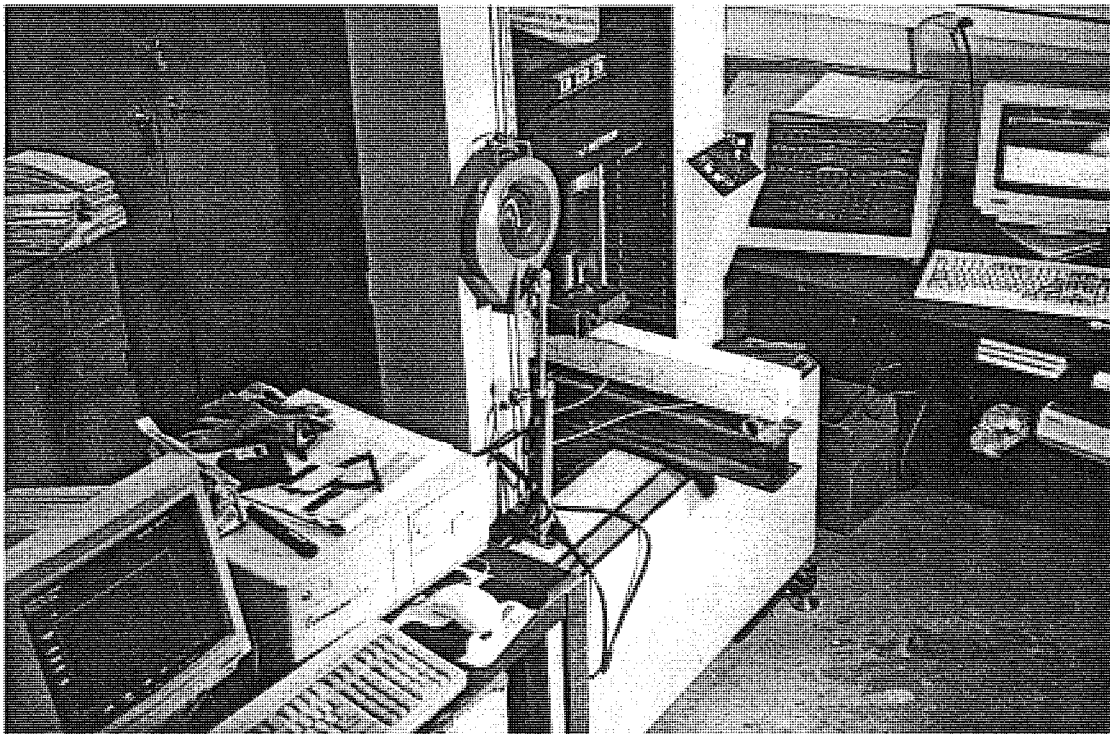
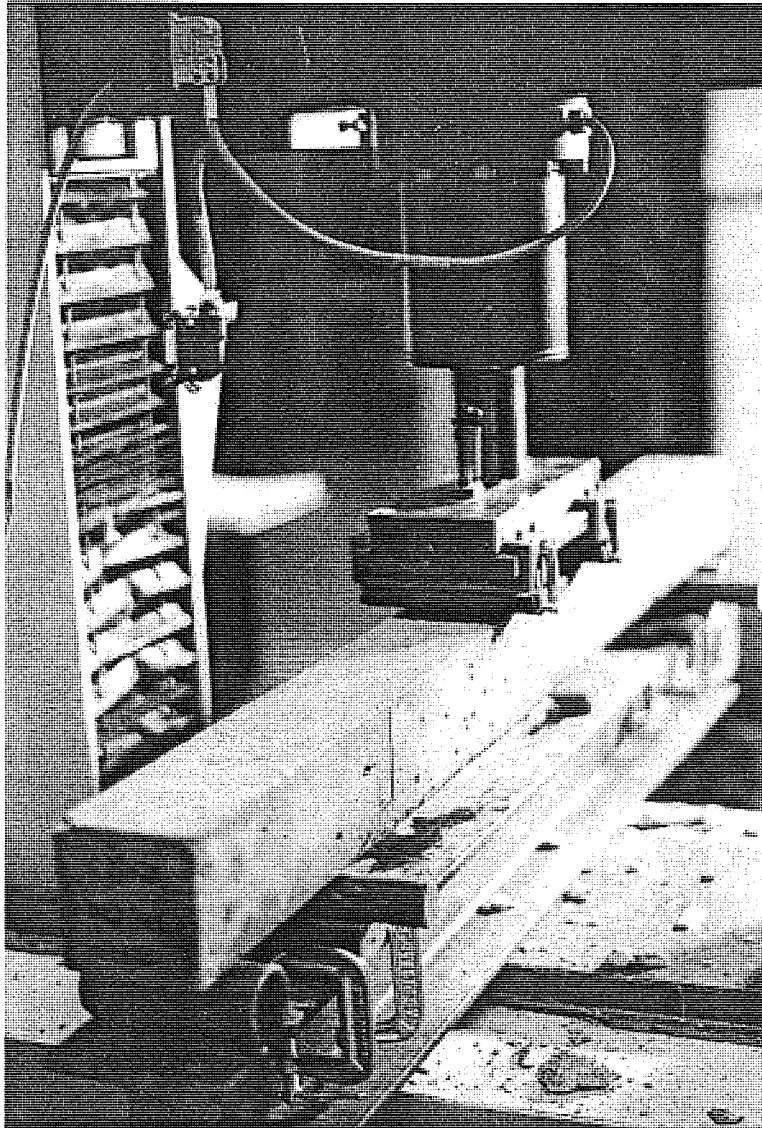


Figure 3. Test Set-Up



**Figure 4. Bending Test of F.T. Specimens**

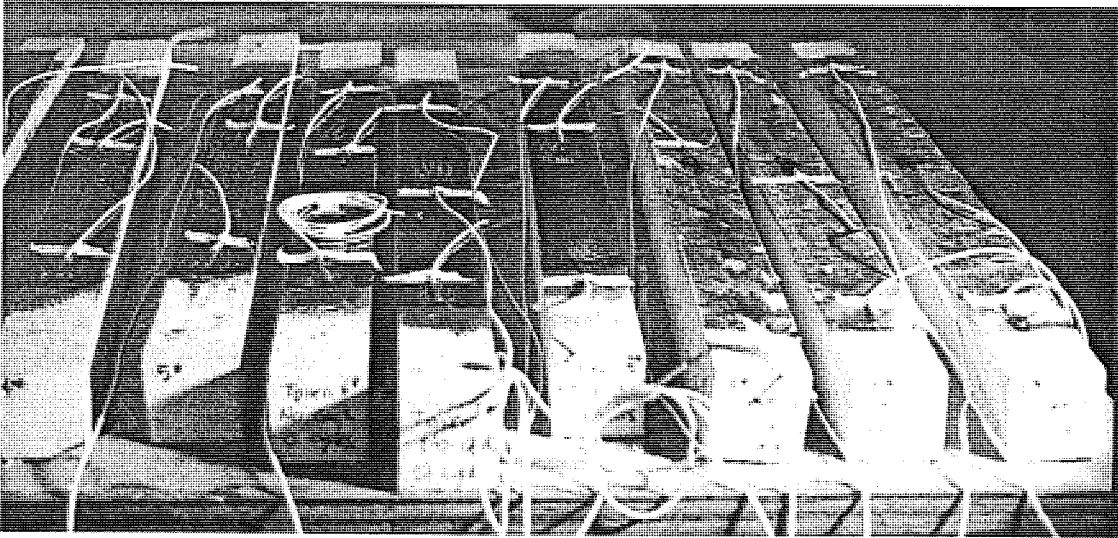


Figure 5. Instrumentation of Specimens at 0 F.T. Cycles

### 3. FAILURE MODES

#### 3.1 Control Specimens (Yielding of the steel reinforcement, flexural cracks)

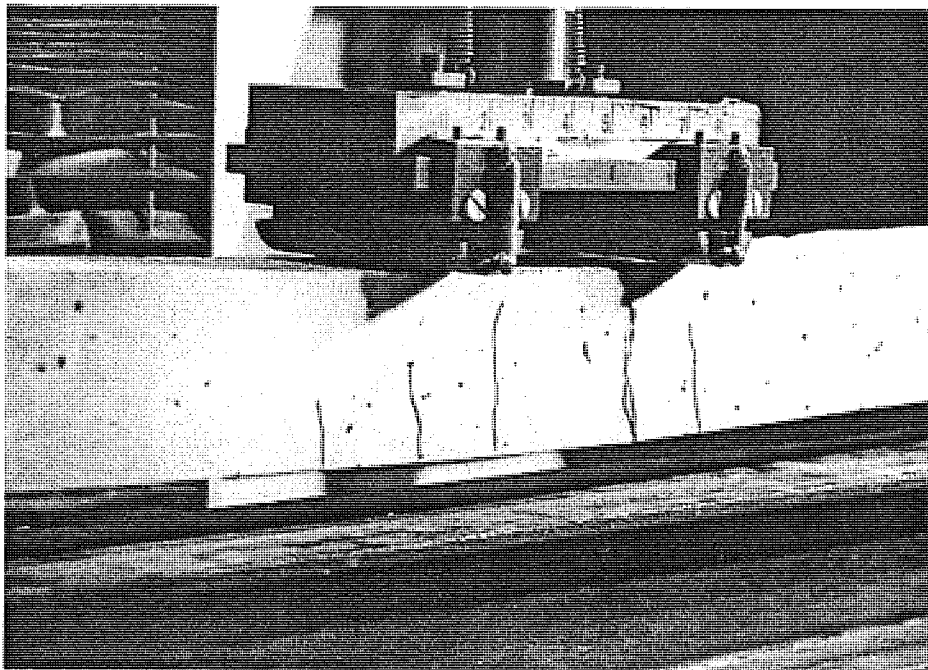
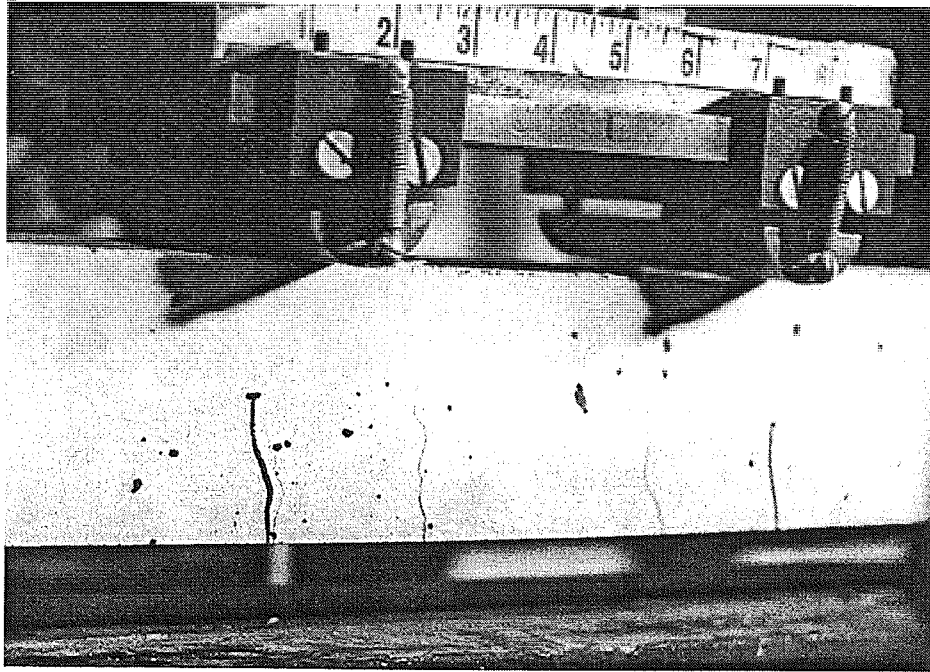


Figure 6. Bending Test of Control Specimens



**Figure 7. Control Specimens (Flexural Cracks)**

3.2 Sika System

**Flexure-Delamination:** CFRP peeling-off initiated at a flexural crack.

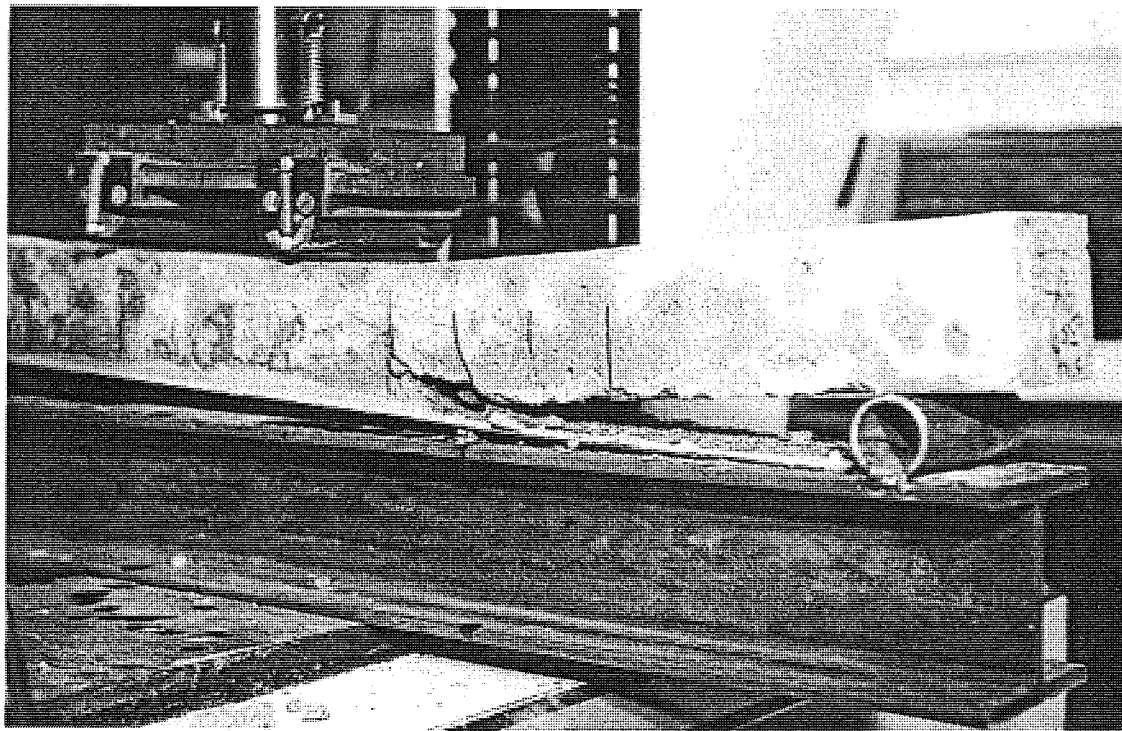


**Figure 8. Sika System. Failure Mode: Flexure-Delamination**

**Shear-Delamination:** CFRP peeling-off initiated at a shear crack.

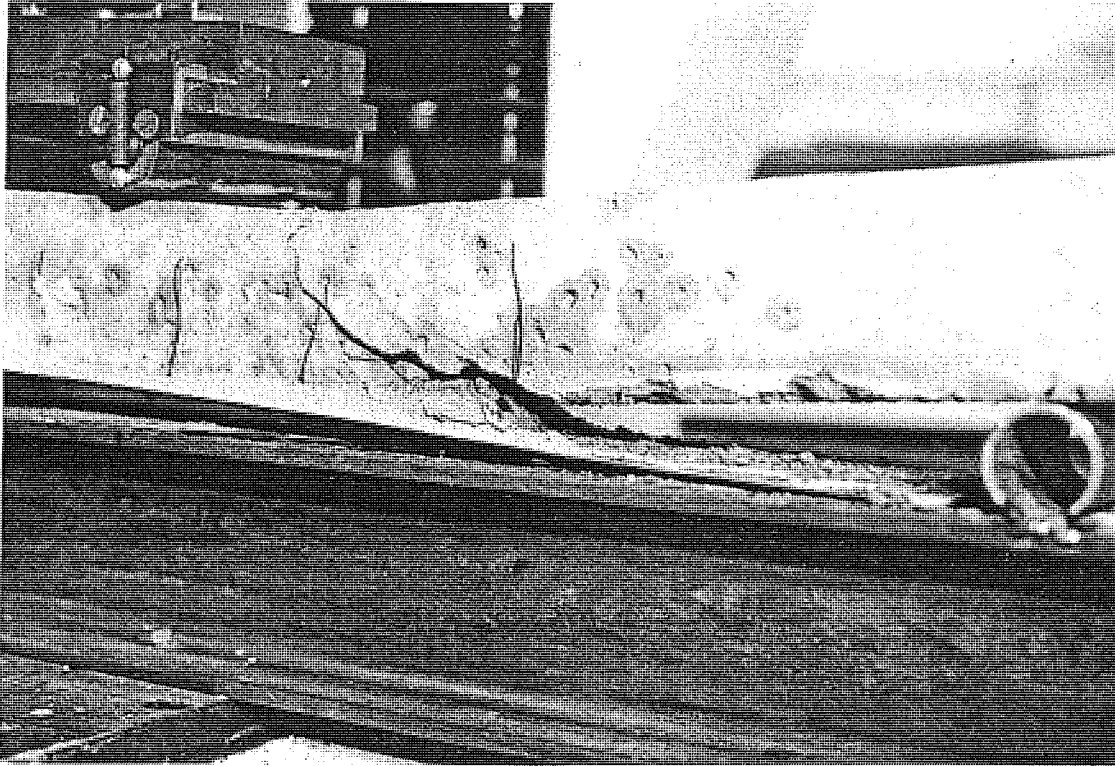


**Figure 9. Sika System. Shear-Delamination Failure**

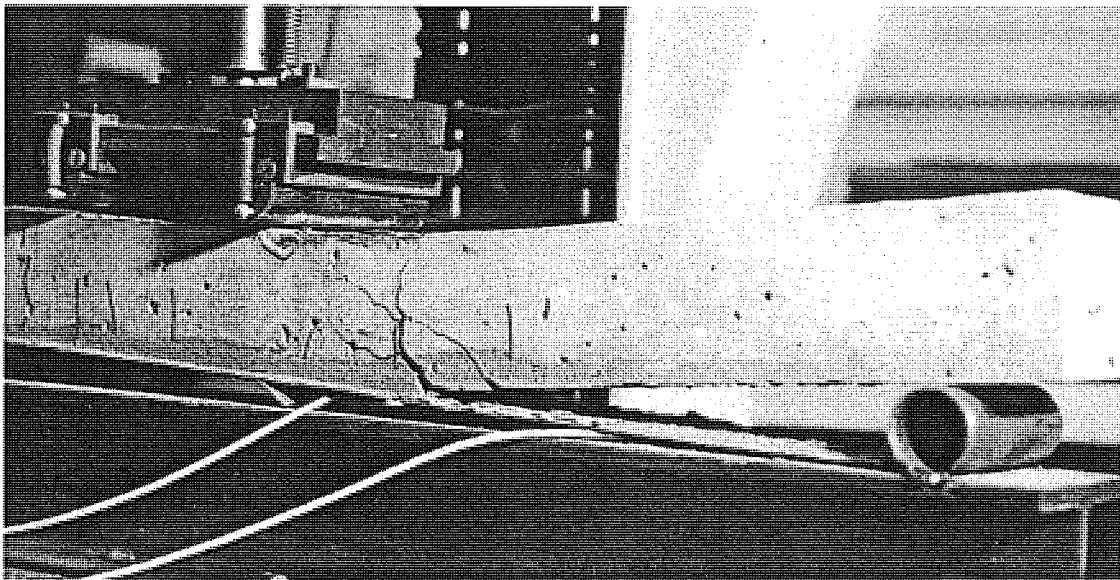


**Figure 10. Sika System. Shear-Delamination Failure**

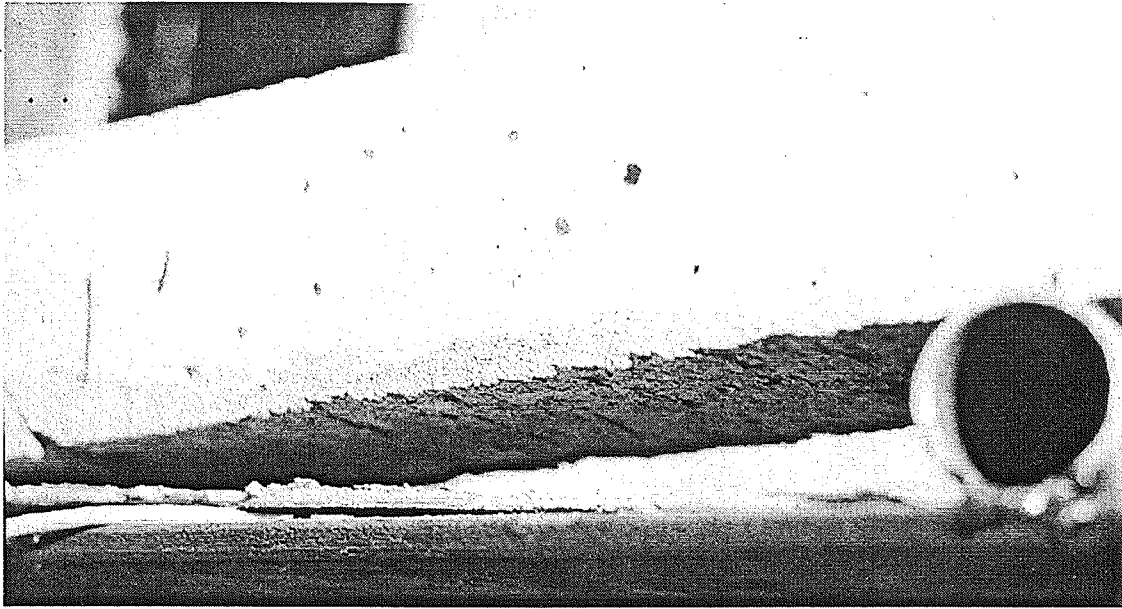


**Figure 11. Sika System. Concrete Surface after CFRP Peeling Off**

**Shear:** Vertical shear failure at the end of the CFRP laminate

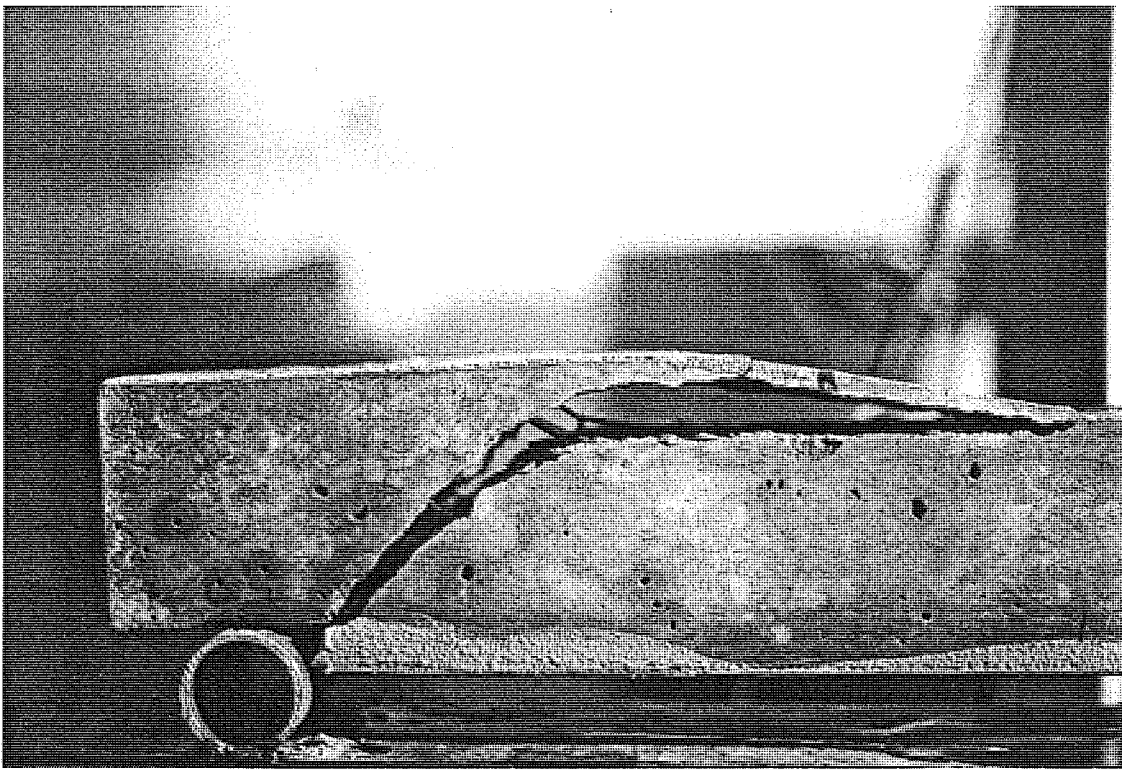


**Figure 12. Sika System. Vertical Shear Failure**

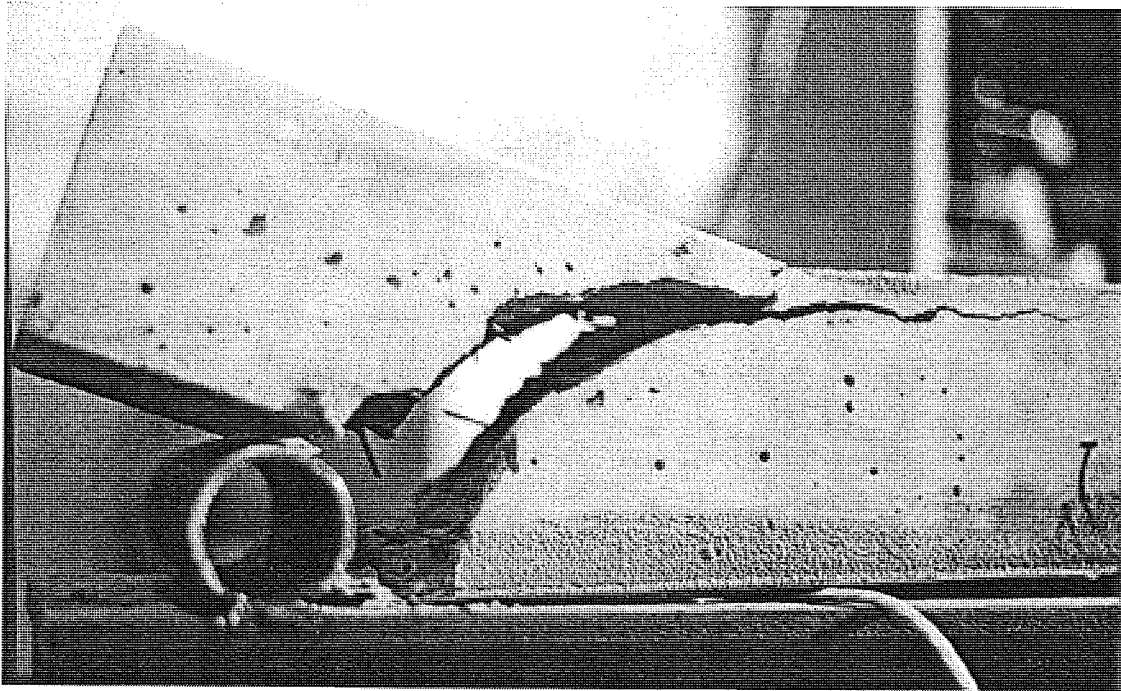


**Figure 13. Vertical Failure of a Specimen Strengthened with Sika System**

### 3.3 Tonen System

**Flexure-Delamination:** CFRP peeling-off initiated at a flexural crack.

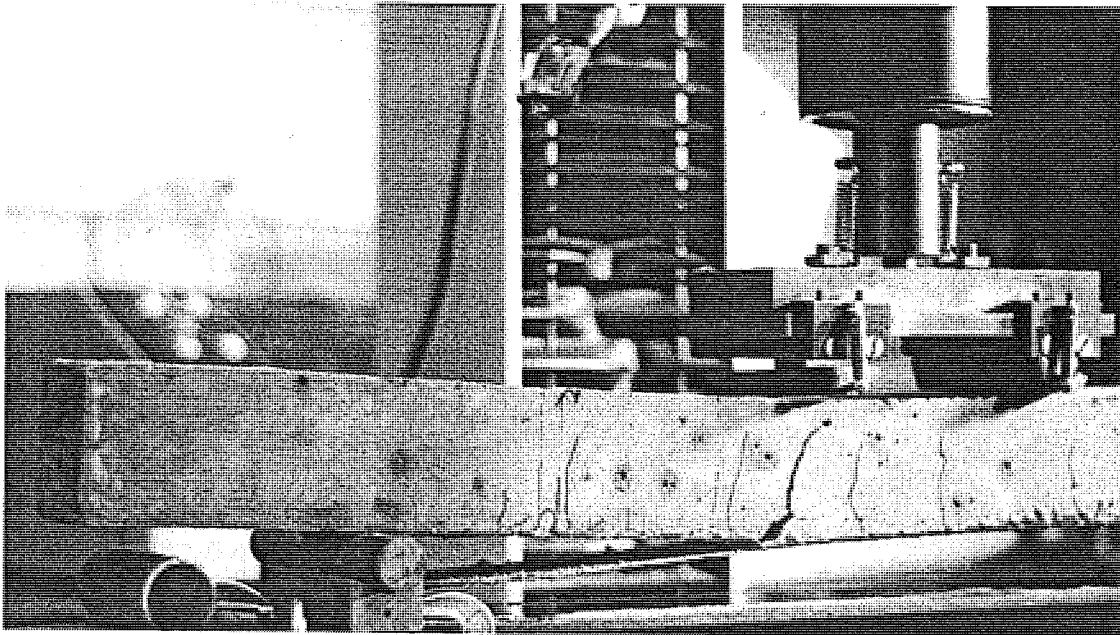


**Figure 14. Tonen System. CFRP Peeling-Off Started at a Flexural Crack**

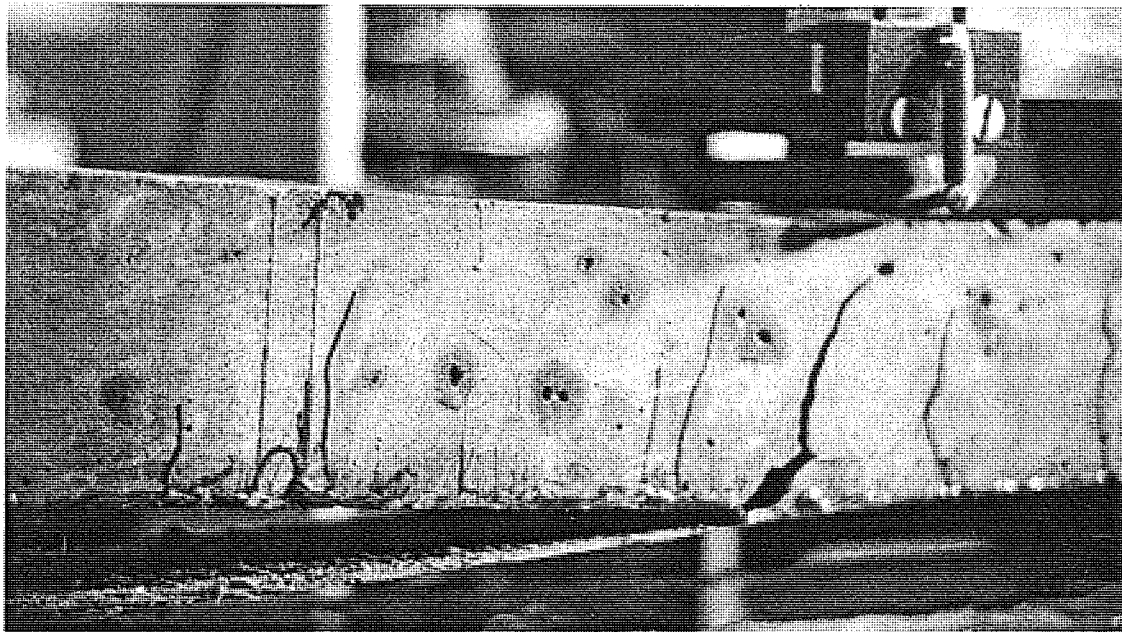


**Figure 15. Tonen System. Flexure-Delamination Failure**

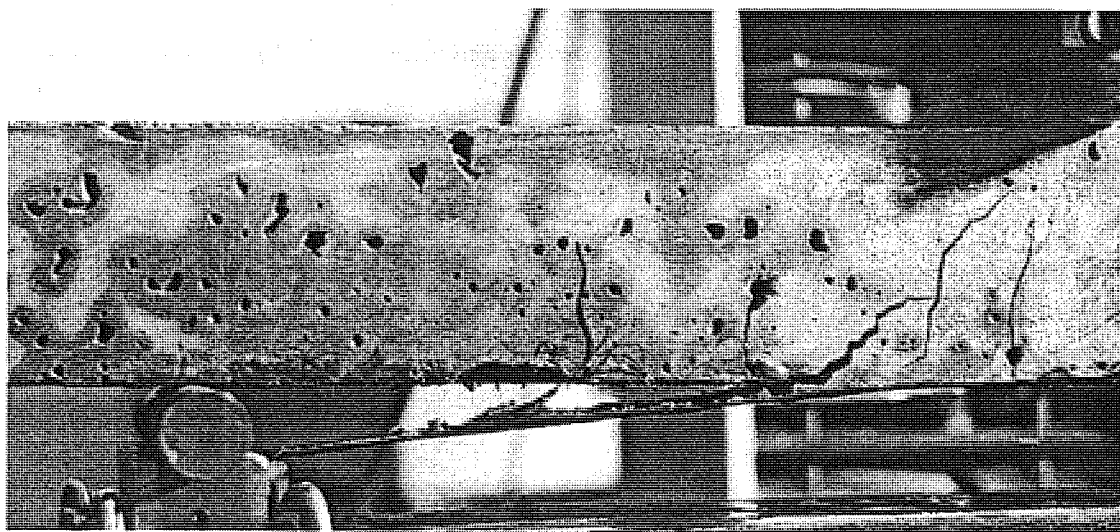


**Figure 16. Tonen System. Flexural Cracks and CFRP Peeling-Off**

**Shear-Delamination:** CFRP peeling-off initiated at a shear crack.

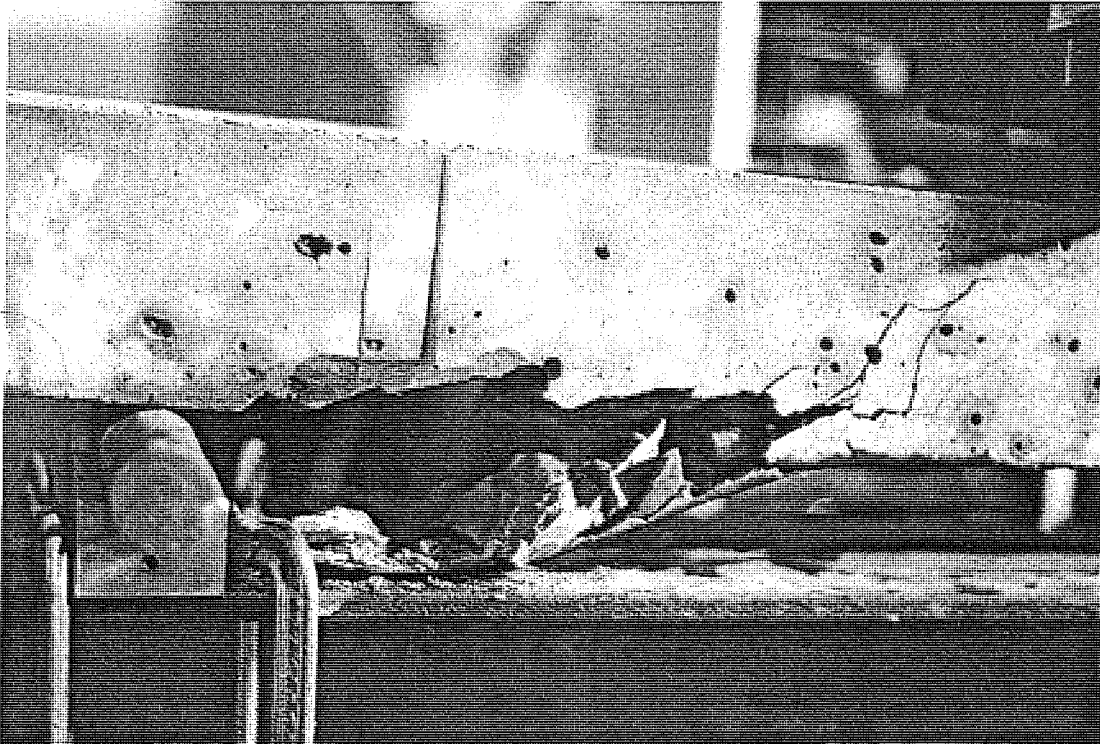


**Figure 17. Tonen System. CFRP Peeling-Off Initiated by a Shear Crack**

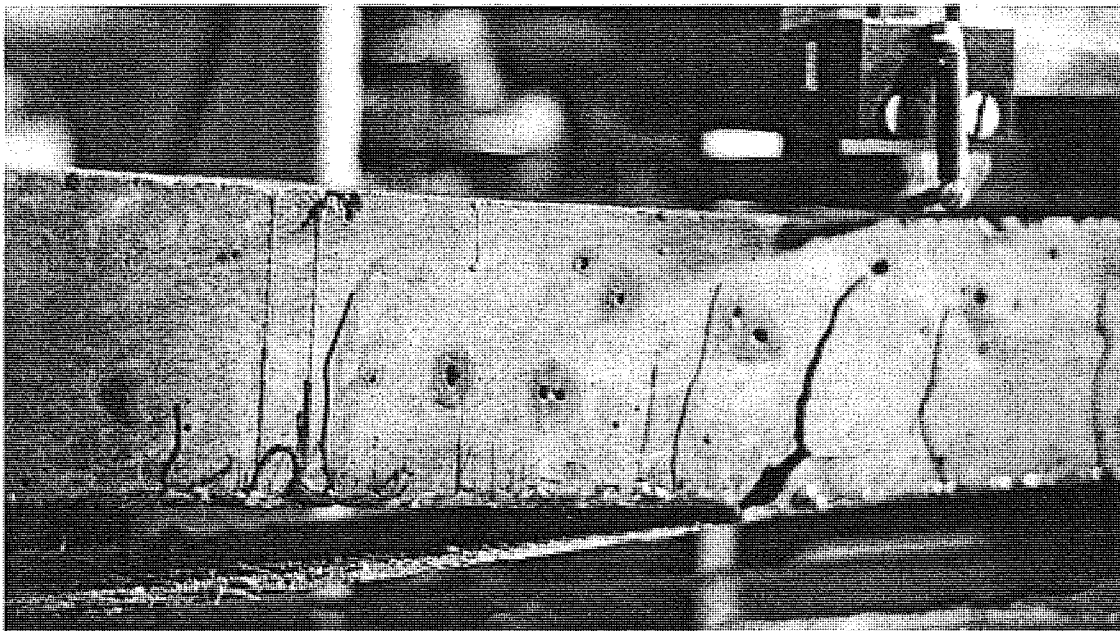


**Figure 18. Tonen System. Shear-Delamination Failure**



**Figure 19. Shear-Delamination Failure of a Specimen with Tonen System**

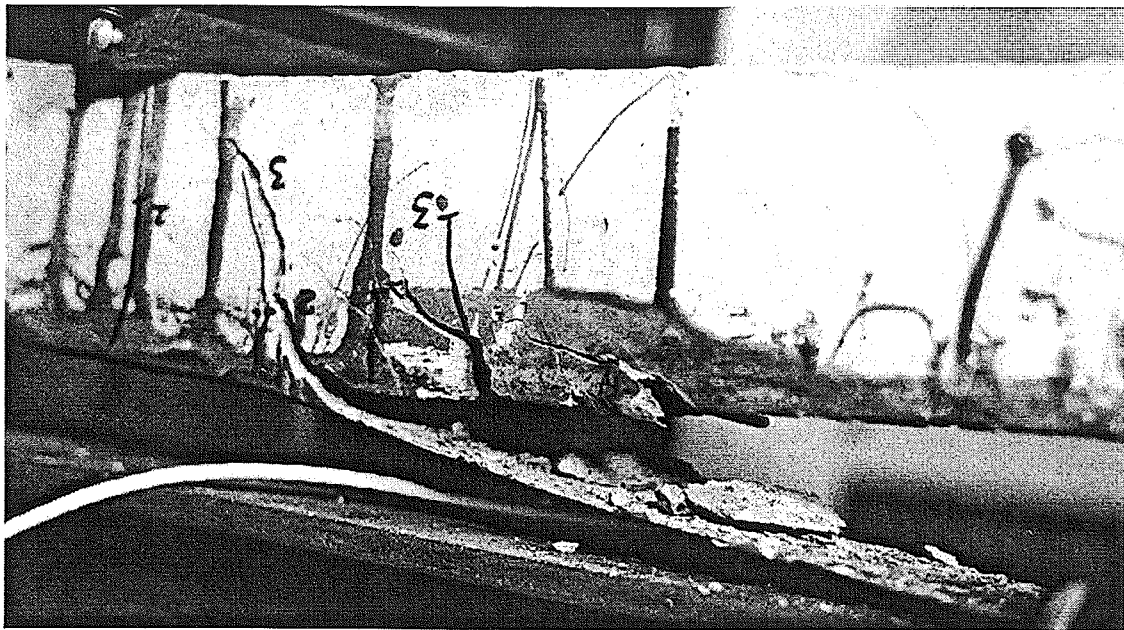


**Figure 20. Tonen system. CFRP Peeling-off. Some Pieces of Concrete remained attached to the Laminate**